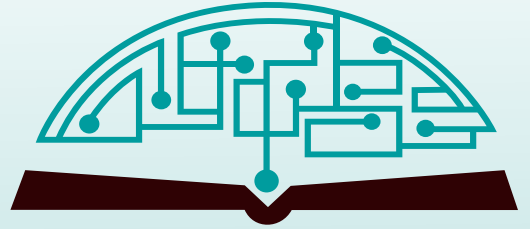


International
Journal of
High School
Research

IJHSR



November 2021 | Volume 3 | Issue 5

ijhighschoolresearch.org

ISSN (Print version) 2642-1046

ISSN (Online version) 2642-1054



GENIUS OLYMPIAD

"Let's build a better future together"



www.geniusolympiad.org

International Environment Project Fair For Grades 9-12



Rochester, New York
Hosted by Rochester Institute of Technology

@GeniusOlympiad



Table of Contents

November 2021 | Volume 3 | Issue 5

01	A Novel Robotic Arm for Tactile Perception Using Tele-Operation and Haptic Feedback <i>Vrinda Anand</i>
06	The Relationship Between Sleep and Cognitive and Physical Health <i>Catherine S. Nemeskal, Jennifer Watrous, Lauren Raine, Charles Hillman</i>
11	The Significance and Evolution of the Stellar Initial Mass Function <i>Ethan Kuperman</i>
16	A Study of The Effect Of Understorey Foliage Density On Bat Diversity and Abundance In The Guyana Shield Rainforest <i>Juliet I. M. Russell</i>
22	Solar Energy Induced Woody Biomass Conversion with a Semiconductor Photoelectrode <i>Claire Y. Lee, Alicia Y. Leem, Hannah Park</i>
28	Key Prognostic Biomarkers of Acute Myeloid Leukemia: Genetic Mutations and Measurable Residual Disease <i>Lok Yin Kwan</i>
36	The Prevalence of Post-Traumatic Stress Disorder in Self-Identified South Asians <i>Sruthi K. Medepalli</i>
40	Carbon-derived Substrate Accelerated the Biodegradation of Low-density Polyethylene <i>Crystal Radinski</i>
44	The Effects of Hybrid Fertilizer on Plant Life <i>Eva Saramya</i>
50	An Analysis of Advantage Factors in Men's Tennis – Handedness, Age, Height, and Rank <i>Shreyes Sridhara</i>
57	The Risk Factors of Adolescent Depression <i>Sia Agarwal</i>
65	Reduction of Heat Resistance of <i>Campylobacter jejuni</i> Using D-limonene from Calamansi Rinds Extract <i>Trinity Bjork M. Coduco, Bea Nicole S. Gacayan, Mary Danielle M. Estrada</i>
71	Geometric Interpretation of Best Rational Approximation and Simple Continued Fractions <i>William Li</i>

**Editorial
Board****International
Journal of
High School
Research****■ CHIEF EDITOR****Dr. Richard Beal**

Terra Science and Education

■ EXECUTIVE PRODUCER**Dr. Fehmi Damkaci,**

President, Terra Science and Education

■ COPY EDITORS**Olivia Colon, Intern,** Terra Science and Education**Taylor Maslin, Intern,** Terra Science and Education**■ ISSUE REVIEWERS****Dr. Rafaat Hussein,** Associate Professor, SUNY ESF**Dr. Junyi Li,** Institute of Electrical and Electronics
Engineers**Dr. Hua Wang,** Qualcomm, Bridgewater, New Jersey, U.S.A**Dr. Yingbin Liang,** Ohio State University**Laura Mufson,** Ph.D., Columbia University**Laura J Dietz,** PhD, University of Pittsburgh**Dr. Tereza Jerabkova,** ESA Research Fellow ESTEC,
Netherlands**Dr. Sinead Kinsella,** Fred Hutchinson Cancer Center**Shelby Keye,** Ph.D., University of Illinois Urbana-
Champaign**Nick Baumgartner,** MS Ph.D. Student, Purdue**Dr. Ana Laura Selzer Ninomiya,** University of Illinois**Dr. Kathryn J. Boor,** Cornell University**Raghavendra Amachawadi,** DVM, MS, PhD**Dr. Ashutosh K. Rai,** Kansas State University**Arlene Lingsang Tabaquero,** Ph.D., Saint Mary's
University**Dr. Anand Krishnamoorthy,** University of Central Florida**Preethika Sainam,** Ph.D., Arizona State University**Senthilkumar Thirupathi,** McGill University**Sanjay Gurunathan,** Global Clinical Sciences Sanofi
Pasteur**Gaby Dee,** Queen's University**Dina Radinskaia,** MD, CCFP (COE) (PC), FCFP**Dr. Kovalchuk, Igor,** University of Lethbridge**Olga Kovalchuk,** MD/Ph.D., University of Lethbridge**Stephanie Clarke,** Ph.D., Stanford University School of
Medicine**Robert H. Lipsky,** Ph.D., Inova Neuroscience and Spine
Institute**Dina Chau,** University of Toronto Toronto**Ricky Cheong,** HKSTP Hong Kong**Dr. Christoph Meyer,** University of Salford**Cassie Hauswald,** Freshwater Ecologist Nature
Conservancy**Amos Chungwon Lee,** Ph.D., University of California**Sae Ryun Ahn,** Sookmyung Women's University Bio
Design Lab**Sungjun Yoon,** Ph.D. RWTH Aachen University**Swati Chhabra,** Shantou University, China**Dr. Tahir Waheed,** Shantou University, China**Hira Waheed,** PostDoc Fellow, Shantou University**Dr. Adnan Khan,** Shantou University

A Novel Robotic Arm for Tactile Perception Using Tele-Operation and Haptic Feedback

Vrinda Anand

Amity International School Vasundhara Sector 1, Ghaziabad, Uttar Pradesh, 201011, INDIA; vrinda.naomi0406@gmail.com

ABSTRACT: In this research, a cost-effective robotic arm was designed and developed, which empowers a user to clasp objects with a third arm and give a sense of touch corresponding to the force that an effector encounters. A cost-effective tele-operated robotic arm was intended to provide surgeons with tactile perception, as well as handle nuclear waste and biohazards. Tele-operation and haptic feedback was achieved with infrared (IR) sensors, servo motors, and force pressure sensors. This arm is capable of lifting 600 g which can be further increased by using pneumatic actuators. The robot could also assist patients with weak arm strength (Amyotrophic lateral sclerosis) and stroke patients as their movements can be controlled by the user's facial expressions.

KEYWORDS: Engineering Mechanics; Mechanical Engineering; Robotic arm; Effector; Tactile, Haptic feedback; Tele-operated robotic arm; Sensors.

■ Introduction

Robots have been proven an efficient workhorse for automotive and other manufacturing industries. In comparison, a robotic arm is a mechanical version of the human arm that is programmable and can perform functions that humans cannot achieve.¹ Such arms can solve many limitations that humans face. The human arm is notable for its ability to perform a great variety of tasks. Although slower, weaker, and less accurate than high-performance robots of today, the human arm is without equal in terms of versatility, robustness and gracefulness. It can help humans to be self-dependent and not rely on others for their daily chores.² A robotic arm can be designed to perform any desired task, such as welding, gripping, spinning, etc., depending on the required application.³ Robots and their components have evolved significantly to be more capable and versatile, but there still exists much room to explore.^{4,5}

This research aimed to design and develop a cost-effective robotic arm. This includes a robotic arm, smart glasses (facial expression detection), and pneumatic muscles. Haptic technology was used to provide a sense of touch, similar to the technology used by surgeons during robot-assisted surgery.

The idea was to replace the expensive technology with an affordable and stable technology that could perform diverse functions. With a novel tactile perception method, it is possible to provide a sense of touch to the users with force pressure sensors exactly equivalent to the force being experienced by the effector. A brain, artificial intelligence (AI), was deliberately not given to the robotic arm to keep it as a tool and designed it in such a way that these are entirely dependent on user inputs.

Further, the McKibben muscles were also included, which could be used as a cheaper version of the arm's actuators. A McKibben muscle is an actuator which converts pneumatic (or hydraulic) energy into mechanical form by transferring the pressure applied on the inner surface of its bladder into the shortening tension.⁶

■ Materials and Methods

The robotic arm consisted of metal, wood, plastic, servo motors, Arduino UNO ATmega 328P, IR Obstacle Sensor Module, Thin Film Force pressure sensors and other low-cost materials.

Servo Motors:

Servo: Detects the operation error of a mechanism, provides feedback and corrects faults. A servo (Figure 1) motor can have alternating current (AC), direct current (DC) or stepper motors. Servo motors are the kinds of motors that can fulfill the commands wanted. They can operate steadily even at very small or very large speeds. A set of servos controlled the wrist and the elbow movement. A micro servo was positioned on the wrist part and a high torque servo on the elbow part.



Figure 1: Servo motor.

Force Pressure Sensor:

Force Sensing Resistors (FSR) are a polymer thick film (PTF) device (Figure 2) which exhibits a decrease in resistance with an increase in the force applied to the active surface. Its force sensitivity is optimized for use in human touch control of electronic devices. This robotic arm was equipped with a sense of touch capability which was achieved by force pressure sensors. Force pressure sensors are placed on the fingertip of the robotic arm and connected to a servo motor with an Arduino Uno to provide haptic technology to the arm.



Figure 2: Force pressure sensor.

Arduino Uno:

Arduino/Genuino Uno (Figure 3) is a microcontroller board based on the ATmega328P (datasheet). It has 14 digital input/output pins (of which 6 can be used as PWM outputs), 6 analog inputs, a 16 MHz quartz crystal, a USB connection, a power jack, an ICSP header and a reset button.



Figure 3: Force pressure sensor.

Infrared Sensors:

An infrared sensor (Figure 4) is an electronic device that emits light in order to sense some aspects of the surroundings. An IR sensor can measure the heat of an object as well as detects the motion. Some infrared sensors were added to a pair of eyeglasses and a controller glove for the robot's tele-operation. These were then attached to the servo motors through an Arduino Uno. The infrared sensor, attached to the front part of the eyeglasses, detects the closing eyelid motion, and sends the signal to the servos, which then moves the fingers of the robotic hand.



Figure 4: Force pressure sensor.

Circuit Diagrams:

For Tele-operation (Figure 5)

In order to achieve tele-operation, connect the IR sensors, servo motors and Arduino board as shown in the circuit (Figure 5).

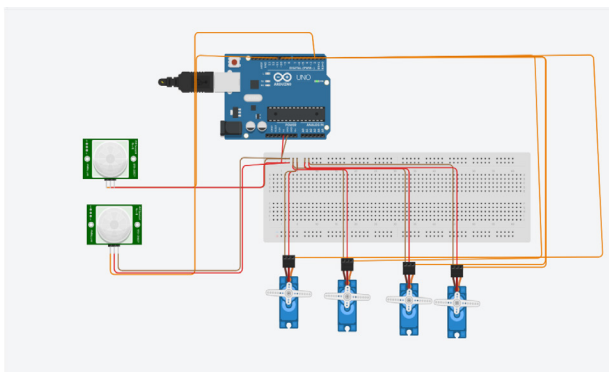


Figure 5: Infrared sensors and servos connected.

Haptic Technology (Figure 6):

For haptic technology, connect a force pressure sensor, servo motor and Arduino board together with a resistor of 10 K ohm.

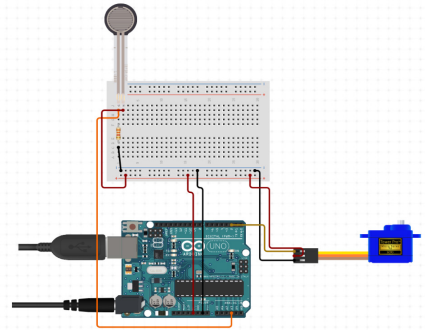


Figure 6: Force pressure sensor and servo connected.

Torque Calculation:

Forearm Torque Calculation:

Length=23cm, Mass=0.06kg

(Where T is Torque, F is force and S is the length of the forearm) (Figure 7)

$$T = F \cdot S$$

$$= 23 \cdot 0.06 \cdot 1/2 \text{ (considering center of mass)}$$

$$\approx 0.7 \text{ kgcm}$$

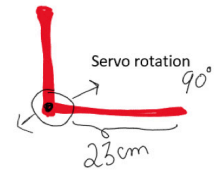


Figure 7: The forearm.

We have used a 15 kg-cm torque servo motor.

NOTE: The torque calculated is only of the forearm.

On Adding Weight (Figure 8)

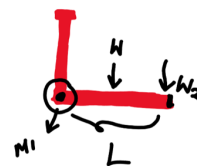


Figure 8: On adding weight on the arm.

$$M1 = S \cdot 1/2 \cdot W1 + S \cdot W2$$

$$= 23 \cdot 1/2 \cdot 0.06 + 23 \cdot W2$$

$$= 0.7 + 23W2$$

As the motor (M1) used has 15 kg cm of torque (T)

$$W2 = 600g$$

Hence, the weight that this forearm can carry is 600 g.

Results and Discussion

Robotic Arm:

The robotic arm has 3D rotation capability. The wrist revolves 180 degrees, 90 degrees of elbow movement, and 360 degrees of bicep rotation (Figure 9). The features ranged from tele-operation to sense of touch. Innovative methods that are quite affordable were used to give this arm such features. A

detailed description of the features, capabilities, and intended uses is provided in the following sections.

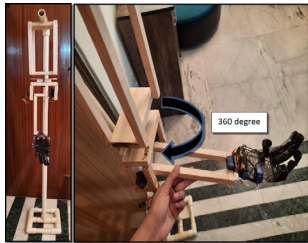


Figure 9: The robotic arm.

Tele-operation:

Tele-operation means operating a machine at a distance. This robot was tele-operated to make the robot copy users' hand movements, which requires correct sensors to be used. Initially, flex sensors were used which were working nicely, but the cost and the durability were a concerning factor. With each sensor costing around \$7, the project's overall cost was too high.

Instead, the sensors were replaced with self-made ones, as shown in (Figure 10). These sensors were made with cardboard, graphite, and some aluminum foil. These flex sensors were working well with the servo motors. However, the challenge was its consistency. The sensors stopped working after a month, which led to a search for sensors that could work with the servos. A variety of sensors were found that exists today, including Brainwave sensors.



Figure 10: Homemade flex sensors attached to the servos.

One can control anything just with the power of your brain; the power that humans have always wanted has now been achieved by some great minds.⁵ Not only Brainwave but also the EMG sensors were pretty eye-catching. The only problem with these sensors is that they are exorbitantly priced. Hence, the reason these sensors were not used in this research.

Finally, it was observed that the infrared sensors were working well with the servos. They were coordinating perfectly with the servo motors. Not just that, but they were economically friendly too, about \$1. So, it was decided to go ahead with these sensors for this project. They were placed inside the controller glove of the left hand under the fingers (Figure 11). After the sensor senses the motion of bending fingers, each servo attached to a robotic finger, rotates, and controls the mechanical fingers as it pulls and releases them (closing and opening of the fingers).

Sense of Touch:

Haptic technology, also known as kinaesthetic communication or 3D touch, refers to any technology that can create an

experience of contact by applying force, vibrations, or motions to the user.



Figure 11: Controller glove with infrared sensors.

There is a force pressure attached to the fingertips of the robotic hand, which upon touching, sends those signals to the servo motor, which is attached to the fingertip of the controller glove that the user is wearing to control the robotic hand (Figure 12). After receiving the signals, the servo rotates according to the pressure frequencies received on the force pressure sensor, making the user feel those sensations. Therefore, if the sensor touches something lightly, the servo rotates just a few degrees giving a lighter sensation. When it is pressed with maximum frequency, the servo rotates a full 180 degrees to provide a much harder sensation (Figure 13).

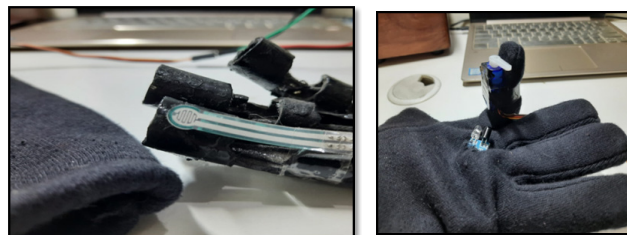


Figure 12: Force pressure sensor attached to the robotic hand.

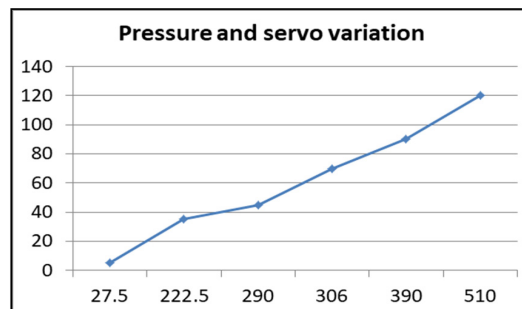


Figure 13: Pressure frequencies received by the force pressure sensor, which shows how the angle of servo increases, with the increase in pressure on the force pressure sensor.

Facial Expression Detection:

This research could also assist patients with weak arm strength such as patients with Amyotrophic lateral sclerosis, stroke patients, etc. For such patients, a technology to control the robot with facial expressions, so that they do not have to use their hands, has also been developed. To serve this purpose, eyeglasses have been used to detect facial expressions. Infrared sensors, attached to the front part of the eyeglasses, detect the closing eyelid motion and send the signals to the servos, which then move the fingers of the robotic hand.

For this, now, when the user usually closed their eyes, the sensor doesn't receive any signal. Still, when the user intentionally closes their eyes harder, the sensor senses the motion due to the harder blink and a slight movement of the eyeglass (due to the muscle movement), making the servos move to make the fingers bend. Infrared sensors placed on either side of the eyeglasses detect the motion of the user's mouth to cause action in the robotic hand (Figure 14). So, with the movement of jaw and smile, the user can rotate the wrist when they move their jaw and bend the elbow of the robotic hand with a smile on their face which would be detected by the sensors. This is also an exciting way to bring a smile to the user's face (Table 1).

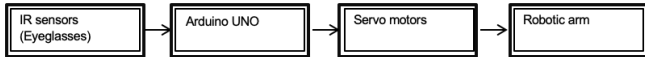


Figure 14: Smart Eyeglasses.

Table 1: Commands for the Control of the Robotic Arm.

Actions	Facial Expressions
1. Bending Fingers	Eye blink
2. Wrist rotation	Moving jaw
3. Elbow rotation	Smiling

Pneumatic Muscles:

The elbow movement can also be controlled by Pneumatic muscles (Mckibben muscles). Each muscle (5 g) can lift 350 g, about 70 times its weight (Figure 15; Table 2). The muscle that this project includes is 20 cm long and at 2 bar pressure, contracts by 1/7th of its length (Figure 16). According to the requirement, several muscles can be used to hold on to extra weight by using them as actuators. These muscles are made with a latex tourniquet tube and a nylon mesh.

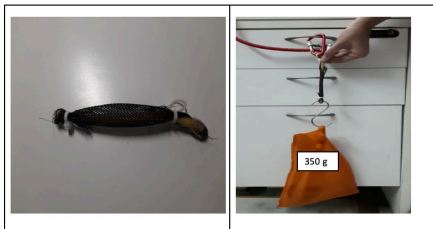


Figure 15: Smart Eyeglasses.

Application as a bionic or a rehabilitation device:

By wearing the robotic hand, the device can act as an assistive rehab device, where the user needs to wear the controller glove on the same hand as the device (Figure 17). With a slight motion of the bending finger/fingers, the user can control the robotic hand. This device could also serve as an inexpensive

bionic hand. For this, the user needs to control the robotic arm with the other hand while he or she wears the device on the other (Figure 18).

Table 2: Experimental parameters.

S.No	WEIGHT (g)	OBSERVATION
1.	100	Lifts up
2.	150	Lifts up
3.	250	Lifts up
4.	350	Lifts up
5.	400	The tube bursts

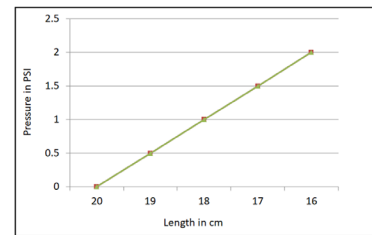


Figure 16: Length variations of pneumatic muscle in response to pressure. The graph shows how the muscle contracts and decreases in length with increase in pressure.



Figure 17: Application as a rehab assistant.

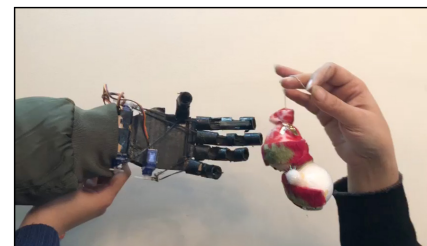


Figure 18: Application as a bionic arm.

Conclusion

In this research, an affordable robotic arm has been designed and developed. The mechanism used is an innovative and inexpensive version of robotic arms. Unlike high-end robotic arms that cost about \$35,000, this project costs under \$100. This research also shows how a sense of touch to the robots (haptic technology) can be added. The study demonstrates that by using different technologies through sensors, the expensive technology can be replaced. However, further research needs to be done in the future to make it fully efficient and stable.

■ Acknowledgements

Without my parent's help and encouragement, this idea would not have been possible. They guided me for eight months. During this journey, they generously funded this project and gave their time, love, and support. I would also like to express my gratitude towards my schoolteachers, who held on to me with their time and patience and helped me whenever possible.

■ References

1. Shaikh, A.S., Panchal, M., Maurya, H., Shaikh, F., Shaikh, N., Surwadkar, T., Juned, M., Ashfaque, M., 2020. Multipurpose Robotic Arm. *Int. J. Res. Appl. Sci. Eng. Technol.* 8, 1635–1639.
2. Cattin, E., Roccella, S., Vitiello, N., Sardellitti, I., Artemiadis, P.K., Vacalebri, P., Vecchi, F., Carrozza, M.C., Kyriakopoulos, K.J., Dario, P., 2008. Design and development of a novel robotic platform for neuro-robotics applications: The NEURobotics ARM (NEURARM). *Adv. Robot.* 22, 3–37. <https://doi.org/10.1163/156855308X291827>
3. Kafuko, M., Singh, I., Wanyama, T., 2015. Design of a Robotic Arm for Teaching Integrated Design. *Proc. Can. Eng. Educ. Assoc.* 1–5. <https://doi.org/10.24908/pceea.v0i0.5827>
4. Changela, B., Kataria, A., 2020. Real-Time Robotic Arm Control using Static Hand Gestures: An Approach towards the Natural Human Machine Interaction. *GRD Journals-Global Res. Dev. J. Eng.* 5, 8–15.
5. Patel, R., 2020. Brain Wave Controlled Robotic Arm for Paralytic and Physically Impaired Patients. *Int. J. Res. Appl. Sci. Eng. Technol.* 8, 1515–1520. <https://doi.org/10.22214/ijraset.2020.30536>
6. Ching-Ping Chou, & Hannaford, B. (1996). Measurement and modeling of McKibben pneumatic artificial muscles. *IEEE Transactions On Robotics And Automation*, 12(1), 90-102. doi: 10.1109/70.481753

■ Author

Vrinda Anand is a twelfth grader attending Amity International School Vasundhara 1. She is interested in mechanical engineering and plans to pursue higher studies in mechanical engineering.

The Relationship Between Sleep and Cognitive and Physical Health

Catherine S. Nemeskal, Jennifer Watrous, Lauren Raine, Charles Hillman

Danvers High School, 60 Cabot Street, Danvers, Massachusetts, 01923, USA; csnemeskal@gmail.com

ABSTRACT: The relationships between sleep and aerobic fitness, intelligence, and cognitive abilities in preadolescent children was investigated in this research. Data from 483 children who were 8 - 9 years old were used to conduct correlational analyses. One parent of each participant completed a questionnaire pertaining to the typical amount of sleep received by the child participant. Each participant completed a maximal oxygen consumption test, a dual energy x-ray absorptiometry (DXA) scan, an Intelligence Test, achievement testing in reading, math, and spelling, and a modified flanker task to assess attentional inhibition. Greater amounts of sleep correlated with aerobic fitness ($r=0.15$, $p\leq 0.001$). Sleep correlated with body composition, measured via body mass index (BMI) ($r=-0.15$, $p\leq 0.001$) and visceral adipose tissue (VAT) ($r=-0.12$, $p=0.02$). Sleep also correlated with crystallized intelligence ($r=0.18$, $p\leq 0.001$) and fluid intelligence ($r=0.16$, $p\leq 0.001$), as well as performance on reading ($r=0.17$, $p\leq 0.001$) and math ($r=0.16$, $p=0.01$) achievement tests. Spelling did not correlate with sleep ($r=0.09$, $p>0.05$). Greater amounts of sleep correlated with congruent flanker task accuracy ($r=0.11$, $p=0.03$) and reaction time ($r=0.13$, $p=0.01$). Finally, sleep correlated with incongruent flanker task accuracy ($r=0.16$, $p\leq 0.001$) and reaction time ($r=0.13$, $p=0.01$). These findings indicate a beneficial relationship of sleep with physical and cognitive health in children.

KEYWORDS: Behavioral and Social Sciences; Cognitive Psychology; Intelligence; BMI; VO₂ Max; Sleep; Attentional Inhibition.

■ Introduction

Human beings spend approximately one-third of their lifetime asleep. Many processes that are necessary for survival occur during sleep cycles: nerve cells communicate and build connections; the body repairs cells, tissues, and muscles; and hormones are produced throughout the body.¹ But how does the time we spend asleep impact the time we spend awake? Children, 8 and 9 years old, are recommended to get 9-11 hours of sleep per night for adequate health and safety.² Adequate sleep is particularly important for children since insufficient sleep is associated with atypical physical and cognitive development.³ According to the National Sleep Foundation, sleeping for under 7 hours or over 12 hours nightly can compromise health and development in preadolescent children and may lead to serious health problems.² There is growing evidence linking sleep and cardiometabolic risk factors in children, particularly in terms of adiposity.⁴ Existing research suggests that more chronic sleep leads to a lower body mass index (BMI) in adolescents, young adults, and older adults.⁵ While this research exists pertaining to sleep and its effects on BMI in adolescents and adults, little is known about the effects of sleep on BMI in preadolescent children. In addition, one study also suggests that sleep influences physical activity, such that unhealthy sleep patterns are related to lower levels of cardiorespiratory fitness.⁶ This may be because exercise has been shown to improve sleep architecture and sleep continuity in children.⁷ Furthermore, research suggests that increased sleep correlates with better academic performance in adolescents.⁸ However, less is known about the effects of sleep on academic performance in preadolescents, as well as its effects on intelligence, both in terms

of crystallized and fluid intelligence. Crystallized intelligence refers to the ability to acquire facts and knowledge. Fluid intelligence refers to the ability to think critically and use reasoning to recognize patterns. Crystallized and fluid intelligence present differently in children, as fluid intelligence increases until adolescence and then declines, whereas crystallized intelligence increases consistently.⁹ Additionally, research from the US Library of Medicine suggests that sleep deprivation impairs attention and inhibition in adult males.¹⁰ Attentional inhibition refers to the ability to suppress irrelevant information in order to concentrate on more pertinent information in the environment. Little is known about the relationship between sleep and attentional inhibition in children. This investigation aimed to assess the relationship between chronic sleep and cognitive and physical health in preadolescent children ages 8 to 9 years. The hypothesis is that hours of sleep received per night will correlate positively with aerobic fitness levels, crystallized and fluid intelligence, and attentional inhibition abilities, as well as correlate negatively with BMI and fat mass (i.e., visceral adipose tissue (VAT)).

■ Methods

A total of 483 children ages 8-9 years old were recruited to participate in this study, of which a subsample ($n=401$) was included in this exploratory analysis. Demographic information can be found in Table 1.

To collect the necessary information to understand the relationships between sleep, fitness, BMI, intelligence, and cognition, a parent of each participant completed a basic questionnaire, which included one question pertaining to chronic sleep behavior: "How much sleep does your child

regularly?” Answers were given in multiple choice format, with options of “under 5,” “5-6,” “6-7,” “7-8,” “8-9,” “9-10,” and “more than 10.” For the purpose of this investigation, answers were rounded down, with the assumption that participants tend to overestimate sleep to satisfy the researcher. For example, if the “8-9 hours of sleep” option was selected, the variable of “8” was utilized (see Figure 1). A limitation of the study was that the questionnaire’s multiple choice options did not go beyond “more than 10” hours of sleep per night, indicated with the variable of “10” on all figures.

Table 1: Participant Demographics.

	Mean ± SE
N	401, 211 females
Age	8.77 ± 0.03
VO ₂ max (ml/kg/min)	39.81 ± 0.37
BMI (kg/m ²)	19.10 ± 0.21
IQ (Standard Score)	109.67 ± 0.66
Sleep (average hrs./ night)	8.29 ± 0.05

Figure 1

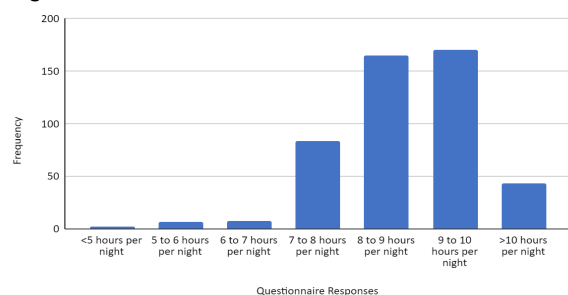


Figure 1: Average hours of sleep per night depicting the participants’ responses to the question “How much sleep does your child get regularly?” The majority of participants indicate receiving 8-10 hours of sleep per night regularly.

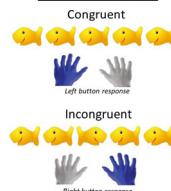
Aerobic fitness was measured using a maximal oxygen consumption test (VO₂ max, ml/kg/min).¹¹ Participants walked or ran on a treadmill at constant speed and incline increasing until they reached volitional exhaustion. Cardiorespiratory fitness was measured as a VO₂peak.¹² Participants’ oxygen consumption was measured using an indirect calorimetry system (ParvoMedics TrueMax 2400). Participants walked/ran at a constant speed on a treadmill with incline increases of 2.5 % every 2 minutes until volitional exhaustion. Participants wore a heart rate (HR) monitor throughout the test to calculate heart rate max. Ratings of perceived exertion (RPE) were assessed every 2 min using the children’s OMNI Scale.^{13,14} (3) respiratory exchange ratio (RER ≥ 1.0),¹⁵ and/or (4) RPE ≥ 8.14 VO₂peak percentile (VO₂peak%) was then determined based on the participants’ sex, age and relative score from normative data.¹⁶ Body composition was examined as BMI and VAT mass. BMI was calculated by dividing body mass (kg) by height (m) squared. Whole body and regional soft tissue were measured by dual energy x-ray absorptiometry (DXA) using a Hologic Discovery bone densitometer (software version 12.7.3; Hologic, Bedford, MA). VAT was estimated by using an automated algorithm that models subcutaneous abdominal adipose tissue (SAAT) at the fourth lumbar vertebra and subtracts it from the regional abdominal adipose tissue.¹⁷

See Drollette *et al.*¹⁸ for further details regarding fitness and body composition assessments.

Intelligence IQ was measured using scores on the Woodcock-Johnson Tests of Cognitive Abilities¹⁹ or the Kaufman Brief Intelligence Test (KBIT),²⁰ both of which are IQ tests for children that include measures of crystallized and fluid intelligence. Each IQ test was standardized on the same scale (mean = 100 ± 15). Academic performance was measured using the Wide Range Achievement Testing (WRAT)²¹ or the Kaufman Tests of Educational Abilities (KTEA), which included math, reading, and spelling. Both the WRAT and KTEA were based on a standard score with a mean of 100 and a standard deviation of 15.

Attentional inhibition was measured in this study using a modified flanker task, which collected measures of reaction time and accuracy²² and was completed on a computer using a response pad. In the flanker task, an array of five fish appeared on a screen (see Figure 2), and the participant was asked to respond to the direction of the central (target) fish. For congruent trials, all five fish faced the same direction. For incongruent trials, the four outer fish (also referred to as flanker fish) faced in the opposite direction of the central fish, requiring the participant to use attentional inhibition to gate out the flanker fish and respond correctly to the direction of the target fish. Each participant completed 150 trials of the flanker task in two blocks of 75 trials.

Modified Flanker Task



All statistical analyses were performed with SPSS 25 (IBM, Armonk, New York) using a family-wise alpha threshold for all tests set at $p=0.05$. Pearson correlations assessed bivariate relationships between sleep and relevant outcome measures.

Figure 2: Example of congruent and incongruent flanker task trials.

■ Results and Discussion

As seen in Table 2, a strong correlation emerged between chronic sleep and aerobic fitness (i.e., relative VO₂ max; $r=0.15$; $p\leq 0.001$; see Figure 3). In addition, there were negative correlations between chronic sleep and BMI ($r=-0.15$; $p\leq 0.001$; see Figure 4), as well as VAT ($r=-0.12$; $p=0.02$; see Figure 5).

Table 2: Pearson Correlation Value Comparison of Measures with Chronic Sleep: As shown, nearly all relationships between sleep and cognitive and physical health measures were significant at the alpha threshold for all tests set at $p=0.05$.

	Pearson Correlation (r)	Significance (p)
Relative VO ₂ Max	0.15*	≤0.001
Body Mass Index	-0.15*	≤0.001
Visceral Adipose Tissue	-0.12*	0.02
Reading Scores (WRAT)	0.17*	≤0.001
Math Scores (WRAT)	0.12*	0.01
Spelling Score (WRAT)	0.09	>0.05
Crystallized Intelligence (WJ), (KBIT)	0.18*	≤0.001
Fluid Intelligence (WJ), (KBIT)	0.16*	≤0.001
Congruent Reaction Time (Flanker)	0.13*	0.01
Congruent Accuracy (Flanker)	0.11*	0.03
Incongruent Reaction Time (Flanker)	0.13*	0.01
Incongruent Accuracy (Flanker)	0.16*	≤0.001

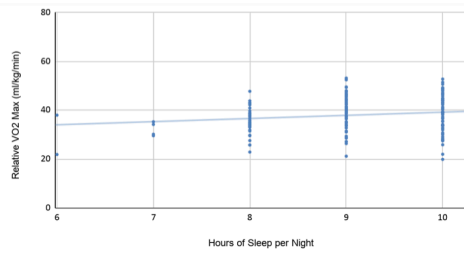


Figure 3: As shown, there is a positive correlation between average hours of sleep per night and VO₂ max performance, indicating a beneficial relationship between chronic sleep and aerobic fitness.

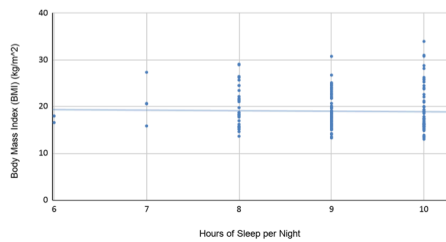


Figure 4: As shown, there is a negative correlation between average hours of sleep per night and BMI, indicating a beneficial relationship between chronic sleep and body composition.

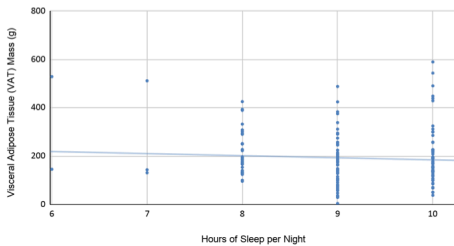


Figure 5: As shown, there is a negative correlation between average hours of sleep per night and VAT mass, indicating a beneficial relationship between chronic sleep and reduced fat mass.

Relative to the intelligence measures (see Figure 6), chronic sleep correlated with crystallized intelligence scores ($r=0.18$; $p \leq 0.001$). Fluid intelligence scores also correlated with chronic sleep ($r=0.16$; $p \leq 0.001$). Crystallized intelligence has a stronger correlation with chronic sleep, relative to fluid intelligence. For academic achievement, both reading ($r=0.17$; $p \leq 0.001$; see Figure 7), and math ($r=0.12$; $p=0.01$; see Figure 8), correlated with chronic sleep, while spelling was unrelated ($r=0.09$; $p > 0.05$; see Figure 9).

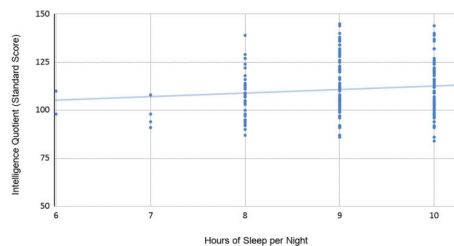


Figure 6: As shown, there is a positive correlation between average hours of sleep per night and IQ, indicating a beneficial relationship between chronic sleep and cognition.

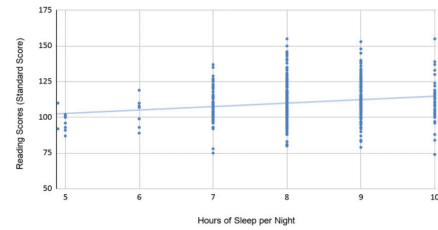


Figure 7: As shown, there is a positive correlation between average hours of sleep per night and reading scores, indicating a beneficial relationship between chronic sleep and academic achievement.

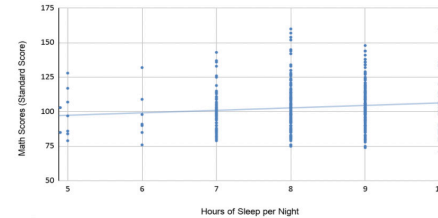


Figure 8: As shown, there is a positive correlation between average hours of sleep per night and math scores, indicating a beneficial relationship between chronic sleep and academic achievement.

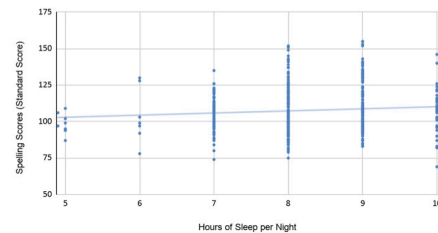


Figure 9: There is no significant correlation between average hours of sleep per night and spelling scores on an academic achievement test.

Finally, children who received more chronic sleep performed better on the flanker task. Congruent flanker trials correlated with chronic sleep, for both accuracy ($r=0.11$; $p=0.03$; see Figure 10), and reaction time ($r=0.13$; $p=0.01$; see Figure 11). Incongruent trials also correlated with sleep, for both accuracy ($r=0.16$; $p \leq 0.001$; see Figure 12), and reaction time ($r=0.13$; $p=0.01$; see Figure 13).

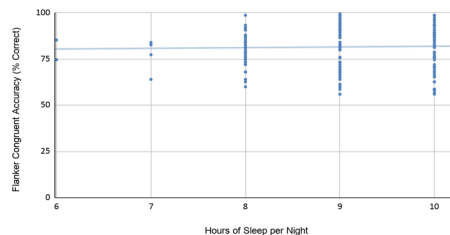


Figure 10: As shown, there is a positive correlation between average hours of sleep per night and accuracy on the congruent flanker task, indicating a beneficial relationship between chronic sleep and cognition.

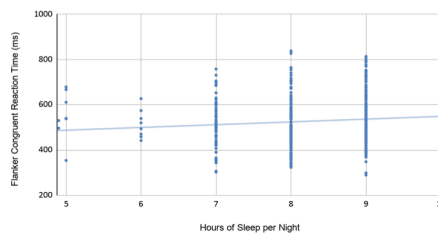


Figure 11: As shown, there is a positive correlation between average hours of sleep per night and reaction time on the congruent flanker task, indicating a beneficial relationship between chronic sleep and cognition.

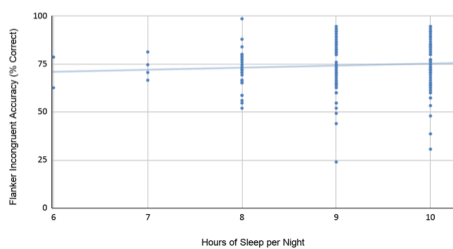


Figure 12: As shown, there is a positive correlation between average hours of sleep per night and accuracy on the incongruent flanker task, indicating a beneficial relationship between chronic sleep and cognition.

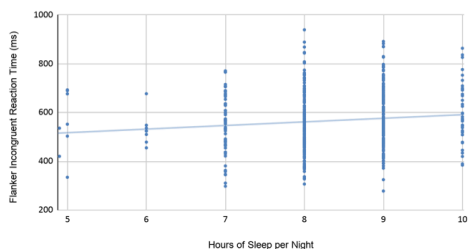


Figure 13: As shown, there is a positive correlation between average hours of sleep per night and reaction time on the incongruent flanker task, indicating a beneficial relationship between chronic sleep and cognition.

The findings demonstrate that chronically adequate amounts of sleep have a positive correlation with physical fitness, body composition, intelligence, and cognitive ability. As for physical fitness, adequate amounts of sleep correlated positively with higher levels of fitness, as demonstrated via correlations with higher VO_2 max values. In addition, findings from our study highlight that chronic amounts of sleep correlated with measures of body composition, as demonstrated via correlations with low BMI, and low VAT mass.

Chronically healthy amounts of sleep correlate positively with crystallized and fluid intelligence, as well as performance on reading and math achievement tests. This suggests that chronic sleep may be beneficial for learning abilities as well as innate intelligence. In contrast, spelling was not correlated with sleep.

A relationship between chronic sleep and attentional inhibition are seen clearly in both congruent and incongruent trials of the flanker task. The correlation between sleep and performance is especially prevalent in the incongruent trials. The incongruent trials are those that require greater amounts of attentional inhibition, as the participant must actively inhibit the flanking stimuli to focus on the central (target) stimulus. The participants who slept more on a regular basis performed better on the most difficult trials. Taken together, these findings suggest that with more sleep, children may be utilizing a strategy whereby they de-emphasize their reaction time in an effort to produce more accurate responses.

Almost all correlations show a steady increase in performance from 4.9 hours of sleep to peak performance at about 8 or 9 hours of sleep per night. Thus, the data suggests that 8-9 hours of sleep may be optimal for cognitive and physical performance. There are a few potential causes for this observed trend, one of which being that the sample used in this study did not contain many participants getting 10 or more hours of sleep per night. A second limitation of the study was that on

the questionnaire used for data collection, the greatest possible amount of sleep that participants could indicate was “>10 hours of sleep per night.” Participants who provided this answer could be achieving any amount beyond 10 hours of sleep per night, including into the oversleeping range. The National Sleep Foundation identifies oversleeping as more than 12 hours of sleep per night for children ages 6-13 years, therefore some members of the “>10 hours of sleep per night” group could be in this category of oversleeping.²³ Oversleeping is implicated in type II diabetes, obesity, and depression, among other diseases and disorders.²⁴ These external factors could be related to their decline in cognitive and physical performance.

Existing research suggests that sleep plays a positive role in the cognitive development and physical growth of infants and children.²⁵ These findings replicate and extend findings from a recent meta-analysis and systematic review that found a significant relationship between objectively measured sleep and cognitive function, particularly for verbal IQ.²⁶ Additionally, existing studies on sleep duration and consistent chronic sleep suggest that more sleep leads to better cognitive performance.²⁷ These conclusions, in conjunction with our findings, suggest that the benefits of sleep are seen in various populations and can be repeated in future studies.

Based on these correlations, there is evidence that sleep is beneficial for preadolescent children in terms of both cognitive and physical health. Children who slept more on a regular basis consistently performed better on academic and cognitive tasks and demonstrated a higher level of physical and aerobic fitness than those who received fewer hours of sleep. This suggests that sleep should be prioritized in childhood to improve cognitive and physical health.

The mechanisms linking sleep to physical and cognitive health in children are poorly understood and still being investigated. However, most data links sleep restriction to an increase in energy intake, which may increase the risk of obesity.⁴ In terms of cognition, sleep has been shown to beneficially impact memory consolidation and learning.²⁸ Longer sleep duration is associated with larger volume in various brain regions such as the prefrontal cortex, which is also important for cognitive function. Specifically, sleep has been shown to mediate the relationship between brain structure and cognition.²⁹

■ Conclusion

In conclusion, consistently healthy amounts of sleep have a beneficial relationship with physical (i.e., aerobic fitness, body composition) and cognitive (i.e., intelligence, attentional inhibition, and academic performance) health. Future research should extend these results using additional, more sophisticated assessments of sleep behaviors (including sleep beyond 10 hours a night), such as accelerometers, with these physical and cognitive health outcomes. Regardless, these findings provide evidence to support sleep as a predictor of childhood health and scholastic performance.

■ Acknowledgements

I acknowledge the support of my mentors, Jennifer Watrous, Lauren Raine, and Charles Hillman for making this project possible.

■ References

1. August 14, (2020). What Happens When You Sleep? *National Sleep Foundation*. <https://www.sleepfoundation.org/articles/what-happens-when-you-sleep>.
2. Paruthi, S., Brooks, L.J., D'Ambrosio, C., Hall, W.A., Kotagal, S., Lloyd, R.M., Malow, B.A., Maski, K., Nichols, C., Quan, S.F., Rosen, C.L., Troester, M.M., Wise, M.S. (2016). Recommended amount of sleep for pediatric populations: a consensus statement of the American Academy of Sleep Medicine. *J Clin Sleep Med*.
3. Bonuck, K., Grant, R. (2012). Sleep problems and early developmental delay: implications for early intervention programs. *Intellectual and Developmental Disabilities*, 50(1), 41-52.
4. Quist, J.S., Sjödin, A., Chaput, J.P., Hjorth, M.F. (October 2016). Sleep and cardiometabolic risk in children and adolescents. *Sleep Medicine Reviews*. <https://www.sciencedirect.com/science/article/abs/pii/S1087079215001203>.
5. Grandner, M.A., Schopfer, E.A., Sands-Lincoln, M., Jackson, N., Malhotra, A. (May 18, 2016). The Relationship between Sleep Duration and Body Mass Index Depends on Age. *US National Library of Medicine*. <https://www.ncbi.nlm.nih.gov/pmc/articles/PMC4700549/>
6. Shang, X., Li, Y., Xu, H., Zhang, Q., Liu, A., Ma, G. (2020). The Clustering of Low Diet Quality, Low Physical Fitness, and Unhealthy Sleep Pattern and Its Association with Changes in Cardiometabolic Risk Factors in Children. *Nutrients*, 12(2), 591.
7. Dworak, M., Wiater, A., Alfer, D., Stephan, E., Hollmann, W., Strüder, H. K. (2008). Increased slow wave sleep and reduced stage 2 sleep in children depending on exercise intensity. *Sleep medicine*, 9(3), 266-272.
8. Dunster, G.P., de la Iglesia, L., Ben-Hamo, M., Nave, C., Fleischer, J.G., Panda, S., de la Iglesia, H.O. (December 12, 2018). Sleepmore in Seattle: Later school start times are associated with more sleep and better performance in high school students. *Science Advances*.
9. Brown, R.E. (2016). Hebb and Cattell: The Genesis of the Theory of Fluid and Crystallized Intelligence. *Frontiers in Human Neuroscience*. <https://www.ncbi.nlm.nih.gov/pmc/articles/PMC5156710/>
10. Chern-Pin Chua, E., Fang, E., Gooley, J.J. (2017). Effects of total sleep deprivation on divided attention performance. *US National Library of Medicine*. <https://www.ncbi.nlm.nih.gov/pmc/articles/PMC5699793/>
11. Khan, N.A., Raine, L.B., Drollette, E.S., Scudder, M.R., Pontifex, M.B., Castelli, D.M., Donovan, S.M., Evans, E.M., Hillman, C.H. (March 31, 2014). Impact of the FITKids Physical Activity Intervention on Adiposity in Prepubertal Children. *Pediatrics*. http://labs.kch.illinois.edu/Research/Labs/neurocognitive-kinesiology/files/Articles/Khan_2014_ImpactOfTheFITKids.pdf
12. Winsley, R.J., Armstrong, N., Middlebrooke, A.R., Ramos-Ibanez, N., Williams, C.A. (2006). Aerobic fitness and visceral adipose tissue in children. *Acta Paediatr*. 95: 1435-1438.
13. Utter, A.C., Robertson, R.J., Nieman, D.C., Kang, J. (January 2002). Children's OMNI Scale of Perceived Exertion: walking/running evaluation. *National Library of Medicine*. <https://pubmed.ncbi.nlm.nih.gov/11782659/>
14. Pescatello, L.S. (2014). ACSM's guidelines for exercise testing and prescription. Wolters Kluwer/Lippincott Williams & Wilkins Health. *American College of Sports Medicine*. 456 p.
15. Bar-Or, O. (1983). Pediatric Sports Medicine for the Practitioner. *Comprehensive Manuals in Pediatrics*.
16. Shvartz, E., Reibold, R.C. (January 1990). Aerobic fitness norms for males and females aged 6 to 75 years: a review. *National Library of Medicine*. <https://pubmed.ncbi.nlm.nih.gov/2405832/>
17. Micklesfield, L.K., Goedecke, J.H., Punyanitya, M., Wilson, K.E., Kelly, T.L. (2012). Dual-Energy X-Ray Performs as Well as Clinical Computed Tomography for the Measurement of Visceral Fat. *Obesity*. 2012;20(5):1109-14.
18. Drollette, E.S., Pontifex, M.B., Raine, L.B., Scudder, M.R., Moore, R.D., Kao, S., Westfall, D.R., Wu, C., Kamijo, K., Castelli, D.M., Khan, N.A., Kramer, A.F., Hillman, C.H. (October 4, 2017). Effects of the FITKids physical activity randomized controlled trial on conflict monitoring in youth. <https://onlinelibrary.wiley.com/doi/epdf/10.1111/psyp.13017>
19. Hasinger, E. (2020). Woodcock-Johnson Test Guide. <https://www.tests.com/Woodcock-Johnson-Testing>
20. Kaufman, A.S., Kaufman, N.L. Kaufman Brief Intelligence Test, Second Edition. <https://www.wpspublish.com/kbit-2-kaufman-brief-intelligence-test-second-edition>
21. Wilkinson, G.S., Robertson, G.J. Wide Range Achievement Test Fifth Edition. Pearson Assessments. <https://www.pearsonassessments.com/store/usassessments/en/Store/Professional-Assessments/Academic-Learning/Brief/Wide-Range-Achievement-Test-%7C-Fifth-Edition/p/100001954.htm>
22. Eriksen, B.A., Eriksen, C.W. (1974). Effects of noise letters upon identification of a target letter in a non-search task. *Perception and Psychophysics*, 16, 143-149.
23. Hirshkowitz, M., Whiton, K., Albert, S.M., Alessi, C., Bruni, O., DonCarlos, L., Hazen, N., Herman, J., Katz, E.S., Kheirandish-Gozal, L., Neubauer, D.N., O'Donnell, A.E., Ohayon, M., Peever, J., Rawding, R., Sachdeva, R.C., Setters, B., Vitiello, M.V., Ware, J.C., Hillard, P.J. (January 14, 2015). National Sleep Foundation's sleep time duration recommendations: methodology and results summary. *National Sleep Foundation*. [https://www.sleephealthjournal.org/article/S2352-7218\(15\)00015-7/fulltext](https://www.sleephealthjournal.org/article/S2352-7218(15)00015-7/fulltext)
24. Oversleeping: Bad for Your Health? *Johns Hopkins Medicine*. <https://www.hopkinsmedicine.org/health/wellness-and-prevention/oversleeping-bad-for-your-health>
25. Tham, E.K.H., Schneider, N., Broekman, B.F.P. (May 15, 2017). Infant sleep and its relation with cognition and growth: a narrative review. *US Library of Medicine*. <https://www.ncbi.nlm.nih.gov/pmc/articles/PMC5440010/>
26. Short, M.A., Blunden, S., Rigney, G., Matricciana, L., Coussens, S., Reynolds, C.M., Galland, B. (June 2018). Cognition and objectively measured sleep duration in children: a systematic review and meta-analysis. *Sleep Health*. <https://www.sciencedirect.com/science/article/abs/pii/S2352721818300135>
27. Mantua, J., Simonelli, G. (March, 2019). Sleep duration and cognition: is there an ideal amount? *Oxford Academic*. <https://academic.oup.com/sleep/article/42/3/zsz010/5288680>
28. Ashworth, A., Hill, C.M., Karmiloff-Smith, A., Dimitriou, D. (December 16, 2013). Sleep enhances memory consolidation in children. *Journal of Sleep Research*. <https://onlinelibrary.wiley.com/doi/full/10.1111/jsr.12119>
29. Cheng, W., Rolls, E., Gong, W., Du, J., Zhang, J., Zhang, X., Li, F., Feng, J. (February 3, 2020). Sleep duration, brain structure, and psychiatric and cognitive problems in children. *Molecular Psychiatry*. <https://pubmed.ncbi.nlm.nih.gov/32015467/>

■ Author

Catherine Nemeskal is a senior at Danvers High School in Danvers, Massachusetts. She will be attending Dartmouth College where she plans to pursue a double major in neuroscience and economics.

The Significance and Evolution of the Stellar Initial Mass Function

Ethan Kuperman

Horace Greeley High School, 70 Roaring Brook Road, Chappaqua, New York, 10514, USA; ethanckuperman@gmail.com

ABSTRACT: It remains undisputed in the current star formation paradigm that the structure and evolution of a star are primarily dependent on its mass. The initial mass function (IMF), the probability distribution function of stellar masses at birth, is consequently a vital function to stellar astrophysics. Since its creation in 1955 by Edwin Salpeter, the IMF has undergone much study and modification, but a definite understanding of the origin and form of the stellar IMF remains elusive. This review will consider the contributions of a multitude of astrophysicists to the study of the IMF in a comprehensive overview and pose several avenues for future research.

KEYWORDS: Physics and Astronomy; Astronomy and Cosmology; Theory; Star Formation; Initial Mass Function.

■ Introduction

Stars have long fascinated humans on Earth. Luminous spheroids of plasma formed from vast clouds of cosmic dust and gas, they captivate us as they shine high on the celestial sphere. We have gone a long way since the first study of stars by Galileo Galilei in 1610, using ever-developing technologies and challenging ourselves to advance the cogent components of theories for star formation—the most integral of which, arguably, is the initial mass function. Stars of varying masses form from interstellar gas and dust, and it is necessary to interpret these masses to understand the characteristics of foreign galaxies.

The IMF, which is based on the initial mass of a star, is a probability distribution which can be used to describe the distribution of stellar masses at birth. The distribution function, fit to a histogram indicating the frequency of stars for mass intervals ranging from m to $m+\Delta m$, is an operational construct defined as either a power law (also known as the Pareto distribution) or a log-normal distribution, the two top contenders for a best-fitting function. Each function has vastly different implications; a power law distributes masses such that any distribution from a given sample will be the same regardless of the size of its progenitor cloud. Contrastingly, the log-normal form is a result of multiplicative processes and implies that several factors contribute to the outcome.¹ As evident from the conclusions drawn intrinsically by each form, the IMF reveals information about the star formation rate of the universe (SFR) and the physical processes which cause star formation and result in a variety of stellar properties by designating the fraction of stars at different masses.² Beyond just measuring star counts and suggesting properties, the IMF is also useful in inferring galaxy characteristics and is often taken into consideration for star formation modeling.³

Past reviews of the IMF and the functional forms that define it cover in great depth its importance and the general course of development, but these reviews are often quite complex by nature. This review aims to discuss the significance and evolution

of the IMF in a clear and succinct manner to highlight its influence in the field of astrophysics. Furthermore, complications with current methods of inferring and representing the IMF and future directions will be established.

■ Discussion

Salpeter and The First IMF:

Since its founding by Austrian astrophysicist Edwin Salpeter, the initial mass function has established itself as a vital component of modern astrophysics. The stellar IMF is closely tied to the star formation rate (SFR), and both are necessary for studies of observed properties and chemical abundances of foreign galaxies. Colors and spectra of groups of stars primarily depend on the SFR and stellar IMF, which are used to interpret various properties based on mass. The publication of Salpeter's 1955 paper, *The Luminosity Function and Stellar Evolution*, gave the definition of the first stellar IMF of the canonical shape $\xi(m)=dN/dm$, with dN representing the number of locally formed stars with masses ranging from m to $m+\Delta m$. The Salpeter IMF is also represented as $\xi(\log m)\approx A(m/M_{\odot})^{-x}$, a relation with a suggested index of $x = 1.35$, limited to the solar neighborhood where $\xi(m)$ is a smooth function of the input m . Salpeter's IMF described the mass distribution for a population of stars of masses between 0.4 and 10 solar masses at birth on the main sequence, but grew uncertain as inputs fell below one solar mass as it is difficult to detect the dim, overlapping population of low-mass stars. As observational equipment and techniques improved, the Salpeter IMF was eventually considered to flatten below one solar mass.⁴ Similarly, massive stars are impossible to fully account for in any observationally determined IMF due to their short lifetimes.

Due to the natural phenomenon of stars moving from the main sequence and becoming red giants and eventually white dwarfs, black holes, and neutron stars as they reach the end of their lifetimes, they must be drawn back to their original positions on the main sequence to infer the IMF. The IMF is a restricted version of a distribution of present-day masses

of stars (the Present-Day Mass Function or PDMF) based on the Luminosity Function, determined by the parameterized luminosity-mass relation $L=M^x$ where x ranges from 1 to 6 and is commonly 3.5 for main-sequence stars. By using the PDMF as a basis for IMF development, only minor constraints must be made to develop the related function for initial mass.

Essentially, the IMF is represented by a mass distribution of stars in a selected area and time, created by designating mass ranges to a continuous set of histogram bins (Figure 1). A time interval can be designated for the purpose of understanding the birth of a sample of stars or for a region over its lifetime. This distribution can signify multiple important properties based on an inference of characteristics due to mass, including the luminosities and lifetimes of stars as well as the contingent energy feedback due to supernovae, which can assist researchers in forming a general picture of the region being studied. When graphed, the power law form of the IMF is commonly placed upon log-log axes such that the intrinsic curve is eliminated, and the function has a linear shape despite its exponential nature on normalized axes.

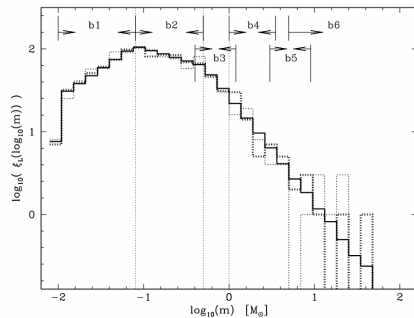


Figure 1: A histogram IMF for 10^6 stars, with thick and thin dotted indicators for two versions of 10^3 star plots. Vertical dotted lines indicate masses where the power law exponent changes, suggesting variation. From Kroupa, 2001.¹²

The Development of the gIMF and cIMF by Integration of IMFs:

Just as star formation exists on scales both small and large, IMFs exist for every range of star forming regions. The galaxy-wide IMF (gIMF) is the summation of IMFs over a galaxy, synonymous with the probability distribution function over said galaxy. In the integrated galaxy theory (IGIMF) theory developed by Pavel Kroupa, the gIMF is calculated by integration over all clusters formed over an epoch of 10 Myr within the galaxy in which the gIMF is applicable.

As mentioned above, but discussed in more depth presently, the shape of the gIMF does not necessarily match the shape of the IMF because low-mass embedded star clusters are implied not to have massive stars.⁵ Specifically, it is insinuated that the gIMF has a steep exponent greater than or equal to 2.8 and does not follow the Salpeter power-law.⁶ The gIMF, however, is similar to the IMF in a galaxy with a star formation rate of approximately one solar mass per year and solar metallicity. The gIMF proposed by the IGIMF varies with the star formation rate and metallicity of its galaxy because, on a smaller scale, the IMF varies among stars formed from their progenitor molecular clouds. Recently, an

important forward step has been taken in the study of the gIMF—the recently developed Python module, GalIMF, is able to calculate the gIMF following the IGIMF theory based on the galaxy-wide star formation rate and metallicity. By synthesizing stellar populations for galaxies, the GalIMF module drives the construction of galactic star formation history empirically.⁷

The cosmic IMF (cIMF, not to be confused with the CIMF, the IMF for star clusters) is similarly the integration of all smaller-scale IMFs. Presently, no definite procedure exists to define the cIMF in entirety, but it is implied that star populations within galaxies must be self-consistent to obtain a cIMF.⁸ This is simply due to the problematic nature of widespread variation if it is confirmed to exist (Figure 2).

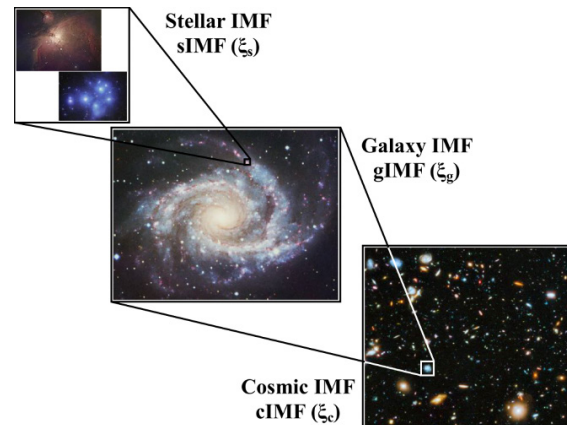


Figure 2: A diagram of regions with theoretically calculable IMFs ranging from the smallest scale (stellar) to the largest (cosmic). Variation within the stellar IMF will affect the universality of the gIMF and, consequently, the same will occur from the gIMF to the cIMF. From Hopkins, 2020.⁴

Inferring the IMF:

The IMF cannot be entirely derived from observations nor is it a singular equation; rather, it is purely a statistical function which varies based on mass input. Therefore, it is an operational construct to characterize galaxies and star formation. In actuality, the clusters necessary for a complete observation of the IMF are either too distant or not massive enough to be observed, with ejections and supernovae further complicating full-scale inferences.⁹ The output varies based on the inferring method used and the characteristics of the region to which it is applied as well as error in measurement. Galaxies forming stars at a rate higher than average tend to have an abundance of massive stars, indicated by a peak further to the right on the x-axis of an IMF histogram.¹⁰ Oppositely, passive galaxies which tend to have excess low-mass stars have a peak further to the left on the x-axis.¹¹ Many ways to infer the IMF exist, all of which have differing methodologies and useful applications. The most essential of these methods will be discussed presently.

The photometric approach determines an IMF through broadband photometry, deriving masses from the mass-luminosity relationship of stars. This method, while popular for usage for individual stars and systems, is uncertain for massive stars.

The spectroscopic approach, a solution to achieving higher accuracy for massive stars, places coordinates on a Hertzsprung-Russell diagram for an x-axis of temperature and spectral class and a y-axis of luminosity, often measured in Kelvin and solar luminosities respectively. An IMF can be inferred through analyzing the dependence of a star's evolutionary properties and therefore stage on the Hertzsprung-Russell diagram on its initial mass.

The integrated light approach infers an IMF and SFR from the strength of H α lines, the brightest emission lines in the visible range, and several colors which determine the characteristics of the region being studied.¹²

The chemical abundance approach focuses on the outcome of supernovae, which enriches the stellar populations influenced by said supernovae and can be used to trace IMFs based on metallicity.¹³

Notably, inferring the IMF for a star cluster is far easier than for field stars due to the nature of stars being born in one cluster at the same time, causing a simpler process of constructing a histogram from their masses at birth.

The Continuous Development of the Salpeter IMF and its Universality:

Whether the IMF is universal or variable has persisted as an essential question for astrophysicists. To better understand the universality of the IMF, various researchers have investigated alternate methods to develop the function. Such efforts included the study of stellar nucleosynthesis and the resulting chemical evolution and UV luminosities which are now more routinely used to trace the intermediate-mass stellar population.¹⁴ In a relatively recent development, the most successful of these alternate methods is gleaned from gravitational lensing, which led to the creation of the IMF mismatch $\alpha \equiv MLDE_{in}/MSPSE_{in}$, the ratio of stellar mass determined by gravitational lensing to that determined by stellar population synthesis models. This ratio agreed with the Salpeter IMF in a reinforcement of its validity.¹⁵ A key result of the application of gravitational lensing to the IMF is the implication that the IMF mismatch increases with the velocity dispersion of a galaxy and implies a non-universal IMF.

Additionally, and also in support of a variable IMF, the application of parameter correction from systematic bias led to discovery of some variation which suggested that the IMF was radically different among the ancient star population.¹⁶ And, as an integration of varying IMFs, the Milky Way gIMF implies both spatial and temporal variability. On the strength of these studies, researchers are presently advocating for a non-universal IMF and, consequently, gIMF as the basis for further studies. This is a step in the direction of a substantial paradigm shift, as the IMF has previously been considered to be universal.

The validity of the Salpeter IMF has also been considered by astrophysicists, as the field of stellar astrophysics has grown vastly since its proposal. For instance, Salpeter's suggestion for the usage of the index 1.35 was disputed due to the fact that the Salpeter IMF was based on the accepted Galaxy disk age at the time, 6 Gyr, which we now know to be approximately 12 Gyr. The index was corrected and instead

suggested to be 1.05.¹⁷ This correction was itself disputed for stars larger than eight solar masses due to a prior observational effort using spectroscopy where 1.35 was determined to be the correct value for massive stars.¹⁸ Presently, the usage of a log-normal functional form and (more commonly) a parameter-based power-law offer irrefutably more accurate IMFs.

Contemporary Log-Normal and Power-Law IMF Forms:

The result of the many aforementioned developments is the surfacing of major advances in understanding and developing new forms of the IMF (Figure 3). During a period where the IMF was considered log-normal-like, the following function form was created by Glenn Miller and John Scalo.¹⁹

$$\log_{10} \xi(\log_{10} m) = A - \frac{1}{2} (\log_{10} \sigma)^2 \left(\log_{10} \frac{m}{m_0} \right)^2$$

Gilles Chabrier introduced another log-normal form which is modifiable with variable parameters applied to both individual stars and systems with masses less than one. Chabrier also restated the power-law form for masses greater than one.²⁰ The variables a, b, and c are used in this review for convenience. This form offered the first jump from Salpeter's original smooth function to a variable IMF.

$$\xi(m) = a \left(\frac{1}{\ln 10 m} \right) \exp \left[\frac{(-\log m - \log b)^2}{(2c^2)} \right]$$

For individual stars, a = 0.158, b = 0.08, and c = 0.69. For binary and multiple systems, a = 0.086, b = 0.22, and c = 0.57.

$$\xi(m) = km^{2.3 \pm 0.3}$$

Also intrinsic are Pavel Kroupa's piecewise parameters for mass ranges for the broken power-law form of the Salpeter IMF for the range m to m + Δm .^{21, 22} Prior to the introduction of this piecewise form, the IMF was a subject of much debate as the topic of universality versus variability grew in popularity. As evidence for variation emerged from improved methods of inferring the IMF, the need for more accurate parameters grew until the following were developed.

$$\xi(m) dm \propto m^\alpha dm$$

$$\xi(m) = 0.26m^{-0.3} \text{ for } 0.01 \leq m < 0.08$$

$$\xi(m) = 0.035m^{-1.3} \text{ for } 0.08 \leq m < 0.5$$

$$\xi(m) = 0.019m^{-2.3} \text{ for } 0.5 \leq m < \infty$$

These parameters offer the most accurate way of empirically estimating the power-law IMF; therefore, the Kroupa IMF is considered to be the standard modern function. Exponents are fairly uncertain at less than 0.5 solar masses. Kroupa's IMF is accepted because it is statistically corrected for systems too far to detect through spectroscopy and too close to be resolved. Prior IMFs which did not account for these errors typically overestimated masses of stars and therefore underestimated their densities. The IMF, previously assumed to be an invariant probability density function, is not commonly known as a parameterized distribution to which Kroupa's power law applies.²³

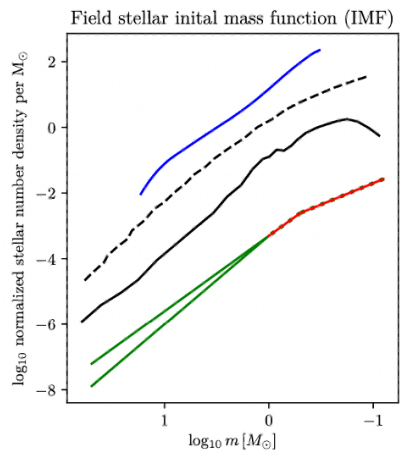


Figure 3: The Salpeter IMF in blue, the Scalo IMF in solid black, the Miller and Scalo IMF in dashed black, the Kroupa IMF in red, and the Scalo IMF as the bottom piece of the Kroupa IMF divergence in green. The Massey IMF for non-field stars, taken from spectroscopy, is the upper piece of the divergence (also in green). From Kroupa, 2019.²⁵

■ Conclusion

Today, the contributions of astrophysicists past and present leave a substantial variety of developments in IMF research, but there are also many unfilled gaps in the current paradigm. The creation of various forms has offered a diverse number of options for stellar astrophysicists, and growth in the usage of modules and data analysis code bodes well for future studies of the IMF. However, ambiguity is commonplace amongst histograms developed using varying methods for different sample sizes and regions, with upper bins often being dropped for low sample sizes, clearly indicating the incompleteness of census data available. As the IMF increasingly shows signs of being variable through census data, it is imperative to leave behind tendencies towards universality and consider parameterized forms and additional distributions.

The upcoming launch of the James Webb Space Telescope offers an incredible opportunity to further investigate star formation by exploring high-redshift systems forming stars, much like the Gaia photometry and parallax mission cataloged census data for over one billion stars in an unprecedentedly complete survey.²⁴ Astrophysicists are hopeful that the information acquired from such a study will offer constraints to the variation of the IMF as well as investigations into its universality.²⁵ A heightened understanding of turbulence and the structure of stars will also provide opportunities to advance the development of the IMF and other frontiers of stellar astrophysics.^{26, 27}

■ References

1. J. Kirkpatrick, C. Gelino, J. Faherty, A. Meisner, D. Caselden, A. Schneider, F. Marocco, A. Cayago, D. Smart, P. Eisenhardt, M. Kuchner, E. Wright, M. Cushing, K. Allers, D. Gagliuffi, A. Burgasser, J. Gagne, S. Logsdon, E. Martin, J. Ingalls, P. Lowrance, E. Abrahams, C. Aganze, R. Gerasimov, E. Gonzales, C. Hsu, N. Andersen, P. Beaulieu, G. Colin, C. Elachi, S. Goodman, L. Gramaize, L. Hamlet, J. Hong, A. Jonkeren, M. Khalil, D. Martin, W. Pendrill, B. Pumphrey, A. Rothermich, A. Sainio, A. Stenner, C. Tenner, M. Thevenot, N. Voloshin, J. Walla, Z. Wedraki. "The Field Substellar Mass Function Based on the Full-sky 20 pc Census of 525 L, T, and Y Dwarfs." *The Astrophysical Journal Supplement Series*. 235, 7 (2021).
2. T. Jerabkova. "Stellar populations in gravitationally bound systems." *The Repository of the University of Bonn*. (2020).
3. J. Scalo. "Five Years of IMF Variation: The Intermediate-Mass Stars." *The Initial Mass Function 50 Years Later*. 1, 23 (2005)
4. J. Scalo. "The Stellar Initial Mass Function." *Fundamentals of Cosmic Physics*. 11, 1 (1986).
5. Z. Yan, T. Jerabkova, P. Kroupa. "The optimally sampled galaxy-wide stellar initial mass function." *Astronomy and Astrophysics*. 607, A126 (2017).
6. P. Kroupa & C. Weidner. "Galactic-Field Initial Mass Function of Massive Stars." *Astrophysical Journal*. 598, 1076 (2003).
7. H. Haghi, V. Amiri, A. Zonoozi, I. Banik, P. Kroupa, M. Haslbauer. "The Star Formation History and Dynamics of the Ultra-diffuse Galaxy Dragonfly 44 in MOND and MOG." *Astrophysical Journal Letters*. 884, 25. (2019).
8. A. Hopkins, Presentation: "Measuring the Stellar Initial Mass Function." (2020.)
9. B. Elmegreen. "The Stellar Initial Mass Function in 2007: A Year for Discovering Variations." 4th Spitzer Science Center Conference. 4, 14 (2007).
10. M. Gunawardhana, A. Hopkins, R. Sharp, S. Brough, E. Taylor, J. Bland-Hawthorn, C. Maraston, R. Tuffs, C. Popescu, D. Wijesinghe, D. Jones, S. Croom, E. Sadler, S. Wilkins, S. Driver, J. Liske, P. Norberg, I. Baldry, S. Bamford, J. Loveday, J. Peacock, A. Robotham, D. Zucker, Q. Parker, C. Conselice, E. Cameron, C. Frenk, D. Hill, L. Kelvin, K. Kuijken, B. Madore, B. Nichol, H. Parkinson, K. Pimbblet, M. Prescott, W. Sutherland, D. Thomas, E. van Kampen. "Galaxy And Mass Assembly (GAMA): The star formation rate dependence of the stellar initial mass function." *Monthly Notices of the Royal Astronomical Society*. 415, 1647 (2011).
11. M. Cappellari, R. McDermid, K. Alatalo, L. Blitz, M. Bois, F. Bournaud, M. Bureau, A. Crocker, R. Davies, T. Davis, P. de Zeeuw, P. Duc, E. Emsellem, S. Khochfar, D. Krajnovic, H. Kuntschner, P. Lablanche, R. Morganti, T. Naab, T. Oosterloo, M. Sarzi, N. Scott, P. Serra, A. Weijmans, L. Young. "A systematic variation of the stellar initial mass function in early-type galaxies." *Nature*. 484, 485 (2012).
12. R. Kennicutt. "The rate of star formation in normal disk galaxies." *Astrophysical Journal*. 272, 54 (1983).
13. T. Gutcke & V. Springel. "Simulating a metallicity-dependent initial mass function: consequences for feedback and chemical abundances." *Monthly Notices of the Royal Astronomical Society*. 482, 118 (2018).
14. J. Audouze & B. Tinsley. "Chemical Evolution of Galaxies." *Astronomy and Astrophysics*. 14, A76 (1976).
15. T. Treu, M. Auger, L. Koopmans, R. Gavazzi, P. Marshall, A. Bolton. "The initial mass function of early-type galaxies." *Astrophysical Journal*. 709, 1195 (2009).
16. P. Kroupa. "On the variation of the initial mass function." *Monthly Notices of the Royal Astronomical Society*. 322, 231 (2001).
17. H. Zinnecker, "Up2010 Introduction: Massive Star Formation and the Upper End of the IMF." *Up2010 ASP Conference Series*. 440, 3 (2010).
18. P. Kroupa, C. Tout, G. Gilmore. "The distribution of low-mass stars in the Galactic disc." *Monthly Notices of the Royal Astronomical Society*. 262, 545 (1993)
19. G. Miller & J. Scalo. "The Initial Mass Function and Stellar Birthrate in the Solar Neighborhood." *Astrophysical Journal Supplement Series*. 41, 513 (1979).
20. G. Chabrier. "Galactic Stellar and Substellar Initial Mass Function."

-
- Publications of the Astronomical Society of the Pacific. 115, 763 (2003).
- 21.P. Kroupa. "The Initial Mass Function of Stars: Evidence for Uniformity in Variable Systems." *Science*. 295, 82 (2002).
- 22.M. Mac Low & R. Klessen. "Control of star formation by supersonic turbulence." *Reviews of Modern Physics*. 76, 125 (2004).
- 23.T. Jerabkova, A. Zonoozi, P. Kroupa, G. Beccari, Z. Yan, A. Vazdekis, Z. Zhang. "Impact of metallicity and star formation rate on the time-dependent, galaxy-wide stellar initial mass function." *Astronomy and Astrophysics*. 620, A39 (2018).
- 24.A. Sollima. "The stellar initial mass function of the solar neighbourhood revealed by Gaia." *Monthly Notices of the Royal Astronomical Society*. 489, 2377.
- 25.T. Jerabkova, P. Kroupa, J. Dabringhausen, M. Hilker, K. Bekki. "The formation of ultra compact dwarf galaxies and massive globular clusters." *Astronomy and Astrophysics*. 608, A53 (2017).
- 26.M. Mac Low. "From Gas to Stars Over Cosmic Time." *Science*. 340, 6140 (2013).
- 27.P. Kroupa & T. Jerabkova. "The Salpeter IMF and its descendants." *Nature*. 3, 482 (2019).

■ Author

Ethan Kuperman is a sophomore at Horace Greeley High School in Chappaqua, New York, studying astrophysics with a focus on star formation and evolution

A Study of The Effect Of Understorey Foliage Density On Bat Diversity and Abundance In The Guyana Shield Rainforest

Juliet I. M. Russell

Shrewsbury School, The Schools, Shrewsbury, Shropshire, SY3 7AT, England; jetty2001@icloud.com

ABSTRACT: This paper aims to look at the effect of understorey foliage density on bat populations, understanding of which may be crucial for conservation of the some 1,400 bat species around the world.¹ With risks posed to their habitats, such as logging and forest clearing,² understanding their interaction with forest foliage may be vital in protecting these species, as nesting sites and food sources are increasingly threatened by human activity.³ Although this study has not been able to show any significant relationship between foliage density and bat abundance, due to lack of data, the use of diversity indices and contingency tables suggests that certain bat species may rely on the presence of particular tree species for roosts and/or food sources. Across two unlogged sites, understorey mist nets were used to catch a total of 221 bats over a two-week period and 'touchpole' data was used as a proxy for foliage density. The results of this study, although inconclusive, suggest that the removal of understorey on bat populations may be greater than previously thought given that bat species dependence on certain tree species is perhaps indicated in this study.

KEYWORDS: Biology, Guyana, Conservation, Bats, Rainforest, Understorey density, Operation Wallacea.

■ Introduction

The Guyana Shield is an area of 270 million hectares of rainforest, spanning multiple South American countries. It is believed to be home to 148 species of bat;⁴ only a tiny proportion of over 3,000 vertebrate species⁵ believed to be found in the forest. Not only home to more common species, it offers habitat for numerous endemic species of both plants and animals and, for this reason, the Shield has become a popular region for conservation studies and projects. Operation Wallacea⁶ runs biodiversity and conservation management research expeditions across the world, recording changes in biodiversity and collecting data on a range of different species.

The author took part in a 2019 trip to the Guyana Shield with Operation Wallacea. The aim of this trip was to study and record the different levels of general biodiversity at two sites. These sites were sufficiently far apart (c.4hrs by bus) for their bat populations (the focus of this study) to be viewed as separate and distinct, with approximately the same level of human disturbance: no logging, sustainable or otherwise, was being carried out near either location. The data collected on the bat populations and vegetation has been used in this study to see if there is a correlation between forest understorey foliage density and bat abundance (and diversity). The hypothesis for this study: as density of understorey foliage increases, bat abundance will decrease. In addition, as foliage becomes denser, a different diversity of species may be found, with species adapted to cluttered forest environments found in greater numbers in areas of denser foliage. Bats are constrained by their wing morphology and echolocation call structure to certain types of habitat;⁷ some guilds of bat are adapted for flight in open areas, with long narrow wings, whereas others with short, broad wings are adapted to the more tightly packed foliage of

a denser understorey. As density of foliage increases, so does the number of obstacles in a bat's flight path and, although it has been shown that their echolocation systems are so accurate that they can avoid obstacles the width of telephone wires,⁸ the more obstacles present, the greater the chance of a potentially damaging/life threatening collision. Additionally, the more foliage, the more changes of direction are required, inevitably slowing a bat down, leading to a potential loss of prey.

For other animals such as birds, higher density understorey foliage may be beneficial since, although it slows them down, it also provides increased protection from predators, of which many are larger birds, which may struggle to pursue them through denser foliage. The thicker understorey also provides a protective layer through which it becomes harder for predators to see them from above and for many birds such as the humming birds and nectar feeders, the risks of predation, when they are relatively stationary whilst at a flower for example, might outweigh the benefits of a clearer flight path. However, for some species of bat, the risk of not finding food is just as dangerous as that of predation; for example, species of vampire bat, such as *Desmodus rotundus*, need to feed at least once every 48 hours or so, or they cannot survive.⁸ Due to their nocturnal habits, predation may be expected to be relatively low in comparison to that of small birds, as predators which rely on sight to catch their prey are limited by the low light intensity. Therefore, the most dangerous times for bats tend to be when they leave their roosts at dusk; a time when they are visible to all possible predators. At this point, perhaps a denser understorey may be beneficial, but after that point it may not. Dense foliage will act as an obstruction to echolocating of prey. If an insect is obscured by a leaf, the bat's high frequency, short wavelength emissions of sound would not detect it. The waves of sound

would bounce back to the bat off the leaf, not reaching the insect and the bat would not, therefore, necessarily be aware of its presence. Bats may suffer from ‘clutter’ echoes.⁹

The density of foliage may have different effects on bats depending on species and on what a particular area is used for by the bats (e.g. roosting or feeding). Bats aim to be as efficient as possible in all flying that they do and in order to conserve energy they need to come to a compromise on speed.⁸ As speed increases, two power inputs increase, but one decreases, and so optimum speeds can differ for different activities. When a bat is making a migratory or long flight, they want to fly fast to spend as little time in the air as possible. For this, they will want a clearer flight path without obstructions and deviations. Similarly, when flying from a roost to a foraging site, bats want to get there fast. If they are too late, they might miss the peak time for insects and lose possible foraging time or be in reach of predators for longer. Again, in this instance they might want a clear path to waste less feeding time. However, when feeding, a bat will want to maximise the time for which they can stay out foraging so therefore speed will most probably decrease. Increased density may then be less of a problem as bats will be swerving and diving to catch insects or find other food. Increased foliage density may also offer more places to find food. But, if too dense, foliage will still hinder a bat’s progress and affect its echolocation. Therefore, a slightly sparser area of forest might be preferable.

■ Results and Discussion

Bat Data:

Data collected showed absolute number, different species and locations of bats (see Table 1). The data indicates that the number of bats caught across the two locations did not differ hugely, but that the species diversity and species ratios were significantly different between Turtle Mountain and Rock Landing.

Table 1: Number of bats captured.

Date	Net Hours	# Bats captured	Bats/Hour	# Bats recaptured
Turtle Mountain				
08/07/2019	6.50	65	10.0	0
09/07/2019	6.00	11	1.8	0
10/07/2019	6.00	20	3.3	0
11/07/2019	6.00	14	2.3	1
12/07/2019	6.50	6	0.9	0
	31.00	116	3.7	1

Date	Net Hours	# Bats captured	Bats/Hour	# Bats recaptured
Rock Landing				
14/07/2019	6.00	42	7.0	1
15/07/2019	6.00	24	4.0	2
16/07/2019	3.50	7	2.0	0
17/07/2019	6.00	17	2.8	2
18/07/2019	4.50	15	3.3	0
	26.00	105	4.0	5

Table 2: Bat species data – Turtle Mountain.

Species	Location					TOTAL
	Turtle Mountain					
DATE	08/07/2019	09/07/2019	10/07/2019	11/07/2019	12/07/2019	
Net Hours	6.5	6.0	6.0	6.0	6.5	
<i>Artibeus gnomus</i>	1	-	-	1	-	2
<i>Artibeus lituratus</i>	4	-	2	1	1	8
<i>Artibeus obscurus</i>	2	-	-	-	-	2
<i>Artibeus planirostris</i>	39	11	13	6	3	72
<i>Carollia perspicillata</i>	9	-	1	2	1	13
<i>Chiroderma trinitatum</i>	-	-	-	-	-	-
<i>Desmodus rotundus</i>	-	-	-	-	-	-
<i>Glossophaga soricina</i>	-	-	-	1	-	1
<i>Glyphonycteris daviesi</i>	1	-	1	-	-	2
<i>Glyphonycteris sylvestris</i>	-	-	-	-	-	-
<i>Lionycteris spurrelli</i>	-	-	-	-	-	-
<i>Lophostoma silvicolum</i>	1	-	-	-	1	2
<i>Mesophylla macconnelli</i>	-	-	-	-	-	-
<i>Micronycteris megalotis</i>	-	-	1	-	-	1
<i>Micronycteris sp.</i>	-	-	-	-	-	-
<i>Mimon bennettii</i>	-	-	-	-	-	-
<i>Mimon crenulatum</i>	-	-	-	-	-	-
<i>Phylloderma stenops</i>	-	-	-	-	-	-
<i>Phyllotomus elongatus</i>	1	-	-	-	-	1
<i>Pteronotus parnellii</i>	5	-	1	2	-	8
<i>Rhinophylla pumilio</i>	1	-	1	-	-	2
<i>Tonatia saurophila</i>	-	-	-	-	-	-
<i>Trachops cirrhosis</i>	1	-	-	-	-	1
<i>Uroderma bilobatum</i>	-	-	-	1	-	1
<i>Vampyriscus bidens</i>	-	-	-	-	-	-
TOTAL	65	11	20	14	6	116

Table 3: Bat species data – Rock Landing.

Species	Location					TOTAL
	Rock Landing					
DATE	14/07/2019	15/07/2019	16/07/2019	17/07/2019	18/07/2019	
Net Hours	6.0	6.0	3.5	6.0	4.5	
<i>Artibeus gnomus</i>	-	1	-	-	1	2
<i>Artibeus lituratus</i>	-	-	-	-	1	1
<i>Artibeus obscurus</i>	7	5	-	3	2	17
<i>Artibeus planirostris</i>	6	4	2	5	3	20
<i>Carollia perspicillata</i>	11	1	1	4	1	18
<i>Chiroderma trinitatum</i>	1	-	-	-	-	1
<i>Desmodus rotundus</i>	-	-	-	-	1	1
<i>Glossophaga soricina</i>	1	-	-	-	1	2
<i>Glyphonycteris daviesi</i>	-	-	-	-	-	-
<i>Glyphonycteris sylvestris</i>	1	-	-	-	-	1
<i>Lionycteris spurrelli</i>	1	-	1	-	1	3
<i>Lophostoma silvicolum</i>	4	1	1	2	1	9
<i>Mesophylla macconnelli</i>	1	-	-	-	-	1
<i>Micronycteris megalotis</i>	-	-	-	-	-	-
<i>Micronycteris sp.</i>	-	1	-	-	-	1
<i>Mimon bennettii</i>	-	-	-	1	-	1
<i>Mimon crenulatum</i>	1	1	-	-	2	4
<i>Phylloderma stenops</i>	1	1	-	1	-	3
<i>Phyllotomus elongatus</i>	2	-	1	1	-	4
<i>Pteronotus parnellii</i>	1	3	1	-	1	6
<i>Rhinophylla pumilio</i>	-	-	-	-	-	-
<i>Tonatia saurophila</i>	1	-	-	-	-	1
<i>Trachops cirrhosis</i>	2	4	-	-	-	6
<i>Uroderma bilobatum</i>	1	-	-	-	-	1
<i>Vampyriscus bidens</i>	-	2	-	-	-	2
TOTAL	42	24	7	17	15	105

Table 4: Total bat numbers at each location over 5 nights.

Species	Location & # of Bats by Species	
	Turtle Mountain	Rock Landing
<i>Artibeus gnomus</i>	2	2
<i>Artibeus lituratus</i>	8	1
<i>Artibeus obscurus</i>	2	17
<i>Artibeus planirostris</i>	72	20
<i>Carollia perspicillata</i>	13	18
<i>Chiroderma trinitatum</i>	-	1
<i>Desmodus rotundus</i>	-	1
<i>Glossophaga soricina</i>	1	2
<i>Glyphonycteris daviesi</i>	2	-
<i>Glyphonycteris sylvestris</i>	-	1
<i>Lionycteris spurrelli</i>	-	3
<i>Lophostoma silvicolum</i>	2	9
<i>Mesophylla macconnelli</i>	-	1
<i>Micronycteris megalotis</i>	1	-
<i>Micronycteris sp.</i>	-	1
<i>Mimon bennettii</i>	-	1
<i>Mimon crenulatum</i>	-	4
<i>Phylloderma stenops</i>	-	3
<i>Phyllotomus elongatus</i>	1	4
<i>Pteronotus parnellii</i>	8	6
<i>Rhinophylla pumilio</i>	2	-
<i>Tonatia saurophila</i>	-	1
<i>Trachops cirrhosis</i>	1	6
<i>Uroderma bilobatum</i>	1	1
<i>Vampyriscus bidens</i>	-	2
TOTAL	116	105

Shannon-Weaver Index of Diversity:

Using the data shown in Table 4, the Shannon-Weaver Index of Diversity has been calculated for each location.

Based on the Shannon index, Rock Landing had a markedly higher bat diversity ($H = 2.528$) than Turtle Mountain ($H = 1.465$).

Simpson's Index of Diversity:

Also using the data shown in Table 4, the Simpson's Index has been calculated for Turtle Mountain and Rock Landing.

This index produces results between 0 (no diversity: no species) and 1 (infinite diversity: many species all with similar/the same relative abundance)

Based on the Simpson's index, Rock Landing has a higher bat diversity ($D = 0.90$) than Turtle Mountain ($D = 0.60$).

Chi-Squared Test:

Both values exceed the critical value of 7.81 for $p = 0.05$ and of 11.34 for $p = 0.01$ at 3 degrees of freedom. Therefore the null hypothesis can be confidently rejected; that bat species are independent of their location as there is less than 1% chance that the difference is down to chance. They are, it seems, dependent, which will be discussed later in the conclusion.

Table 5: Tree species recorded in each location.

Tree Species*	Sub-Total rock	Sub-Total turtle	TOTAL
Aromata	1	1	2
Awasakuli	-	6	6
Balataballi	2	2	4
Baromali	3	17	20
Black Kakarali	2	5	7
Black Yari Yari	2	1	3
Bloodwood	4	-	4
Bohocoda	1	-	1
Bulletwood	3	-	3
Cecropia	2	1	3
Charlie's wood	1	-	1
Cherry	2	-	2
Crabwood	-	3	3
Curryweed	-	1	1
Dead	-	1	1
Dead unknown	-	3	3
Dukabali	1	-	1
Glasswood	4	-	4
Guavabali	2	6	8
Halawa	2	-	2
Hakibali	1	-	1
Inga	2	5	7
Kakocali	2	1	3
Kakarali	11	1	12
Kakibali	-	1	1
Kauta	15	10	25
Kautabali	2	4	6
Kukurit palm	8	-	8
Kuru palm	-	1	1
Large palm	1	-	1
Letterwood	1	-	1
Locust	2	-	2
Maho	13	2	15
Manikol palm	1	-	1
Mapurakong	-	1	1
Monkey Pot	-	1	1
Mora	27	11	38
Purpleheart	1	-	1
Sand baromali	1	6	7
Sand mora	-	6	6
Smooth leaf	-	-	-
Kakarali	1	10	11
Soft Wallaba	-	1	1
Spongewood	3	-	3
Suya	8	2	10
Suyabali	1	-	1
Trysel	-	86	86
Unknown	36	55	91
Vine	1	-	1
Wadara	-	1	1
Wamara	7	12	19
Weyerballi	2	6	8
Wild Cherry	2	3	5
Wild guava	7	-	7
Wild starapple	2	-	2
Yari Yari	2	1	3
Yarola	-	4	4
TOTAL # Trees	192	276	468
*local names			

Forestry Data:

a) Shannon-Weaver

Using the data from Table 6; Based on the Shannon index the diversity of trees was higher in Rock Landing ($H = 3.368$)

than in Turtle Mountain ($H = 2.561$), just as it was with the bats.

Table 6: Touchpole measurements.

Transect	0.5m	1.0m	1.5m	2.0m	2.5m	3.0m	Total Touches
TURTLE							
Birds	5	17	17	14	19	31	103
Bird0	9	14	16	21	29	9	98
SR3	17	30	27	27	42	23	166
SR4	26	22	10	33	27	27	145
SR2	35	8	10	8	5	4	70
BA2	12	13	4	2	11	8	50
BA1	11	14	5	17	7	8	62
FS17	8	18	10	6	15	12	69
FS16	10	13	8	12	14	23	80
FS21	11	16	22	20	28	41	138
FS20	12	16	12	11	19	8	78
ROCK							
Transect	0.5m	1.0m	1.5m	2.0m	2.5m	3.0m	Total Touches
BA5	109	34	27	31	37	31	269
BA6	50	25	6	13	11	13	118
FS39N	8	7	3	4	19	22	63
FS40N	12	11	18	9	22	17	89
Bird6	32	14	9	16	24	34	129
Bird5	12	8	3	6	1	8	38
FS41	36	18	8	15	19	34	130
FS37	23	12	2	3	7	23	70
FS42	48	15	11	12	25	9	120
SRRL3	18	24	17	11	13	12	95
FS38N	36	30	16	17	28	33	160
SRRL4	35	16	9	6	17	6	89

b) Mann-Whitney U Test:

Using data from Table 7;

The outcome for $U_1 = 88.5$, and for $U_2 = 43.5$.

The lower of the two U values was then compared to the critical value, at $p = 0.05$, for sample sizes of 11 and 12. The relevant critical value in this instance is 33; this is exceeded by the lowest U value of 43.5 and therefore null hypothesis is accepted. This means that there is no significant difference between the understorey foliage density at the Turtle Mountain and Rock Landing sites. This suggests that the difference between bat diversities should, therefore, be due to another factor.

Discussion

Bats:

The statistical tests on the bat data show that there were differences between the bat assemblages in the two locations. Whilst Turtle Mountain may have had more bats caught over the time the author was there (although the nets were also open for marginally longer due to bad weather conditions at Rock Landing), there were fewer different species than were found at Rock Landing. The diversity indices demonstrate that the two locations are home to not only different species, but different numbers of species.

Whilst the chi-squared test does not indicate the number of bats found in an area, it does demonstrate that the populations are, in some way, dependent on their location.¹⁰ This test could not consider all the data due to low numbers of certain species, but it may nevertheless be representative of the whole sample. Unfortunately, it cannot indicate any correlation between understorey foliage density and numbers or species of bats.

Forestry:

Whilst this cannot be statistically shown with only two sets of data, it can be seen that where there is increased tree diversity there is also higher bat diversity and from this it can be inferred that there may be a positive correlation between the two factors. This may be down to chance given the lack

of sufficient data to form a proper correlation, but it may also be related to niche availability: with a higher tree diversity there is likely to be a wider range of food available to different bat species, opening up more niches for them to fill. A wider range of trees offers a wider range of habitats and food sources to support more different bat species; this might be down to the fruits growing on trees or the insects living in them or the roosts available. The data indicates that different species of bats prefer habitats containing certain tree species. In the Turtle Mountain area, 86 Trysel trees were recorded whilst none were found at Rock Landing and 72 *Artibeus planirostris* were found at the former and only 20 at the latter. Whilst the data is not sufficient to indicate this statistically, it appears that there may be a correlation between certain tree species and a particular species of bat, either due to roosting or feeding preferences.

The touch pole data did not provide any significant results, with the median values for the data sets from the two sites being fairly similar. More data is required to assess a possible correlation between the bat and forestry data.

■ Conclusion

Unfortunately, due to lack of data, it has not been possible to show any significant link between understorey foliage density and bat population numbers, as, on analysis, although the bat populations and species distribution vary between the two locations, “Turtle Mountain” and “Rock Landing” appear to have similar understorey foliage density, suggesting that this is not the influencing factor in the differences seen between the bat populations. It suggests that other factors are determining bat numbers and species’ occurrence. The two areas differed in altitude, tree species diversity and slope gradient, all of which could affect the numbers and species of bats found in each area. The data does seem to support a link between tree species diversity and bat diversity.

In addition to not having collected enough data whilst out in Guyana, the data collection was not set up with this hypothesis in mind. The main aim of Operation Wallacea is to collect data for conservation purposes – to record how individuals and populations of animal and plant species across the Guyana Shield are surviving and changing from year to year. In order to obtain data suited to this hypothesis, at least one more site (and preferably many more) would have to have been visited, collecting forestry and bat data in order to confirm a correlation.

Problems also occurred with the method of capture. Mist nets need to be very fine so that bats do not detect them. As a result, they are likely to fly straight into the nets. But, because of this, the nets are also very prone to tearing if snagged or bitten. Therefore, holes would often be left in the nets if a stick or insect were removed from the nets without enough care or, more frequently, if a bat chewed their way out. This not only allows for the captured bats to escape without being recorded, but also for other bats to fly through the holes which had been made. Although both sets of data were recorded at similar times of year (both at the end of the rainy season), they were a week apart. Ideally, the data would have been collected during the same week in both locations to minimise the num-

ber of uncontrolled variables. Aiming to minimise the number of variables in data collection, or to record any discrepancies between the two sites, humidity, air temperature and wind speed, for example, all could have been recorded.

As has been seen above, to make any conclusions as to the effect that understorey foliage density would have on bat populations in these two areas it turns out that at least one further data set (and preferably more) is needed to test reliably for a negative or positive correlation between the two. This would allow a Spearman’s Rank test then to be carried out but, as it is, a connection between the forestry and bat data is difficult to make. It can be seen where possible trends may arise, like with bat and tree species diversity, but without more data it cannot be certain although other authors have suggested that there is indeed a correlation.⁹

To get a better idea of the entire bat assemblage of each location, ideally taller nets, and a method of extracting bats from higher up in those nets, would have been used. This would provide data not only on the low flying, smaller, understorey feeders, but also the often-larger canopy feeders that tend to be found flying higher than the nets used. The collection was of data on only a fraction of the bats known to be present in the rainforests across Guyana.

If nets were checked more frequently, the likelihood of bats having time to chew their way out of the net would be smaller and therefore fewer holes would be made and so fewer bats missed.

Carrying out this project has made evident that it would be interesting to look further into the relationship between tree diversity and bat diversity. This study has shown that there may well be a connection and it would make sense for there to be correlation. It would be particularly interesting to look more closely at individual species preferences, like that possibly shown by *Artibeus planirostris*. Additionally, investigating the effect of sustainable logging on bat populations in surrounding areas could be very informative. One of the sites in the Iwokrama reserve, that unfortunately was not part of this data collection, is an area involved in sustainable logging. The effect of loss of potential food sources and roosting sites could be huge on the bat populations and since bats are such good indicators and maintainers of ecosystem health, on biodiversity generally; they distribute seeds and keep insect numbers down but are highly susceptible to changes in their environment.¹¹

■ Methods

Data was collected over a two-week period in the first half of July 2019, towards the end of the Guyanan rainy season. At this time of year, the temperature ranges from c. 30°C to low 20s at night, with high daytime humidity levels (fairly standard for this time of year). Rainfall was sporadic and heavy, often during netting hours in the evening, frequently accompanied by thunderstorms.

Study sites:

a) Turtle Mountain (‘Turtle’):

The mountain has an elevation of 164m surrounded by a flat region of forest. The bat net site was slightly above the base of the mountain, on a slight slope, above the river. It was further from water than the site at Rock Landing, but

nearer to the Essequibo river. The Essequibo is c.500m wide at the nearest point to the net site and may have deterred frequent movement of many bats over such an exposed distance, perhaps slightly isolating bat populations from those on the opposite bank. The nets were c.2km from the main river and c.20m higher than it.

b) Rock Landing ('Rock'):

These nets were near water level (c.3m above) on a relatively flat area compared to the Turtle Mountain site. The nets were set up close to a small river, which would be easy for bats to traverse and may also offer a good food source in the form of insects and larvae, particularly for trawler feeder bats such as *Noctilio albiventris*.¹²

Bat Data Collection:

A series of mist nets were set up to trap the bats and the relevant information (as described later) was recorded between each netting period before setting them free.

Nets were set up as follows:

"Mist nets" are made of very fine black nylon c.2cm mesh. They have 4 horizontal furling strings; Figure 1.¹³

One block of 18 "mist nets", in each location, were set up in pairs at right angles to form 'L' shapes in a 3x3 grid as shown in Figure 2. Nets were set up in this way as bats are known to zigzag in flight and so there was a higher chance of catching them in this layout than had the nets been in straight lines.

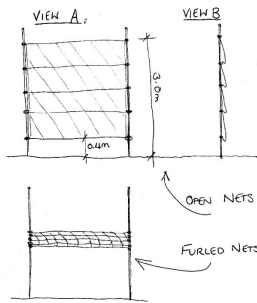


Figure 1: Mist net appearance.

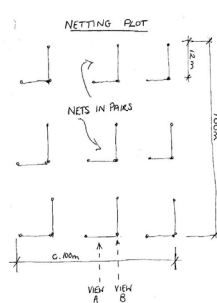


Figure 2: Mist net layout.

Each net was 2.6m high x 12m wide and c. 0.4m above ground level, reaching to 3m above ground level when open. Nets were suspended on poles secured to trees (see Figure 1). The grid of nets was located roughly in the centre of the area in which forestry measurements were taken and they spanned one of the forestry plots. The gap between the bottom of the net and the ground was to ensure that no small animals, foraging along the floor got ensnared in or ripped the nets. Net heights any higher than 3m would have been difficult to extract bats from. The nets, split into four shelves, were slightly slack to prevent bats from bouncing off on contact or tearing straight through.

Trapping times:

Nets were left furlled between closing and reopening the next night. They were opened at 17:30, shortly before dusk, and checked at 1.5-hour intervals until 23:30 when they were furlled, c.6 hours after opening. On opening, nets were checked for insects or debris and these were removed as anything of this nature could be detected by the bats and avoided, causing them to avoid the nets altogether. Bats caught in the nets were

removed, placed in individual bags which were securely knotted and held by the string to minimise physical contact with the bat. These bats were carried back to camp a few minutes away. The nets stayed open until c.23:30 unless closed due to heavy rainfall as bats tend not to fly in bad weather. Any holes made by bats were mended to prevent others flying through.

Bat release:

Bats were released from camp. As the nets were quite close to camp and given the distances bats fly and their ability to navigate so effectively, it was not a problem to release them a short distance away from where they had been found. Sub-adults found in the nets alongside an adult of the same species were released together, on the grounds that they may have been parent and offspring. Any bats appearing to have sustained injury from being in the net (predation, exhaustion etc.) were given a small volume of sugar water in an attempt to give them energy to return to their roosts and heal.

Data recording:

Weight of bat was recorded (weight of empty bag subtracted from weight of bag with bat). Forearm length (mm) was measured; the bat forearm is homologous to our own. Sex of the bat was also recorded, along with the age; adult or sub-adult (age is determined from examination of the bony protrusions on the front of the bat's forearms. Juveniles have smooth joints until they fully fuse, becoming more uneven and knobby and recognisably adult).

Bats were then checked for recapture marks. If a bat was a new capture, a small wing punch was made in the bottom of the left wing membrane, between blood vessels. This does not endanger the bat as they heal over relatively fast and only leave a residual mark. As a natural part of life, bats receive multiple tears and rips in their wings, from predation and collisions, all of which heal over leaving a scar. If a bat had a mark from a previous wing punch, it was recorded as a recapture (see Table 1). The teeth were examined, and bats were then photographed (whole body, head and teeth). Dichotomous keys^{10,14} were then used to determine its species (see Tables 2 and 3).

Forestry Data Collection:

Data was collected over an area of c.3km x 3km at each of Turtle Mountain and Rock Landing; data were taken from 11 plots at Turtle Mountain and 12 at Rock Landing. The 20m x 20m plots were roughly equally distributed across each site.

Five types of data were recorded in each plot, two of which are used in this paper.

Number of each species of tree was recorded (see Table 4) – data used for this study. Understorey foliage density was estimated in this study using 'touchpole' measurements as a proxy for foliage density. Poles were 3m high (matching mist net heights). Measurements were taken at 1m horizontal intervals along one East-West transect of the plot and one North-South transect. i.e. 2 x 20 measurements across the plot, 40 in total (please refer to Figure 3) – data used for this study.

The following data were not used in this study but could be used, for example, when investigating the effect of density of canopy foliage on the higher-flying bat species. The

diameter at Breast Height (DBH) of trees was recorded: trees with diameter >10cm were measured. Taken together with approximate tree height, this data allows for a potential estimate of timber density/volume in each plot. Canopy density was then measured: a 'densiometer' was used to measure relative density of upper canopy in each plot, with 5 readings taken per plot and averaged. The points of light penetrating the canopy and seen on the densiometer were used as a proxy for foliage density. (The Spherical Crown Densiometer is a: reflective, shallow convex dome of c.70mm diameter marked with c.5mm grid. Points of light on grid intersections are counted and recorded whilst holding densiometer steady.) Five readings of leaf litter depth were taken per plot using graduated stick. Results were averaged. This data also has not been used for this study.

Touchpole measurements taken along dotted axes

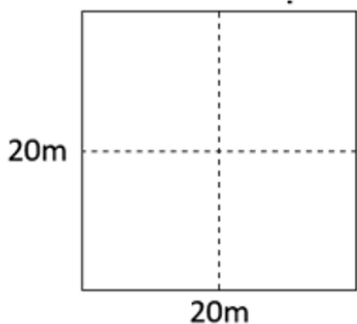


Figure 3: Touchpole transect.

At each of the 40 points, the number of vegetation touches on each pole was recorded (graduations not used for this study). In this study, a simple aggregate of total pole touches on all 40 poles was taken as an estimate of relative understorey density (see Table 5).

Data Analysis:

i. Bat Data:

The species data collected has been analysed using both the Shannon-Weaver and Simpson's indices to establish which of the two sites, Turtle Mountain or Rock Landing, have a higher diversity of bat species, as outlined later on.

a) Shannon-Weaver Index of Diversity :

Accounts for how 'evenly the total number of individuals in a sample is apportioned between each species'.¹⁵

It does not take into account how many species are present, but how even the numbers of each species are.

It usually ranges from c.1-3.5, but can only be used to compare like with like as it gives relative values.

$$H = - \sum p_i \ln p_i$$

Where:
H = diversity
p_i = proportion of a particular species.

$$H = - \left[\left(\frac{2}{166} \right) \times \ln \frac{2}{166} + \frac{8}{166} \times \ln \frac{8}{166} + \frac{2}{166} \times \ln \frac{2}{166} + \frac{72}{166} \times \ln \frac{72}{166} \dots + \frac{1}{166} \times \ln \frac{1}{166} \right]$$

=1.465

b) Simpson's Index of Diversity :

Measures species "evenness" (no. of individuals of each species) and "richness" (no. of different species).

This differs from Shannon-Weaver; a location could have only four species, but if those species are evenly represented, it would have a high diversity. With Simpson's, a high diversity comes from evenness but also the number of different species. Fewer species and/or less even distribution of those species mean lower diversity.

$$D = 1 - \frac{\sum n(n-1)}{\sum N(N-1)}$$

Where:

D = diversity
n = no. of individuals of one species
N = no. of individuals of all species
e.g.

$$D = 1 - \frac{2(2-1)+8(8-1)+2(2-1)+72(72-1)+\dots+1(1-1)}{166(166-1)} = 0.60$$

Contingency Table and Chi-squared test :

A Chi-squared test was used to compare the bat species ratios between the two locations and therefore to indicate whether bat species are dependent on their location.

A contingency table is used to work out the expected values for the chi-squared test (see Table 5). For the contingency table, only four species of bat were used. More could not be used, as their numbers were too few and would have led to expected values of below 5 which would have made the results of following calculations inaccurate and unreliable.

The species used are shown in Table 5.

The Chi-squared test compares observed and expected values (bat numbers). Expected bat numbers are calculated using a null hypothesis for the contingency table that assumes that ratios of each bat species are the same across both locations.

H0: bat species are independent of their location (therefore we would expect the same ratios of each bat species at both locations)

H1: bat species not independent of their location (ratios would be different between locations)

The expected values were worked out from the observed values:

$$E = \frac{[\text{row total}] \times [\text{column total}]}{[\text{total number of bats}]}$$

e.g. *A. planirostris*

$$E = \frac{92 \times 95}{156} = 56.024$$

Table 7: Contingency Table.

Species	TOTAL Observed		Row total	TOTAL Expected	
	Turtle	Rock		Turtle	Rock
<i>Artibeus obscurus</i>	2	17	19	11.571	7.429
<i>Artibeus planirostris</i>	72	20	92	56.024	35.974
<i>Carollia perspicillata</i>	13	18	31	18.878	12.122
<i>Pteronotus parnellii</i>	8	6	14	8.526	5.474
Column total	95	61	156		

Using the calculated expected values, a Chi-squared test can be carried out.

$$\chi^2 = \sum \frac{(O - E)^2}{E}$$

Where:

O = observed values

E = expected values

$$\text{e.g. } \chi^2 = \frac{(2-11.571)^2}{11.571} + \frac{(72-56.024)^2}{56.024} \dots = 14.334$$

Turtle Mountain:

$$\chi^2 = 14.334$$

Rock Landing:

$$\chi^2 = 22.325$$

Degrees of freedom = $(n-1)(m-1)$

$$= (4-1)(2-1) = 3$$

ii. Forestry Data:

Forestry data has been analysed using:

1) the Shannon-Weaver test for diversity in the tree populations for each site

2) the Mann-Whitney U test to find out if there is a statistically significant difference between the understorey density of each location, using the touch pole data as a proxy for that density.

a) **Shannon-Weaver :**

$$H = - \sum p_i \ln p_i$$

b) **Mann-Whitney U Test:**

This test determines whether the medians of the two sets of data are significantly different.

$$U_1 = n_1 \times n_2 + 0.5n_2(n_2 + 1) - \sum R_2$$

$$U_2 = n_1 \times n_2 + 0.5n_1(n_1 + 1) - \sum R_1$$

Where:

n_1 = sample size of first set of data

n_2 = sample size of second set of data

$\sum R_1$ = sum of ranks of first set of data

$\sum R_2$ = sum of ranks of second set of data

Touchpole data from both Turtle Mountain and Rock Landing is combined and ranked from smallest to largest. The sum of each location's ranks is then put into the relevant equation along with the sample size of the set.

■ Acknowledgements

The author is grateful to all members of Operation Wallacea with whom she was lucky enough to spend a fascinating and informative two weeks in the Guyana Shield and in particular Iona Cunningham-Eurich and Johnny Wilson with whom bat and forestry data were gathered on site and also to Scott Sveiven and Dr. Burton Lim for generously sharing the data collected during the time the author was in Guyana. Thanks also to Dr. Richard Case and Mr Jerome Armstrong for their guidance on the writing of this study.

■ References

1. Bat Trust. Types of bats - About Bats - Bat Conservation Trust. <https://www.bats.org.uk/about-bats/what-are-bats> (accessed Sep 11, 2020).
2. Razing the land to feed massive timber hunger. https://wwf.panda.org/knowledge_hub/where_we_work/amazon/amazon_threats/other_threats/logging_amazon/ (accessed Sep 11, 2020).

3. Law B., Park K.J., Lacki M.J. Insectivorous Bats and Silviculture: Balancing Timber Production and Bat Conservation. In *Bats in the Anthropocene: Conservation of Bats in a Changing World*, Voigt C., Kingston T., Eds.; Springer: Cham, CH, 2016.
4. Lim, B.; Engstrom, M. Mammals Of Iwokrama Forest. *Proc. Acad. Nat. Sci. Philadelphia* 2005, 154, 71-108.
5. The Essential Guiana Shield-Guyana Chronicle. <https://guyanachronicle.com/2018/11/28/the-essential-guiana-shield/#:~:text=The%20area%20is%20the%20only,and%20it%20must%20be%20protected> (accessed Sep 11, 2020).
6. Operation Wallacea | Conservation Research Expeditions <https://www.opwall.com/> (accessed Sep 11, 2020).
7. Denzinger, A.; Schnitzler, H. Bat Guilds, A Concept To Classify The Highly Diverse Foraging And Echolocation Behaviors Of Microchiropteran Bats. *Frontiers in Physiology* 2013, 4.
8. Altringham, J. *Bats: From Evolution To Conservation*; 2nd ed.; Oxford University Press: New York, 2011.
9. Caras, T.; Korine, C. Effect Of Vegetation Density On The Use Of Trails By Bats In A Secondary Tropical Rain Forest. *Journal of Tropical Ecology* 2009, 25, 97-101.
10. Lim, B.; Engstrom, M. Species Diversity Of Bats (Mammalia: Chiroptera) In Iwokrama Forest, Guyana, And The Guianan Subregion: Implications For Conservation. *Biodiversity and Conservation* 2001, 10, 613-657.
11. Medellin, R.; Equihua, M.; Amin, M. Bat Diversity And Abundance As Indicators Of Disturbance In Neotropical Rainforests. *Conservation Biology* 2000, 14, 1666-1675.
12. Lundrigan, B.; Kamarainen, A. *Noctilio albiventris* (lesser bulldog bat). https://animaldiversity.org/accounts/Noctilio_albiventris/ (accessed Sep 11, 2020).
13. Gilroy, D.; Sveiven, S.; O'Shea, D.; Lim, D.; Hallett, M.; Fitzpatrick, D.; Pierre, M.; Bonat, S. *Monitoring Biodiversity By Operation Wallacea In The Iwokrama And Surama Forests*, Guyana; 2015.
14. Lopez-Baucells, A.; Rocha, R.; Bobrowiec, P.; Bernard, E.; Palmeirim, J.; Meyer, C. *Field Guide to the Bats of the Amazon*; 1st ed.; INPA, 2016.
15. Fowler, J.; Cohen, L.; Jarvis, P. *Practical Statistics for Field Biology*; 2nd ed.; Wiley: Hoboken, 2013.

■ Author

The author studied at Shrewsbury School and is going on to Oxford University to study Biological Sciences. This paper was inspired by a visit to Guyana over a period of two weeks during which field work allowed for data collection.

Solar Energy Induced Woody Biomass Conversion with a Semiconductor Photoelectrode

Claire Y. Lee, Alicia Y. Leem, Hannah Park

Fayetteville-Manlius High School, 8201 E Seneca Turnpike, Manlius, New York 13104, USA; clairelee5g@gmail.com, yuminkleem@gmail.com

ABSTRACT: An abundance in lignocellulosic biomass can be an effective solution for increasing fuel and chemical demands. Lignocellulosic biomass is composed of cellulose, hemicellulose, and lignin – all components that are vital to its ability to be converted into various value-added chemicals. Despite its abundance and subsequent potential, the depolymerization of lignin remains a big technical challenge. This experiment entailed the oxidation of corn stover with the dye sensitized solar cell (DSSC) as a pretreatment process for easy depolymerization. In the photoelectrochemical reaction, raspberry extract coated titanium dioxide (TiO₂) electrode and a visible LED light source were used to see if solar energy could be used. It was observed that the absorption spectra changes, which infers structural changes in corn stover through UV-vis spectroscopy, finding the possibility of depolymerization of lignin in mild conditions at a low cost.

KEYWORDS: Energy; Chemical; Solar Materials; Woody biomass; Photoelectrochemical Cell; Sustainable Energy. Manhattan had a more pronounced upward when compared to the data gathered from the stations in relatively less populated areas.

Introduction

Wood is composed of three components: microfibrils of cellulose (35-50%), hemicellulose (20-35%), and lignin (15-20%) – all shown in Figure 1. Lignin is the largest non-carbohydrate component in the lignocellulosic biomass (LCB) and the most abundant aromatic polymer (LCB contains up to ~20% lignin) but is currently underutilized. Most of the lignin is used for producing heat energy but instead, it can be converted to valuable chemicals (i.e. ethanol, phenol).¹ Previous studies show that lignin can be decomposed at high temperatures and pressure, resulting in the production of value-added chemicals.² Recently, several research groups developed effective methods to break down lignin into small molecules by utilizing visible or solar light, a naturally abundant, safe, and cost efficient source.³ More importantly, these solar-powered reactions allow for improvement in selectivity and the yield of lignin decomposed, especially under mild conditions such as room temperature air. Inspired by the recent studies about visible light induced lignin depolymerization, a unique method was reported to modify lignin into decomposed lignin with a dye-sensitized solar cell under the illumination of visible light. Composed of light absorbing molecules, fruit dyes extracted from raspberries, blueberries, and blackberries were utilized as a component of the dye sensitized solar cell, because it can absorb photons which make up light.

Solar energy is considered an alternative renewable and sustainable energy source. As a result of using fossil fuels, global warming and air pollution are problems that substantially degrade the environment today. In 2017, 81% of the world's consumed energy was oil, coal, and natural gas and nearly fifteen billion metric tons of fossil fuels are consumed every year.⁴ At this rate, it's predicted that the world will run out of fossil fuels in seventy years' time.⁵ Not only is this a strain on our available energy sources, but it presents a health crisis as well.

The resulting air pollution alone, which has been on the rise since 2016, contributes to 9% of global deaths.⁶

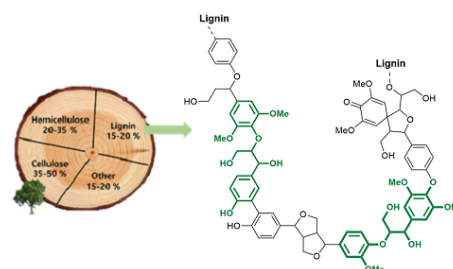


Figure 1: Wood components and the structure of lignin (The green lined structures represent the major molecular structure in lignin).

To find a solution to this global issue, researchers are creating modernized ways to acquire energy by using natural resources such as solar radiation. Among these modernized alternatives is the dye sensitized solar cell. These cells produce electric energy by absorbing the rich visible light radiated from the sun and applying the principles of plant photosynthesis (Figure 2). The process of chlorophyll utilizing solar energy is mimicked by the dye in these cells. Similar to how plants absorb solar energy to turn it into chemical energy, these cells are able to absorb solar energy and process it into usable electric energy as shown in Figure 3. Like the process of photosynthesis where chloroplasts capture light energy to convert into chemical energy (ATP, NADPH in chloroplast), the fruit dye in the dye sensitized solar cell attaches to the TiO₂ particles to absorb light. The dye then gives its electrons to allow the flow of energy throughout the cell, which is kept in a cycle by the iodine mediator that is added.

Goal of the project:

In the following project, the isolated lignin gained from a range of pretreatments will be used as feedstock to produce mono-aromatic compounds and/or dicarboxylic acids. A

range of aromatic compounds, often used as another renewable source for petroleum-based chemical building blocks, will be produced from lignin through depolymerization with a final goal of improving the economics of LCB- based biorefineries.

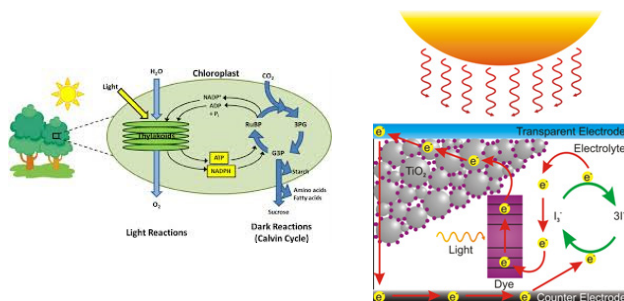


Figure 2: Process of photosynthesis.⁷ **Figure 3:** Process of dye sensitized solar cell.⁸

As a pretreatment process, the dye sensitized solar cell was fabricated and checked for the possibility of lignin depolymerization in corn stover through photo-oxidation using solar energy. Corn stover is the non-grain portion of corn crop and considered to be a substantial potential biorefining resource and often used for lignin decomposition research. Untreated corn stover has ~20% lignin.

■ Methods

Chemicals:

Sunscreen (Bare republic, Titanium Dioxide 6.4%), raspberries, blueberries, and blackberries were purchased from Wegmans, NY. Isopropyl alcohol (~99%) was purchased from Amazon. Hydrogen peroxide (3%) and acetone (~99%) were purchased from CVS without the purification. The Leem and Yoo research groups at SUNY ESF provided TiO₂ paste, corn stover, FTO glass, and electrolyte solution.

General fabrication of Dye Sensitized Solar Cells:

The three dyes were extracted from blueberries, raspberries, and blackberries by crushing the fruit and filtering out the dye using vacuum filtration. The dyes were then diluted with water and each was used to measure the UV-visible absorbance spectrum to understand the absorption of the dyes. The next step was to fabricate the dye sensitized solar cell using sunscreen containing TiO₂ and other ingredients. Before applying anything to the fluorine doped tin oxide (FTO) glass, it was placed in isopropyl alcohol for ten minutes in the sonicator to cleanse the glass surface of any small particles. After the glass was cleansed, the sunscreen was evenly coated on the FTO glass by using different layers of tape on the perimeter to create various thicknesses and placed in the oven at 120 °C for one hour. After depositing the sunscreen on FTO glass at high temperature, the concentrated dye solution from fruit juice was dropped on top of the dry sunscreen coated FTO glass. After twenty minutes, any excess dye on the glass was gently rinsed off with solvents. The counter electrode was then prepared, which was a carbon coated FTO glass made by using graphite pencil. The two glass pieces, one with the fruit dye coated TiO₂ containing sunscreen and the other electrode with the carbon coating, were sandwiched together and held together with two binder clips. Drops of redox elec-

trolyte solution (0.5M iodide electrolyte solution) were then placed between the two glass samples and spread throughout its inner surface by clipping and unclipping the binder clips.⁹ The cell was assembled with an electric wire connected to a multimeter, which was used to find the maximum current of the cell when placed in front of different LED light sources, Red, Green, and Blue.

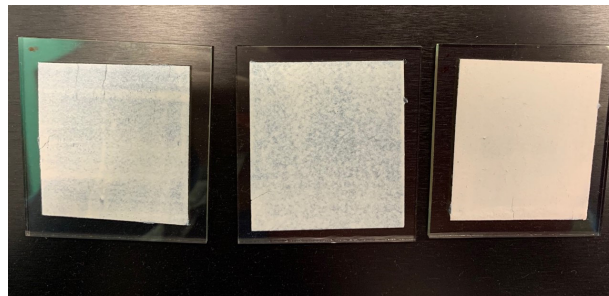


Figure 4: FTO glass substrate coated with sunscreen containing TiO₂ with various thickness. (from left 1 layer, 2 layers and 3 layers of tape)

Instead of a small component of TiO₂ in sunscreen, another dye-sensitized solar cell was prepared by using pure TiO₂ paste and graphite carbon. Various samples of glass were evenly coated with TiO₂ (Figure 4). The active area was controlled by adjusting the number of layers of scotch tape placed around the edges. When all the glass samples were coated with TiO₂ paste, they were then placed on a hot plate at 80°C for twenty minutes. After drying, the concentrated raspberry dye solution was dropped on the preheated TiO₂ electrode (Figure 5). The counter electrode, carbon coated FTO glass, was fabricated by coating the conductive side of the glass with graphite pencil. Then, the two electrodes, the dye attached TiO₂ electrode, and the carbon coated FTO electrode, were sandwiched and held together with two binder clips. Iodide electrolyte solution was dropped between the two glass samples and spread throughout the inner surface by clipping and unclipping the binder clips. The electrodes, with an electric wire, were connected to a multimeter which was used to find the maximum current of the cell in Figure 6 and 7.¹⁰ The photocurrent density data was obtained with different distances between the electrodes and the different LED light sources: Red, Green, and Blue.

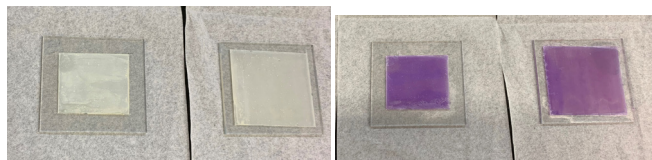


Figure 5: FTO glass substrate coated with TiO₂ paste and raspberry extract.

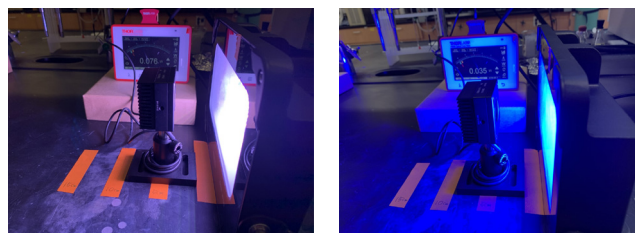




Figure 6: Measuring light intensity with optical power meter in various distance and various light colors.



Figure 7: Measuring electrical current of DSSC with multimeter.

Photoelectrochemical Oxidation of Lignin:

In a 100 ml beaker, 10 ml of acetone and 20 ml of 3% hydrogen peroxide were put in water as an oxidizing agent. In addition, 1.0g of corn stover was added. To set up the photoelectric oxidation experiment, the raspberry dye coated TiO₂ electrode was used as a working electrode. Then, platinum wire was used as a counter electrode and an Ag/AgCl electrode as a reference electrode. The solution was heated to 60°C for an hour shown in Figure 8.^{10,11} The photocurrent, approximately 10⁻⁶ A/cm², was monitored under visible light illumination.

In another 100 ml beaker, the same procedures were followed as above except for the absence of electrodes as a control experiment in order to compare the effectiveness of the dye sensitized solar cell (Figure 8).



Figure 8: Photoelectrochemical oxidation experiment of corn stover.

Results and Discussion

UV-visible absorbance spectra of various fruit dyes:

In Figure 9, maximum absorbance in the visible light range was 494 nm for blackberries and 508 nm for raspberries, but the blueberry dye solution barely showed any peak in the visible range. Previous studies reported the broad absorption of light between 400 and 600 nm in blackberry.¹² This UV-vis data is largely consistent with our observation based on the visible absorbance spectrum of the blackberry dye. According to the solar radiation spectrum, visible light is most abundant between 400 nm and 700 nm (Figure 10). To maximize the usage of solar energy, fruit dyes are appropriate due to their absorption in the visible region. Among the fruits, raspberry dye was chosen based on its efficient absorption in the visible range, showing it can absorb the most visible light for the use of dye sensitized solar cells.

Dye Sensitized Solar Cell (DSSC) with Sunscreen:

TiO₂ is widely used as a semiconductor in DSSCs because it is easy to synthesize and has a low cost. Sunscreen, which contains TiO₂, was used for the DSSC tests. Unfortunately, a photocurrent was not detected due to the small amount of

TiO₂ (6.4%) and other organic ingredients in the sunscreen.

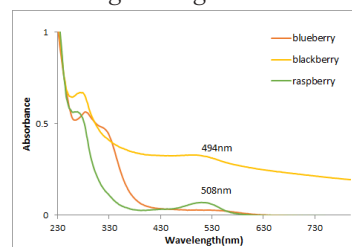


Figure 9: UV-vis absorption spectrum of various fruit extracts.

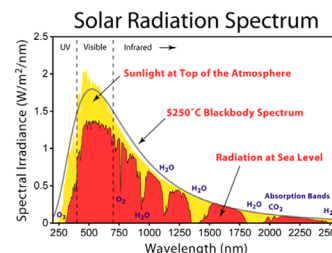


Figure 10: Solar radiation spectrum.

Dye Sensitized Solar Cell (DSSC) with TiO₂ Paste:

Using an LED light source, the electrical currents were measured from (1) the different active areas and (2) the distance between the light source and the DSSC. Interestingly, it was observed that greater surface areas with closer distances to the light source produced higher electrical currents (Table 1). Essentially, the closer distance between the light source and the DSSC exhibited higher light intensity and the larger surface area allowed for more light absorption. In Figure 11, the electrical current was plotted per cm² versus power density. Based on this graph, it was concluded that the two measurements were very similar at the same distance.

Table 1: Measurement of electrical current in various areas and distances.

Distance	Light Intensity	4.5cm*5cm	3.5cm*4cm
5cm	76 mW/cm ²	53.7μA (2.39 μA/cm ²)	37.2μA (2.66 μA/cm ²)
10cm	36 mW/cm ²	47.2μA (2.10 μA/cm ²)	31.8μA (2.27 μA/cm ²)
15cm	19 mW/cm ²	39.6μA (1.76 μA/cm ²)	27.3μA (1.95 μA/cm ²)

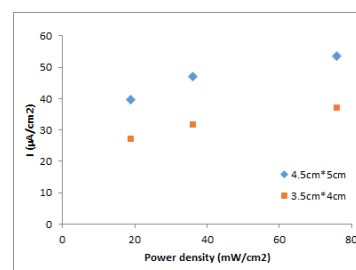


Figure 11: Graph of power density vs electrical current.

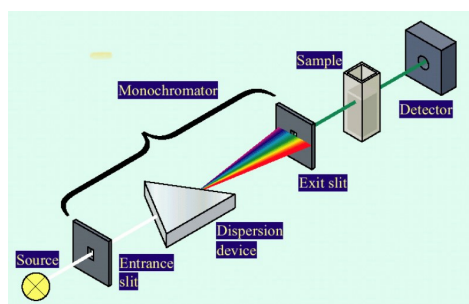
Measurements of the Electrical Current by Colors of the Light Source:

The wavelengths varied based on the colors of the light source (Table 2). Out of the three colors that were experimented (blue, green, red), the blue light produced the highest electrical current. From the previous experiment above, it was shown that the raspberry dye absorbs the most visible light in the blue wavelength. This evidence explains how the blue light produced the most electrical current.

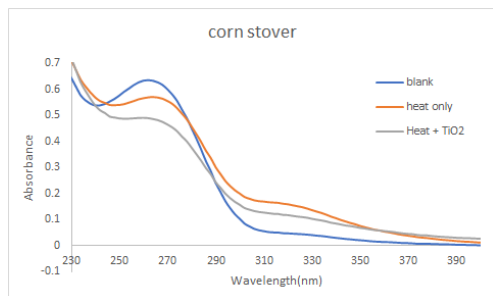
Table 2: Measurement of electrical current with various light colors.

light color	Distance	light intensity	2cm*2cm	4cm*4cm
white	5cm	76 mW/cm ²	9.8 μ A	12.4 μ A
	10cm	36 mW/cm ²	8.8 μ A	10.2 μ A
	15cm	19 mW/cm ²	8.2 μ A	8.6 μ A
blue	5cm	35 mW/cm ²	9.0 μ A	10.8 μ A
	10cm	16 mW/cm ²	8.6 μ A	8.3 μ A
	15cm	8 mW/cm ²	8.2 μ A	6.5 μ A
green	5cm	20 mW/cm ²	7.4 μ A	7.9 μ A
	10cm	9 mW/cm ²	6.3 μ A	6.2 μ A
	15cm	4 mW/cm ²	5.7 μ A	5.9 μ A
red	5cm	23 mW/cm ²	4.8 μ A	7.7 μ A
	10cm	10 mW/cm ²	4.6 μ A	5.8 μ A
	15cm	5 mW/cm ²	4.5 μ A	4.7 μ A

Photoelectrochemical oxidation of lignin obtained by corn stover:

**Figure 12:** Basic design of UV-vis spectrophotometer.¹⁴

Next, the photoelectrochemical oxidation of lignin extracted by corn stover was carried out and the solution samples were characterized using UV-vis spectroscopy. UV-vis absorption spectroscopy is the measurement of the attenuation of a beam of light after it passes through or reflects from a sample surface (Figure 12). Different structures of molecules absorb different wavelengths from the light source. According to Planck's equation ($E = h \cdot c / \lambda$), the shorter the wavelength, the more energetic the photon, which are the particles that make up light.

**Figure 13:** UV-vis absorption spectrum of corn stover.

In Figure 13, the UV-vis absorption level decreased around a wavelength of 260 nm and increased around 320 nm. This change implies that the molecular structure was altered so that the molecule absorbs lower energy. This absorption data could indicate that lignin is oxidized photochemically or thermochemically under the illumination of visible light. In the basis

of the previous study, the observation of lignin degradation can monitor the absorption band between 310 nm and 320 nm. This specific wavelength can be the evidence of the presence of a carbonyl bond or ethylene type double bond in conjunction with benzene groups.¹⁵ Therefore, it was concluded that photoelectrochemical reactions using solar energy can be used as a pretreatment for depolymerization of lignin in mild conditions. The photochemical reactions of lignin are currently under investigation.

Conclusion

Among the three fruits, raspberry, blackberry, and blueberry, raspberries showed the strongest absorption in the visible range, and thus were chosen for the dye sensitized solar cells to utilize abundant visible light in solar energy. After fabricating the DSSC with TiO₂ paste and raspberry coating, electric currents were measured in various light intensities and light colors. As a result, shorter distances from the light source showed stronger light intensities and stronger electric currents. In the measurement with different light colors, DSSCs showed the strongest electric current in blue light, besides white light, which can be explained with UV-vis absorption spectrum showing that raspberry has an absorption peak at 508 nm wavelength. In the photoelectrochemical reaction of corn stover with DSSC, a UV-vis absorption spectrum change was observed. The peak at 270 nm decreased and the peak at 320 nm increased. This means that there was a molecular structural change in which the reaction's products absorbed less energy. Therefore, the experiment suggests the potential of lignin depolymerization using solar energy in mild conditions and at a low cost.

Acknowledgements

Special thanks to Mrs. Hyun Yu as our mentor and supervisor for helping us use the UV-visible spectrophotometer and supervising the whole project at State University of New York College of Environmental Science and Forestry (SUNY ESF). We also thank Drs. Gyu Leem and Chang Geun Yoo at SUNY ESF, Syracuse, NY, USA for providing TiO₂ paste, corn stover, and electrolyte solution. This work was supported in part by the USDA National Institute of Food and Agriculture, McIntire-Stennis project number: 1026335.

References

- Tayyab, M., Noman, A., Islam, W., Waheed, S., Arafat, Y., Ali, F., Zaynab, M., Lin, S., Zhang, H. & Lin, W. (2018). Bioethanol production from lignocellulosic biomass by environment-friendly pretreatment methods: A review. *Appl. Ecol. Env. Res.*, 16, 225-249.
- Brebu, M., & Vasile, C. (2010). Thermal degradation of lignin—a review. *Cellulose Chemistry & Technology*, 44(9), 353.
- Li, S., Li, Z. J., Yu, H., Sytu, M. R., Wang, Y., Beeri, D., Zheng, W., Sherman, B., Yoo, C. & Leem, G. (2020). Solar-Driven Lignin Oxidation via Hydrogen Atom Transfer with a Dye-Sensitized TiO₂ Photoanode. *ACS Energy Letters* 5(3), 777-784.
- <https://blog.resourcewatch.org/2019/05/02/which-countries-use-the-most-fossil-fuels/>
- <https://mahb.stanford.edu/library-item/fossil-fuels-run/>
- <https://ourworldindata.org/air-pollution#summary>.
- Rasmussen, M., & Minteer, S. D. (2014). Photobioelectrochemistry: solar energy conversion and biofuel production with photosynthetic catalysts. *Journal of The Electrochemical Society*, 161(10),

- H647-H655.
8. Operation of a Grätzel cell. Retrieved from https://en.wikipedia.org/wiki/Dye-sensitized_solar_cell
 9. Takechi, K., Muszynski, R., & Kamat, P. V. (2009). Fabrication procedure of dye-sensitized solar cells. *Retrieved on Feb.*
 10. Smestad, G. P., Gratzel, M. (1998). Demonstrating electron transfer and nanotechnology: a natural dye-sensitized nanocrystalline energy converter. *Journal of chemical education*, 75(6), 752.
 11. Mittal, A., Katahira, R., Donohoe, B. S., Black, B. A., Pattathil, S., Stringer, J. M., & Beckham, G. T. (2017). Alkaline peroxide delignification of corn stover. *ACS Sustainable Chemistry & Engineering*, 5(7), 6310-6321.
 12. Galloway, K. R., Bretz, S. L., & Novak, M. (2015). Paper chromatography and UV-Vis spectroscopy to characterize anthocyanins and investigate antioxidant properties in the organic teaching laboratory. *Journal of Chemical Education*, 92(1), 183-188.
 13. Solar radiation spectrum. Retrieved from https://commons.wikimedia.org/wiki/File:Solar_Spectrum.png
 14. Basic design of UV-vis spectrophotometer. Retrieved from <http://ssi.shimadzu.com>
 15. Janshekar, H., Brown, C., & Fiechter, A. (1981). Determination of biodegraded lignin by ultraviolet spectrophotometry. *Analytica Chimica Acta*, 130(1), 81-91.

■ Author

Alicia Leem is a current sophomore at Fayetteville-Manlius High School and a member of Yoo and Leem research groups at State University of New York College of Environmental Science and Forestry, Syracuse, New York since 2018. Her current research focuses on biomass conversion. She has volunteered during National Chemistry Week for the Central New York American Chemical Society (CNY ACS). In her free time, she enjoys reading, painting, and snowboarding.

Claire Lee is a current sophomore at Fayetteville-Manlius High School and a member of Yoo and Leem research groups at State University of New York College of Environmental Science and Forestry, Syracuse, New York since 2018. Her current research focuses on solar energy conversion. She enjoys science and hopes to enter the medical field. During her free time she enjoys drawing and running.

Key Prognostic Biomarkers of Acute Myeloid Leukemia: Genetic Mutations and Measurable Residual Disease

Lok Yin Kwan

HKUGA College, No.9 Nam Fung Road, Wong Chuk Hang, Hong Kong; lokyin.kwan@yahoo.com.hk

ABSTRACT: Acute myeloid leukaemia (AML) continues to be one of the most fatal forms of leukaemia, with a high recurring relapse rate (RR) even in patients who have achieved complete remission (CR). Although there is no remedy, certain genetic mutations and measurable residual disease (MRD) play an important role as a prognosticator in monitoring disease progression in AML. This review illustrates some of the most conventional biomarkers that predict patient outcomes in AML, including MRD, fusion genes RUNX-family- transcription-factor-1-RUNX1-partner-transcriptional-co-repressor-1 (RUNX1-RUNX1T1), core binding factor beta subunit-smooth muscle myosin heavy chain 11 (CBFB-MYH11) and promyelocytic leukaemia-retinoic acid receptor (PML-RARA) and genetic mutations such as nucleophosmin 1 (NPM1). Collectively, results have shown that independent mutation factor, NPM1^{mut} and MRD are currently the most accurate indicators for relapse in AML upon CR. Whereas DTA mutations (i.e. mutations in epigenetic regulators DNA methyltransferase 3A (DNMT3A), ten-eleven-translocation-2 (TET2) and additional sex comb-like 1 (ASXL1)) are likely preleukemic clones that persist throughout therapy, and their association with leukemogenesis and older patients leaves their functionality in prognosis uncertain. Studies suggest that genetic mutations isocitrate dehydrogenase (IDH) and fins-like tyrosine kinase 3 (FLT3) as standalone biomarkers are unreliable, but under the condition of concomitant NPM1^{mut}, their prognostic validity is enhanced. Outcomes from the increasingly personalised risk-adapted treatments, via patient stratification based on their MRD risk status, have revealed that the previous “one-size-fits-all” approach to AML treatment should be abandoned, whereas a more personalised treatment should be adopted to maximise chances of survival.

KEYWORDS: Biomedical and Health Sciences; Genetics and Molecular Biology of Disease; Hematology; Acute Myeloid Leukemia; Measurable Residual Disease.

■ Introduction

AML is an aggressive heterogenous group of disorders, characterised by uncontrolled clonal proliferation of myeloid progenitor cells (blasts) and differentiation arrest.¹⁻³ Making up approximately 25 % of all adult-onset leukaemias in Western countries,² with an incidence rate of 4.3 cases per 100,000 adults per year,⁴ AML is the most common type of leukaemia with the lowest mortality rate.⁵ According to the World Health Organisation (WHO), AML is classified by ≥ 20 % of blasts in the bone marrow (BM) or peripheral blood (PB). In addition, the expression of precursors such as cluster of differentiation (CD) markers CD13, CD33, CD34, CD117 and HLA-DR^{pos} are used to confirm the immaturity of blasts and myeloid maturation.^{4,6} Per the initial stage of induction therapy, chemotherapy (CT) drugs, cytarabine and anthracycline are prescribed, followed by either repeated cycles of high-dose cytarabine and/or haematopoietic stem cell transplant (HSCT),⁷ e.g. allogeneic stem cell transplant (AlloSCT) or autologous stem cell transplant (AuSCT). However, despite the increasing understanding of the disease, little improvement has been made in controlling disease progression, particularly in older patients. There is still a 50 % relapse rate (RR) in patients who have achieved morphological complete remission (CR),⁸ as the highly varied factors affecting prognostic results, such as age, recurring genetic mutations, cytogenetic and somat-

ic clonal chromosomal abnormalities, remains a challenge to clinicians.^{5,9} The common understanding of CR is defined by fulfilling three criteria: 1) less than 5 % myeloblasts present in the bone marrow, 2) peripheral blood absolute neutrophil count of greater than 1,000 cells/ μ L, and 3) peripheral blood platelet count of over 100,000 platelets/ μ L.¹⁰ In addition to the existing criteria, a new response category “complete remission without MRD” is added by the 2017 European LeukemiaNet (ELN).¹¹

In recent years, clinicians and researchers have been studying the significance of MRD in AML patients, where small numbers of persisting neoplastic cells are detected after treatment.¹² Commonly used biomarkers that account for high relapse rates in AML are as follows:

NPM1^{mut}: are amongst the most prevalent genetic aberrations found in AML patients, composing up to 25 % - 35 % of the cases.¹³ The presence of NPM1mut results in abnormal expression of the NPM1 protein in the cytoplasm,^{1,13} activating myeloid proliferation.

RUNX1-RUNX1T1 fusion gene: is formed from t(8;21)(q22;q22) translocation, where the majority of the coding region of RUNX1T1 gene is fused to the RUNX1 mino terminus containing the DNA-binding runt homology domain generate a RUNX1- RUNX1T1 fusion protein.¹⁴ It is also a

RUNX1- RUNX1T1 fusion protein.¹⁴ It is also considered one of the most common fusion genes found in AML patients, and represents a favorable prognosis.

CBFB-MYH11 fusion gene: is formed due to the Inv(16) (p13q22) associated AML subtype M4Eo, the chromosomal rearrangement leads to the fusion of the MYH11 gene with Cbfb locus. Other genes may combine with Cbfb-MYH11 to induce leukemia.¹⁵

PML-RARA fusion gene: is formed by the fusion of PML proteins and RARA. The PML protein is pivotal in several cellular processes and tumor suppression mechanisms. It has a dominant negative action on transcription which inhibits the proliferation of myeloid progenitors and causes maturation arrest at the promyelocytic stage.¹⁶

MRD: is the term for a small group of leukemic cells that remains in the patient during or after treatment in CR. It is considered an independent prognostic and post-diagnosis indicator with a highly accurate prediction in patient outcome, particularly in AML where relapse occurs recurrently. Many studies have proven that the presence of MRD is associated with higher RR and lower event-free survival (EFS) in acute leukemia.^{6,17,18} An empirically distinctive MRD level with a logarithmic scale or a quartile segregation in correlation to the OS is being set up as a threshold to define MRD^{pos} and MRD^{neg}. Currently, the ELN MRD Working Party suggests that MRD denotes the presence of leukemia cells at levels of 1:10⁴ to 1:10⁶ white blood cells, which is compared with 1:20 in morphological examinations.¹⁹ The party also recommends a threshold of 0.1 % to distinguish between MRD^{pos} and MRD^{neg}, in addition to the peripheral blood absolute neutrophil count $\geq 1 \times 10^9/L$ and platelet count $\geq 100 \times 10^9/L$, for defining CR.²⁰ But due to an already lower threshold level, for example, from 0.01 % to 0.1 %, for measuring leukemia associated immunophenotype (LAIP), a 0.1 % may signify MRD positivity in LAIP patients.²¹ In later sections, this review will explore the more reliable technologies of MRD detection in facilitating the reflection of MRD's functionality as a biomarker.

Although certain genetic mutations are often detected in AML patients prior and after treatment, it is said that the following mutations when independently evaluated demonstrate a degree of uncertainty in prognostic implications:

DNMT3A^{mut}: are epigenetic modifiers that are usually sorted with ten to eleven translocation 2 (TET2) and additional sex comb-like 1 (ASXL1) under the umbrella term - DTA mutations. DNMT3A is a recurrent mutation found in 22 % of AML patients,¹³ arising from somatic mutations, they persist throughout therapy and remission.

FLT3^{mut}: are identified in one third of AML patients,² with two main types: internal tandem duplications (ITD), which mainly occurs in exons 14 and 15 of the juxtamembrane domain; and tyrosine kinase domain (TKD), which are point mutations of D835 and 836.¹³ FLT3 activates downstream signalling of the RAS, MAPK and STAT5 pathways, stimulating cellular proliferation.⁹

stream signalling of the RAS, MAPK and STAT5 pathways, stimulating cellular proliferation.⁹

IDH^{mut}: cause an alteration to the oxidative role of IDH enzymes in the Krebs cycle, such that the original product, α -ketoglutarate (α -KG), is reduced to 2-hydroxyglutarate, a cancer-related metabolite.² IDH^{mut} have an occurrence of up to 15 % in AML patients, in which its subtypes IDH1 and IDH2 are mutually exclusive.¹³

This literature review aims to provide insight on the rationale behind selecting the appropriate markers for greater accuracies in prognostic outcomes, as well as guiding the direction of prospective development in treatment strategies for recurring relapse in AML patients.

■ Results and Discussion

Genetic Mutations as Biomarkers:

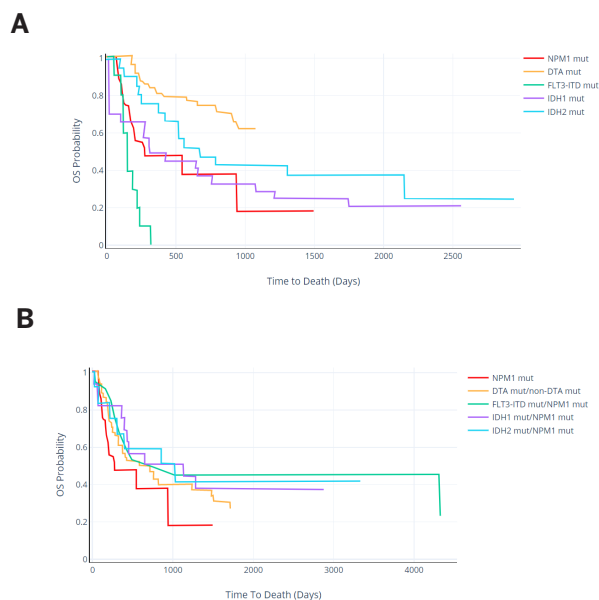


Figure 1: Summarised data from previous research on the OS probability of patients with independent mutations and concomitant mutations with NPM1^{mut}.

(A):

OS probability of patients with the mentioned independent mutations (i.e. NPM1^{mut},²² DTA^{mut},²³ FLT3-ITD^{mut},²³ IDH1^{mut},²⁴ and IDH2^{mut}),²⁴ excluding cohorts with other coexisting mutations;

(B):

OS probability of patients with concomitant mutations with NPM1^{mut} (i.e. NPM1^{mut},²² DTA^{mut}/NPM1^{mut},²⁵ FLT3-ITD^{mut}/NPM1^{mut},²⁶ IDH1^{mut}/NPM1^{mut},²⁴ and IDH2^{mut}/NPM1^{mut})²⁴, excluding combinations with other types of mutations. NPM1^{mut} is the relative point of comparison for the prognostic value of other mutated alleles, the coherence of OS in other mutated alleles with the trend in NPM1^{mut} can only be seen when the supposedly inconclusive gene mutations (e.g. DTA^{mut}, FLT3-ITD^{mut}, IDH1^{mut}, and IDH2^{mut}) coexist with NPM1^{mut}.

In a study by Bertoli *et al.* (2020),²⁷ 540 patients were documented at diagnosis for NPM1^{mut}. 430 of them were in CR1 (67.6 %) and 160 patients relapsed (46.2 %). Among

the 142 CR1 patients with NPM1^{mut}, 67 relapsed (47.2 %). 58.2 % of the relapses occurred during the first year and 34.3 % occurred after 3 years onwards. Among the 288 NPM1 wild-type (NPM1^{wt}) patients in CR1, there were 160 relapses (55.6 %), 60 % occurred in the first year, and only 11.2 % of relapses were after the 3-year mark. Though the duration of complete remission is seemingly more favorable in patient cohorts of NPM1^{mut} AML, risks of late relapses were significantly higher. Moreover, the notion proposed by Salipante et al. (2014)¹² on NPM1 as a representation of early genetic lesions in AML, an indicator that its mutation serves as one of the few driver mutations in this disease, is refuted in this paper with the reason that NPM1^{mut} cells are responsive to treatment and disappeared in 40 % of the patients with late relapse. Which is why the paper recommends the use of MRD detection in long term complete remissions due to half of the patient's undetectable levels of NPM1^{mut}.

As for whether the NPM1^{wt} is a reflective of potential relapse, insights form another recent investigation by Höllein et al. (2018)²⁸ states that patients with NPM1^{wt} are more susceptible to relapse, suggesting that preleukemic cells with NPM1^{wt} may be a subsequent cause of relapse due to clonal haematopoiesis in AML. Though it is uncertain whether NPM1^{mut} has a higher prognostic value than NPM1^{wt}, it is evident that NPM1^{mut} is a strong indicator of patient outcome, particularly in short-term recovery.

In a study designed by Jongen-Lavrencic et al. (2018),²⁵ DTA mutations are the most common in age-related malignancies. Persistent mutations were detected with targeted NGS, where it was prevalent in 51.4 % of the 430 patient bone marrow samples collected. Within the proportion of persistent mutations, rates of persistent mutation in DNMT3A was at 78.7 %, 54.2 % for TET2 and 51.6 % for ASXL1, all of which are significantly greater than other variant alleles. The distribution of residual mutation-bearing cells could be shown by the large discrepancies in individual variant allele frequencies (VAF), thus existing in virtually negligible volumes to populating most of the cells. It is suggested that morphologic CR is achieved when heterozygous mutations <2.5 %, but levels of DTA in the samples were noticeably above the cut-off during remission. By contrast, non-DTA alleles (e.g. NPM1) only occasionally persisted at >2.5 % levels after induction CT, typically the number of mutations are drastically reduced during CR. The outcome of the research highlights the adverse effects of non-DTA mutations in both training and validation cohorts. The overall survival (OS) and relapse rate (RR), regardless of the presence of persistent DTA mutations, are noticeably lower than patient samples with no detection of non-DTA mutation.

The research by Debarri et al. (2015),²⁹ further supports the notion that DNMT3A mutations are repopulated non-leukemic clones, meaning that they are not associated with increased relapse risk in the short term. Results were obtained from patient samples of BM and PB, in order to compare the makeup of cell subpopulations NPM1, DNMT3A and IDH1/2. The study employed NPM1 as a reference marker for the relative changes in the levels of other indicators, as well as the basis for accuracy in prediction of relapse. The detection limits of 0.07 % and 0.11 % were set for IDH1/2 AND DNMT3A

of 0.07 % and 0.11 % were set for IDH1/2 AND DNMT3A mutation analyses respectively. A trend of decrease in patient's mutated IDH1/2 is visible since diagnosis, although a slight increase after initial post induction (MRD1) period is present in the cohort (n=4) with both IDH1/2 and NPM1 mutations during remission period throughout post consolidation. Compared with the patient cohort with discordant DNMT3A and NPM1 mutations (n=6), the percentage of mutated DNMT3A slightly decreases in MRD1 from the initial levels measured at diagnosis, the numbers continue to rise despite the continual period of post consolidation and complete remission. Another notable feature in this cohort is the long remission period, in which relapse happened in the previously mentioned patients with mutated IDH1/2 significantly early on their post consolidation stages, whereas patients in this cohort remained at remission at an average of 57 months as of the time the investigation has taken place. A major limitation of this study is its small sample size. In patient 5, there was a discrepancy detected in the changes amongst IDH1/2 and NPM1 levels, whereas in patient 2 a correlation is shown. The paper claims that IDH1/2 mutation-based MRD better predicts relapse incidence than NPM1 mutation-based MRD, but observations were made based on the outcome of selected individual samples, where some evidence did not meet the claim.³⁰ Therefore, the validity of IDH1/2 analyses has yet to be determined by further investigation. However, with prior research on the effects of DTA on complete remission, this paper supports the previously mentioned hypothesis that DNMT3A mutations are insufficient to trigger proliferation of cancer cells. DNMT3A^{mut} patients are significantly older, with an increasing mutation frequency until reaching a plateau in the range of 40 to 60 years.^{25,31} Hence, it remains uncertain whether these mutations (IDH1^{mut}, IDH2^{mut} and DNMT3A^{mut}) will play a role in contributing to the driving force of leukemogenesis or relapse in older patients. An opposing finding by Brambati et al. (2016),³² presents the prospective significance of DNMT3A and IDH1/2 mutations in future detection of AML relapse. The study used ddPCR to determine the percentage relapse of patients with molecular alterations, in which 9 out of 17 patients in a longitudinal follow up relapsed and the remaining 8 did not. The results between relapsed to non-relapsed samples are: DNMT3A (77.8 vs 25 %), NPM1 (66.7 vs 25 %), IDH1 (- vs 12.5 %), IDH2 (22.2 vs 87.5 %). However, the outcome only accounts for the number of patients with the said mutated alleles, rather than an evaluation regarding the impact of the genetic abnormalities. Therefore, results that seemingly present significance in DNMT3A, IDH1 and IDH2 are inconclusive. Thus, in reference to the consensus from the ELN MRD Working Party, it is agreed that the prevalence of the aforementioned non-DTA mutations and IDH1/2 alone, without the discordant NPM1^{mut} in view, are inadequate interpretations of prognostic outcome.¹⁹

FLT3-ITD is often associated with increased RR and poor OS, whereas FLT3-TKD is thought to have a neutral effect on patient outcome in normal karyotype AML (NK-AML). They are discouraged by the ELN to be employed as markers of MRD due to their constantly altering allele ratio of ITD to TKD in various stages of treatment, in which they are occa

sionally undetectable at relapse and often only significant at initial diagnosis.³³ In a study by Santos *et al.* (2011),³⁴ of the 272 patients with NK-AML, 22 % had isolated FLT3-ITD^{mut}, 7 % had isolated FLT3-TKD^{mut}, and 4 % had both. Patients with FLT3-ITD^{mut} are reported with higher WBC counts and higher BM blast percentages than patients with FLT3^{wt}. There was no significant difference in the CR rate between patients with FLT3-ITD mutations and patients with wt-FLT3, but the results demonstrate patients with FLT3-ITD had inferior EFS, DFS, and OS, in which those with low FLT3-ITD burden had a longer OS. In patients carrying FLT3-TKD^{mut}, there was no significant difference in the CR rate when compared with FLT3^{wt}, and no particular impact on EFS and OS despite varying FLT3-TKD burden.

Another point to note is in the results of patients with FLT3-ITD mutations and concomitant NPM1, OS appears to be higher than cohorts with only FLT3-ITD mutations (Figure 1B). Suggested by some studies, the coexistence of NPM1 and low ratio FLT3-ITD^{wt} is demonstrated in patients with lower relapse rates,^{11,35} and can be regarded as a favourable prognostic indicator, along with the co-occurrence of FLT3-TKD and NPM1 mutations.³⁶ Recently, a novel analysis program, getITD, has been developed to identify and annotate all of the ITDs tested, as well as its insertion sites, length and variant allele frequency, facilitating the investigation on the influence of ITD in MRD.³⁷ Although the validity of this technology has yet to be reviewed in other lab and clinical settings, the technology offers a prospective vision on the utility of FLT3 in MRD monitoring throughout the patient's recovery. Thus, the prognostic significance and potentials of FLT3 should not be undermined solely because of its minimal utility as an MRD biomarker.

MRD Monitoring:

Multiparametric flow cytometry (MFC)

Diagnostic immunophenotyping is one of the most common applications of MFC.^{6,38} A distinctive feature of this technology is the ability to simultaneously characterise mixed cell populations via the detection and combination of cell surface markers present on leukemic blasts. MFC is divided into two major approaches - the leukemia associated immunophenotype (LAIP) and the different from normal (DfN).⁶ According to ELN recommendations, both approaches are integrated to define and identify individual specific surface markers that differentiate leukemic cells from healthy cells, in order to track aberrations during and after diagnosis.¹⁹ A major distinction of the MFC technology is its applicability to over 90 % of patients,⁶ such that MFC-based MRD is also considered an independent prognostic indicator of AML. However, it has limited standardisation and slightly lower sensitivity than other newly developed methods.

Polymerase chain reaction (PCR)

Quantitative polymerase chain reaction (qPCR):

qPCR uses fluorescent labelling techniques and identifies targets under three aspects: transcription ratio at diagnoses, reduction kinetics of leukemic clones and early detection of recurring clones.³⁹ Thus the detection of fusion genes and molecular biomarkers are typically conducted via qPCR. Unlike

MFC, it is a standardized technique with notably higher sensitivity, providing high-throughput detection and quantification of target DNA sequences via simultaneous amplification.^{6,40} However, functional targets detected are only present in half of the patients, and several mutations do not facilitate MRD monitoring (e.g. FLT3^{mut}).

Digital droplet polymerase chain reaction (ddPCR):

A novel modification of the conventional qPCR assays, encompassing an even higher sensitivity (up to 0.001 % mutated allele frequency) for tracking gene mutations.³² ddPCR, uses a combination of microfluidics and proprietary surfactant chemistries to emulsify samples,⁴¹ fractioning samples into droplets,³² in order to distinguish wild-type versus mutant gene copies.⁴² But despite its high sensitivity and absolute quantification ability, results produced by ddPCR are often highly variable due to the novelty of the technology, lower accuracy in quantification of larger amplicons, higher risk of contamination due to the open nature of the operating system and high cost in acquiring instrumentation.

Next Generation Sequencing (NGS):

NGS enables a comprehensive and highly sensitive detection of somatic mutations, as well as the identification of hotspots and abnormal blasts.^{43,44} It enables simultaneous sequencing in large amounts of DNA or RNA, revealing a broad spectrum of molecular alterations in patient samples. However, due to the novelty of NGS, this technology is not yet widely available, and requires complex interpretation of data, which not all labs can provide.

MRD as a Biomarker:

Considering an investigation carried out by Short *et al.* (2019),⁴⁵ 141 adult patients were analysed retrospectively for their MRD levels before and after salvage treatment. 61 % were patients with MRD^{neg} or had undetectable MRD, their results indicate a lower cumulative incidence of relapse and better RFS. Moreover, RR within 1.4 months in second remission were 13 % higher among MRD^{pos} patients without CR, compared with MRD^{neg} patients who have achieved CR. The paper concludes that patients with MRD^{neg} and CR had the best outcomes in 2-year cumulative incidence of relapse, RFS, and OS.⁴⁵ In a similar research by Walter *et al.* (2013),⁴⁶ 253 patients undergoing first myeloablative HCT were assessed for the presence of MRD after achieving morphological CR. 54 patients were MRD^{pos} and 199 others were MRD^{neg}. After adjustments of factors using multivariate models proposed by the international working group (2003) and the ELN (2010), the hazard ratios of MRD^{pos} to MRD^{neg} were 3.14 for overall mortality, 4.72 for failure of DFS and 6.78 for relapse.⁴⁶ The results from both studies and many more conclusively suggest that MRD is a highly accurate and useful measure in disease progression and prognosis at diagnosis, relapse and during CR.^{6,17,18}

While it is evident that MRD is an independent biomarker in many cases, molecular MRD monitoring often incorporates the quantification of fusion genes RUNX1-RUNX1T1, CBFB-MYH11 and PML-RARA, as well as NPM1^{mut}, which is the best-validated molecular marker for MRD. Though it is commonly believed that the mentioned fusion genes are

strong indicators of favourable outcomes, their high copy numbers pose a fatal threat to patient outcome as it signifies the presence of MRD^{Pos}, in which case patients with persistent MRD^{Pos} seldom survive in the long term.³⁹ In a research conducted by Kern *et al.* (2007),³⁹ amongst relapsing patients with core binding factor leukemias (AML with RUNX1-RUNX1T1 or CBFβ-MYH11), there is an increase in MRD levels during CR. Another observation was that an increase in patient transcript ratios indicated molecular relapses 1 to 5 months prior hematologic and cytogenetic relapses. This is supported by Ommen *et al.* (2010),⁴⁷ in CBFβ-MYH11 leukemias where it performed the earliest prediction of relapse in 50 % of the patients tested RQ-PCR positive in BM 8 months prior. By contrast, patients with high copy numbers of RUNX1-RUNX1T1 and PML-RARA showed more rapid relapse kinetics as 50 % of the patients relapsed within 3 to 3.5 months of testing positive. With evidence from Stentoft *et al.* (2005)⁴⁸ concluding that virtually all cases of relapse occur with persistent levels of MRD^{Pos} in patients with core-binding factor leukemia.

As for high NPM1^{mut} allele burden, it, in various instances, has been shown to be related to MRD positivity in first complete remission. This notion is supported by the findings of Patel *et al.* (2018)⁴⁹, where it is suggested that the ability of high-burden NPM1 mutated hematopoiesis to persist after induction chemotherapy reflects the difficulty in full eradication, which correlates to a higher likelihood of MRD. Other results obtained from the University Hospital Leipzig between January 2001 and January 2016 by Bill *et al.* (2018),²² shows that 33.3 % of the patients were found to be mutated NPM1 MRD^{Pos} before HSCT. It was observed that mutated NPM1 MRD^{Pos} occurred more frequently during AlloSCT in patients' second complete remission (CR2) after relapse in first complete remission, than during their first complete remission (CR1). Amongst pre-transplant mutated NPM1 MRD^{Pos} after AlloSCT, the 2-year cumulative incidence of relapse (64.7 vs 6.0 %) was significantly higher than MRD^{neg} patients, which translates into a lower overall survival rate (38.8 vs 71.7 %). There is a clear correlation between the prevalence of mutated NPM1 that is followed by MRD^{Pos}, leading to increased chances of relapse rates and mortality. However, despite the seemingly indicative outcome, cases of false positives and negatives are reported. In the group of mutated NPM1 MRD^{Pos} patients, 17 of 51 patients (23.5 %) did not relapse, and 2 cases of MRD^{neg} patients (6 %) relapsed prior HSCT. Further analysis was not possible due to the small sample size. The false negative is suggested to be explained by the limited sensitivity of ddPCR, which despite the presumed accuracy of the technology, may still be at times fallible due to multiple factors (e.g. the equipment available in the clinical setting, and proficiency in employing the technique, etc.), and most importantly the uncertain influence of the NPM1^{wt} subclone.

In conclusion, it is well established that early detection of MRD is indeed crucial for identifying impending relapse, staging intervention as predicted from longitudinal prognosis, assessing objective establishment of remission status and producing accurate prognostic analyses.⁵⁰ Although the bio-

markers of MRD are distinctive in nature, they are all equally essential in monitoring recovery status during CR.

Defining High and Low Risk Stratification:

The current approach of devising treatment plans for AML patients involves referencing the corresponding risk stratification of the patient. According to the ELN, risk stratifications are generally categorised into three conditions: favourable (FR), intermediate (IR), and poor (PR) (Table 1).¹

Table 1: 2017 ELN molecular, genetic and cytogenetic mutation risk stratification.^{1,31}

Risk category	Genetic abnormality
Favourable	t(8;21)(q22;q22.1); RUNX1-RUNX1T1 inv(16)(p13.1q22) or t(16;16)(p13.1;q22); CBFβ-MYH11 Mutated NPM1 without FLT3-ITD or with FLT3-ITD- Biallelic mutated CEBPA
Intermediate	Mutated NPM1 and FLT3-ITD- Wild-type NPM1 without FLT3-ITD or FLT3-ITD- (normal karyotype) t(9;11)(p22;q23);MLL3-KMT2A Cytogenetic abnormalities not classified as favourable or poor/adverse
Poor/Adverse	t(6;9)(p23;q34.1); DEK-NUP214 t(v;11q23.3); KMT2A rearranged inv(3)(q21.3q26.2) or t(3;3)(q21.3;q26.2); GATA2,MECOM(EV1) -5 or del(5q); -7; -17/abn(17p) Complex karyotype; monosomal karyotype Wild-type NPM1 and FLT3-ITD- Mutated RUNX1/ASXL1/TP53

Genetic Mutation and MRD in Therapeutic Guidance:

The respective conditions provide prognostic value to OS and relapse predictions, in which age >60 is, on its own, an independent risk factor for poor prognosis and therapeutic outcome. Thus low-risk patients, MRD^{neg} with favourable and intermediate conditions, are shown to present significantly higher probability of relapse free survival and lower relapse rates than high-risk patients, MRD^{Pos} and FLT3-positive.¹³ In the GIMEMA AML1310 trial of risk-adapted, MRD-directed therapy for young adults with newly diagnosed AML,⁵¹ entailing four tiers: favourable-risk (NCCN-FR), intermediate-risk (NCCN-IR), poor-risk (NCCN-PR) and intermediate-risk without LAIP identification (NCCN-IR-no LAIP). NCCN-IR-Neg and NCCN-FR (low risk) patients were submitted to AuSCT, whereas NCCN-IR-Pos and NCCN-PR (high risk) patients received AlloSCT. Combining the results of this study with the investigation of Zhu *et al.* (2013)⁵² and Hourigan *et al.* (2020)²³ on risk-adapted treatments (Figure 2), the results reveal that high doses of cytarabine, myeloablative conditioning (MAC) and AlloSCT are the most well received in high risk cohorts, showing an improvement in OS probability. By contrast, the patients in the low risk cohort benefitted the most in CT, with a relatively better OS outcome under reduced-intensity conditioning (RIC) treatment. The effects of CT are significantly more responsive in low risk cohorts, however the lowest probability of OS occurring in high risk patients was from cohorts undergoing CT. Moreover, the effects of the various therapeutic intensities for high and low risk patients are similar in both OS and disease-free survival (DFS) probabilities, conclusively indicating high intensity therapy and AlloSCT are more suitable in high risk patients (Figure 2), whereas low intensity chemotherapy approaches may be more beneficial to low risk patients than transplantation. Therefore, patients should receive transplants based on the treatment plan

devised for their risk stratification, and not because of donor availability.²³

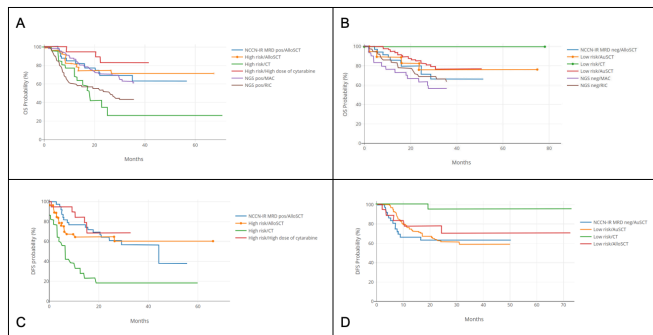


Figure 2: Summarised data from previous research on the OS and DFS probabilities in different treatment methods in high and low risk patient cohorts.

(A) Treatment effects to OS probability in high risk cohorts receiving AlloSCT,⁵² CT,⁵² high-dose cytarabine,³¹ and NCCN-IR MRDpos (which is essentially a subdivision from the high risk cohorts) receiving AlloSCT.⁵¹ Effects of MAC and RIC are contrasted in NGS MRD^{POS} patients;¹¹

(B) Treatment effects to OS probability in low risk cohorts receiving AlloSCT,⁵² CT,⁵² AuSCT,⁵¹ and NCCN-IR MRDneg patients receiving AlloSCT.³¹ Effects of MAC and RIC are contrasted in NGS MRD^{NEG} patient;¹¹

(C) Effects of treatment to DFS probability in high risk cohorts receiving AlloSCT,⁵² CT,⁵² high-dose cytarabine,⁵¹ and NCCN-IR MRD^{POS} patients receiving AlloSCT;⁵¹

(D) Effects of treatment to DFS probability in low risk cohorts receiving AlloSCT,⁵² CT,⁵² AuSCT,⁵¹ and NCCN-IR MRD^{NEG} patients receiving AuSCT.⁵¹ Overall, the OS and DFS are most benefitted in low risk cohorts receiving CT and RIC, whereas the OS and DFS are most well received by high risk cohorts undergoing AlloSCT and MAC.

Conclusion

Recent technological advancements have increased the ability to detect and analyze gene mutations as well as MRD in AML patients. Novel instruments have been shown to reduce technical limitations with a heightened sensitivity in monitoring prognostic biomarkers in AML, as well as facilitating the discovery of concomitant and independent mutations associated with poor prognoses, locating an array of leukemic clones and transcription factors for the investigation of potential mutation drivers in hematopoiesis. As reviewed, certain gene mutations not only encompass a high prognostic value, but also provides a valid biomarker to MRD monitoring, an even more sensitive measure of patient recovery. An in-depth review of the potentials and shortcomings of our enhanced understanding of how genetic mutations and MRD affect the actual clinical outcomes is out of scope for this review. Moreover, the question of whether full eradication of NPM1^{mut} or achieving MRD^{neg} is necessary before treatment remains open to further research and discussion. Evidently, monitoring key molecular biomarkers of AML is a quintessential part of standard care and should be continued, but at the same time, the impact of less conventional biomarkers should not be undermined, for they are all possibilities in furthering the progression of AML prognosis and treatment development. Hopefully, costs of standard, as well as less conventional technologies for detection of genetic aberrations will decrease in the future, enabling

more advanced discovery in the field of AML prognosis with less financial constraints.

Acknowledgements

I would like to thank Dr. Aston Tam for his valuable and constructive feedback on my initial drafts.

References

- Saultz, J.N.; Garzon, R. Acute Myeloid Leukemia: A Concise Review. *J. Clin. Med.* 2016, 5, 33.
- DiNardo, C. D.; Cortes, J. E. Mutations in AML: Prognostic and Therapeutic Implications. *Hematology Am. Soc. Hematol. Educ. Program* 2016, 1(1), 348–355.
- Xu, Z.-J.; Gu, Y.; Wang, C.-Z.; Jin, Y.; Wen, X.-M.; Ma, J.-C.; Tang, L.-J.; Mao, Z.-W.; Qian, J.; Lin, J. The M2 Macrophage Marker CD206: A Novel Prognostic Indicator for Acute Myeloid Leukemia. *Oncoimmunology* 2020, 9 (1), 1683347.
- Abbasi, S.; Diab, O.; Mohyuddin, G. R.; Singh, A. K. In-Hospital Morbidity and Mortality among Acute Myeloid Leukemia Patients Admitted for Hematopoietic Stem Cell Transplants between 2002–2014. *Blood* 2019, 134 (Supplement_1), 2147–2147.
- Deschler, B.; Lübbert, M. Acute Myeloid Leukemia: Epidemiology and Etiology. In *Acute Leukemias*; Springer Berlin Heidelberg: Berlin, Heidelberg, 2008; pp 47–56.
- Dix, C.; Lo, T.-H.; Clark, G.; Abadir, E. Measurable Residual Disease in Acute Myeloid Leukemia Using Flow Cytometry: A Review of Where We Are and Where We Are Going. *J. Clin. Med.* 2020, 9 (6), 1714.
- Seiter, K. Acute Myeloid Leukemia (AML) Medication. <https://emedicine.medscape.com/article/197802-medication> (accessed Nov 6, 2020).
- Leukemia & Lymphoma Society. Acute Myeloid Leukemia, 2019 Leukemia & Lymphoma Society Website. https://www.lls.org/sites/default/files/file_assets/PS32_AML_Booklet_2019_FINAL.pdf (accessed Nov 6, 2020)
- Gaballa, S.; Saliba, R.; Oran, B.; Brammer, J. E.; Chen, J.; Rondon, G.; Alousi, A. M.; Kebriaei, P.; Marin, D.; Popat, U. R.; Andersson, B. S.; Shpall, E. J.; Jabbour, E.; Dayer, N.; Andreeff, M.; Ravandi, F.; Cortes, J.; Patel, K.; Champlin, R. E.; Ciurea, S. O. Relapse Risk and Survival in Patients with FLT3 Mutated Acute Myeloid Leukemia Undergoing Stem Cell Transplantation. *Am. J. Hematol.* 2017, 92 (4), 331–337.
- Carlson, K.-S. B.; Guzman, M. L. Is Minimal Residual Disease Monitoring Clinically Relevant in Adults with Acute Myelogenous Leukemia? *Curr. Hematol. Malig. Rep.* 2013, 8 (2), 109–115
- Döhner, H.; Estey, E.; Grimwade, D.; Amadori, S.; Appelbaum, F. R.; Büchner, T.; Dombret, H.; Ebert, B. L.; Fenau, P.; Larson, R. A.; Levine, R. L.; Lo-Coco, F.; Naoe, T.; Niederwieser, D.; Ossenkoppele, G. J.; Sanz, M.; Sierra, J.; Tallman, M. S.; Tien, H.-F.; Wei, A. H.; Löwenberg, B.; Bloomfield, C. D. Diagnosis and Management of AML in Adults: 2017 ELN Recommendations from an International Expert Panel. *Blood* 2017, 129 (4), 424–447.
- Salipante, S. J.; Fromm, J. R.; Shendure, J.; Wood, B. L.; Wu, D. Detection of Minimal Residual Disease in NPM1-Mutated Acute Myeloid Leukemia by next-Generation Sequencing. *Mod. Pathol.* 2014, 27 (11), 1438–1446.
- Buccisano, F.; Maurillo, L.; Del Principe, M. I.; Del Poeta, G.; Sconocchia, G.; Lo-Coco, F.; Arcese, W.; Amadori, S.; Venditti, A. Prognostic and Therapeutic Implications of Minimal Residual Disease Detection in Acute Myeloid Leukemia. *Blood* 2012, 119 (2), 332–341.
- Duployez, N.; Nibourel, O.; Marceau-Renaut, A.; Willekens, C.; Helevaut, N.; Caillaud, A.; Villenet, C.; Celli-Lebras, K.; Boissel, N.; Jourdan, E.; Dombret, H.; Figeac, M.; Preudhomme, C.;

- Renneville, A. Minimal Residual Disease Monitoring in t(8;21) Acute Myeloid Leukemia Based on RUNX1-RUNX1T1 Fusion Quantification on Genomic DNA: Minimal Residual Disease Monitoring Int(8;21) Acute Myeloid Leukemia. *Am. J. Hematol.* 2014, 89 (6), 610–615.
15. Kundu, M.; Liu, P. P. Function of the Inv(16) Fusion Gene CBFβ MYH11. *Curr. Opin. Hematol.* 2001, 8 (4), 201–205.
16. Noguera, N. I.; Catalano, G.; Banella, C.; Divona, M.; Faraoni, I.; Ottone, T.; Arcese, W.; Voso, M. T. Acute Promyelocytic Leukemia: Update on the Mechanisms of Leukemogenesis, Resistance and on Innovative Treatment Strategies. *Cancers (Basel)* 2019, 11 (10), 1591.
17. Norkin, M.; Katragadda, L.; Zou, F.; Xiong, S.; Chang, M.; Dai, Y.; Hsu, J. W.; Moreb, J. S.; Leather, H.; Murthy, H. S.; Farhadfar, N.; Li, Y.; Hromas, R.; Brown, R. A.; Cogle, C. R.; Wingard, J. R. Minimal Residual Disease by Either Flow Cytometry or Cytogenetics Prior to an Allogeneic Hematopoietic Stem Cell Transplant Is Associated with Poor Outcome in Acute Myeloid Leukemia. *Blood Cancer J.* 2017, 7 (12), 1–8.
18. Šálek, C.; Folber, F.; Froňková, E.; Procházka, B.; Marinov, I.; Cetkovský, P.; Mayer, J.; Doubek, M.; Czech Leukemia Study Group - for Life. Early MRD Response as a Prognostic Factor in Adult Patients with Acute Lymphoblastic Leukemia. *Eur. J. Haematol.* 2016, 96 (3), 276–284.
19. Schuurhuis, G. J.; Heuser, M.; Freeman, S.; Béné, M.-C.; Buccisano, F.; Cloos, J.; Grimwade, D.; Haferlach, T.; Hills, R. K.; Hourigan, C. S.; Jorgensen, J. L.; Kern, W.; Lacombe, F.; Maurillo, L.; Preudhomme, C.; van der Reijden, B. A.; Thiede, C.; Venditti, A.; Vyas, P.; Wood, B. L.; Walter, R. B.; Döhner, K.; Roboz, G. J.; Ossenkoppele, G. J. Minimal/Measurable Residual Disease in AML: A Consensus Document from the European LeukemiaNet MRD Working Party. *Blood* 2018, 131 (12), 1275–1291.
20. Verma, D.; Kantarjian, H.; Faderl, S.; O'Brien, S.; Pierce, S.; Vu, K.; Freireich, E.; Keating, M.; Cortes, J.; Ravandi, F. Late Relapses in Acute Myeloid Leukemia: Analysis of Characteristics and Outcome. *Leuk. Lymphoma* 2010, 51 (5), 778–782.
21. Ravandi, F.; Walter, R. B.; Freeman, S. D. Evaluating Measurable Residual Disease in Acute Myeloid Leukemia. *Blood Adv.* 2018, 2 (11), 1356–1366.
22. Bill, M.; Grimm, J.; Jentzsch, M.; Kloss, L.; Goldmann, K.; Schulz, J.; Beinicke, S.; Häntschel, J.; Cross, M.; Vucinic, V.; Pönsch, W.; Behre, G.; Franke, G.-N.; Lange, T.; Niederwieser, D.; Schwind, S. Digital Droplet PCR-Based Absolute Quantification of Pre-Transplant NPM1 Mutation Burden Predicts Relapse in Acute Myeloid Leukemia Patients. *Ann. Hematol.* 2018, 97 (10), 1757–1765.
23. Hourigan, C. S.; Dillon, L. W.; Gui, G.; Logan, B. R.; Fei, M.; Ghannam, J.; Li, Y.; Licon, A.; Alyea, E. P.; Bashey, A.; Deeg, H. J.; Devine, S. M.; Fernandez, H. F.; Giralt, S.; Hamadani, M.; Howard, A.; Maziars, R. T.; Porter, D. L.; Scott, B. L.; Warlick, E. D.; Pasquini, M. C.; Horwitz, M. E. Impact of Conditioning Intensity of Allogeneic Transplantation for Acute Myeloid Leukemia with Genomic Evidence of Residual Disease. *J. Clin. Oncol.* 2020, 38 (12), 1273–1283.
24. Paschka, P.; Schlenk, R. F.; Gaidzik, V. I.; Habdank, M.; Krönke, J.; Bullinger, L.; Späth, D.; Kayser, S.; Zucknick, M.; Götze, K.; Horst, H.-A.; Germing, U.; Döhner, H.; Döhner, K. IDH1 and IDH2 Mutations Are Frequent Genetic Alterations in Acute Myeloid Leukemia and Confer Adverse Prognosis in Cytogenetically Normal Acute Myeloid Leukemia with NPM1 Mutation without FLT3 Internal Tandem Duplication. *J. Clin. Oncol.* 2010, 28 (22), 3636–3643.
25. Juliusson, G.; Jädersten, M.; Deneberg, S.; Lehmann, S.; Möllgård, L.; Wennström, L.; Antunovic, P.; Cammenga, J.; Lorenz, F.; Ölander, E.; Lazarevic, V. L.; Höglund, M. The Prognostic Impact of FLT3-ITD and NPM1 Mutation in Adult AML Is Age-Dependent in the Population-Based Setting. *Blood Adv.* 2020, 4 (6), 1094–1101.
26. Jongen-Lavrencic, M.; Grob, T.; Hanekamp, D.; Kavelaars, F. G.; al Hinai, A.; Zeilemaker, A.; Erpelinck-Verschueren, C. A. J.; Gradowska, P. L.; Meijer, R.; Cloos, J.; Biemond, B. J.; Graux, C.; van Marwijk Kooy, M.; Manz, M. G.; Pabst, T.; Passweg, J. R.; Havelange, V.; Ossenkoppele, G. J.; Sanders, M. A.; Schuurhuis, G. J.; Löwenberg, B.; Valk, P. J. M. Molecular Minimal Residual Disease in Acute Myeloid Leukemia. *N. Engl. J. Med.* 2018, 378 (13), 1189–1199.
27. Bertoli, S.; Tavitian, S.; Bérard, E.; Mansat-De Mas, V.; Largeaud, L.; Gadaud, N.; Rieu, J.-B.; Vergez, F.; Luquet, I.; Hugué, F.; Sarry, A.; Delabesse, E.; Récher, C. More than Ten Percent of Relapses Occur after Five Years in AML Patients with NPM1 Mutation. *Leuk. Lymphoma* 2020, 61 (5), 1226–1229.
28. Höllein, A.; Meggendorfer, M.; Dicker, F.; Jeromin, S.; Nadarajah, N.; Kern, W.; Haferlach, C.; Haferlach, T. NPM1 Mutated AML Can Relapse with Wild-Type NPM1: Persistent Clonal Hematopoiesis Can Drive Relapse. *Blood Adv.* 2018, 2 (22), 3118–3125.
29. Debarri, H.; Lebon, D.; Roumier, C.; Cheok, M.; Marceau Renaut, A.; Nibourel, O.; Geffroy, S.; Helevaut, N.; Rousselot, P.; Gruson, B.; Gardin, C.; Chretien, M.-L.; Sebda, S.; Figeac, M.; Berthon, C.; Quesnel, B.; Boissel, N.; Castaigne, S.; Dombret, H.; Renneville, A.; Preudhomme, C. IDH1/2 but Not DNMT3A Mutations Are Suitable Targets for Minimal Residual Disease Monitoring in Acute Myeloid Leukemia Patients: A Study by the Acute Leukemia French Association. *Oncotarget* 2015, 6 (39), 42345–42353.
30. Patel, J. L.; Schumacher, J. A.; Frizzell, K.; Sorrells, S.; Shen, W.; Clayton, A.; Jattani, R.; Kelley, T. W. Coexisting and Cooperating Mutations in NPM1 -Mutated Acute Myeloid Leukemia. *Leuk. Res.* 2017, 56, 7–12.
31. Gaidzik, V. I.; Schlenk, R. F.; Paschka, P.; Stölzle, A.; Späth, D.; Kuendgen, A.; von Lilienfeld-Toal, M.; Brügger, W.; Derigs, H. G.; Kremers, S.; Greil, R.; Raghavachar, A.; Ringhoffer, M.; Salih, H. R.; Wattad, M.; Kirchen, H. G.; Runde, V.; Heil, G.; Petzer, A. L.; Girschikofsky, M.; Heuser, M.; Kayser, S.; Goehring, G.; Teleanu, M.-V.; Schlegelberger, B.; Ganser, A.; Krauter, J.; Bullinger, L.; Döhner, H.; Döhner, K. Clinical Impact of DNMT3A Mutations in Younger Adult Patients with Acute Myeloid Leukemia: Results of the AML Study Group (AML5G). *Blood* 2013, 121 (23), 4769–4777.
32. Brambati, C.; Galbiati, S.; Xue, E.; Toffalori, C.; Crucitti, L.; Greco, R.; Sala, E.; Crippa, A.; Chiesa, L.; Soriani, N.; Mazzi, B.; Tresoldi, C.; Stanghellini, M. T. L.; Peccatori, J.; Carrabba, M. G.; Bernardi, M.; Ferrari, M.; Lampasona, V.; Ciceri, F.; Vago, L. Droplet Digital Polymerase Chain Reaction for DNMT3A and IDH1/2 Mutations to Improve Early Detection of Acute Myeloid Leukemia Relapse after Allogeneic Hematopoietic Stem Cell Transplantation. *Haematologica* 2016, 101 (4), e157–61.
33. Levis, M. FLT3 Mutations in Acute Myeloid Leukemia: What Is the Best Approach in 2013? *Hematology Am. Soc. Hematol. Educ. Program* 2013, 2013 (1), 220–226.
34. Santos, F. P. S.; Jones, D.; Qiao, W.; Cortes, J. E.; Ravandi, F.; Estey, E. E.; Verma, D.; Kantarjian, H.; Borthakur, G. Prognostic Value of FLT3 Mutations among Different Cytogenetic Subgroups in Acute Myeloid Leukemia. *Cancer* 2011, 117 (10), 2145–2155.

35. Pratorcorona, M.; Brunet, S.; Nomdedéu, J.; Ribera, J. M.; Tormo, M.; Duarte, R.; Escoda, L.; Guàrdia, R.; Queipo de Llano, M. P.; Salamero, O.; Bargay, J.; Pedro, C.; Martí, J. M.; Torredadell, M.; Díaz-Beyá, M.; Camós, M.; Colomer, D.; Hoyos, M.; Sierra, J.; Esteve, J.; Grupo Cooperativo Para el Estudio y Tratamiento de las Leucemias Agudas Mieloblásticas. Favorable Outcome of Patients with Acute Myeloid Leukemia Harboring a Low-Allelic Burden FLT3-ITD Mutation and Concomitant NPM1 Mutation: Relevance to Post-Remission Therapy. *Blood* 2013, 121 (14), 2734–2738.
36. Boddu, P.; Kantarjian, H.; Borthakur, G.; Kadia, T.; Daver, N.; Pierce, S.; Andreeff, M.; Ravandi, F.; Cortes, J.; Kornblau, S. M. Co-Occurrence of FLT3-TKD and NPM1 Mutations Defines a Highly Favorable Prognostic AML Group. *Blood Adv.* 2017, 1 (19), 1546–1550.
37. Blätte, T. J.; Schmalbrock, L. K.; Skambraks, S.; Lux, S.; Cocciardi, S.; Dolnik, A.; Döhner, H.; Döhner, K.; Bullinger, L. GetITD for FLT3-ITD-Based MRD Monitoring in AML. *Leukemia* 2019, 33 (10), 2535–2539.
38. McKinnon, K. M. Flow Cytometry: An Overview. *Curr. Protoc. Immunol.* 2018, 120 (1), 5.1.1–5.1.11.
39. Kern, W.; Haferlach, C.; Haferlach, T.; Schnittger, S. Monitoring of Minimal Residual Disease in Acute Myeloid Leukemia. *Cancer* 2008, 112 (1), 4–16.
40. Kralik, P.; Ricchi, M. A Basic Guide to Real Time PCR in Microbial Diagnostics: Definitions, Parameters, and Everything. *Front. Microbiol.* 2017, 8, 108.
41. Bio-Rad Laboratories, Inc. Droplet Digital™ PCR (ddPCR™) Technology. <https://www.bio-rad.com/en-uk/applications-technologies/droplet-digital-pcr-ddpcr-technology?ID=MDV31M4VY> (accessed Nov 4, 2020).
42. Grimwade, D.; Freeman, S. D. Defining Minimal Residual Disease in Acute Myeloid Leukemia: Which Platforms Are Ready for “Prime Time”? *Blood* 2014, 124 (23), 3345–3355.
43. Levine, R. L.; Valk, P. J. M. Next-Generation Sequencing in the Diagnosis and Minimal Residual Disease Assessment of Acute Myeloid Leukemia. *Haematologica* 2019, 104 (5), 868–871.
44. Mack, E. K. M.; Marquardt, A.; Langer, D.; Ross, P.; Ultsch, A.; Kiehl, M. G.; Mack, H. I. D.; Haferlach, T.; Neubauer, A.; Brendel, C. Comprehensive Genetic Diagnosis of Acute Myeloid Leukemia by Next-Generation Sequencing. *Haematologica* 2019, 104 (2), 277–287.
45. Short, N. J. Complete response, minimal residual disease negativity linked to lower relapse risk in relapsed/refractory AML. <https://www.healio.com/news/hematology-oncology/20191213/complete-response-minimal-residual-disease-negativity-linked-to-lower-relapse-risk-in-relapsedrefrac> (accessed Jan 12, 2021).
46. Walter, R. B.; Buckley, S. A.; Pagel, J. M.; Wood, B. L.; Storer, B. E.; Sandmaier, B. M.; Fang, M.; Gyurkocza, B.; Delaney, C.; Radich, J. P.; Estey, E. H.; Appelbaum, F. R. Significance of Minimal Residual Disease before Myeloablative Allogeneic Hematopoietic Cell Transplantation for AML in First and Second Complete Remission. *Blood* 2013, 122 (10), 1813–1821.
47. Ommen, H. B.; Schnittger, S.; Jovanovic, J. V.; Ommen, I. B.; Hasle, H.; Østergaard, M.; Grimwade, D.; Hokland, P. Strikingly Different Molecular Relapse Kinetics in NPM1c, PML-RARA, RUNX1-RUNX1T1, and CBFβ-MYH11 Acute Myeloid Leukemias. *Blood* 2010, 115 (2), 198–205.
48. Stentoft, J.; Hokland, P.; Østergaard, M.; Hasle, H.; Nyvold, C. G. Minimal Residual Core Binding Factor AMLs by Real Time Quantitative PCR—Initial Response to Chemotherapy Predicts Event Free Survival and Close Monitoring of Peripheral Blood Unravels the Kinetics of Relapse. *Leuk. Res.* 2006, 30 (4), 389–395.
49. Patel, S. S.; Kuo, F. C.; Gibson, C. J.; Steensma, D. P.; Soiffer, R. J.; Alyea, E. P., 3rd; Chen, Y.-B. A.; Fathi, A. T.; Graubert, T. A.; Brunner, A. M.; Wadleigh, M.; Stone, R. M.; DeAngelo, D. J.; Nardi, V.; Hasserjian, R. P.; Weinberg, O. K. High NPM1-Mutant Allele Burden at Diagnosis Predicts Unfavorable Outcomes in de Novo AML. *Blood* 2018, 131 (25), 2816–2825.
50. Bader, P.; Kreyenberg, H.; Ossenkoppele, G. Monitoring Minimal Residual Disease in ALL and AML. In *The EBMT Handbook*; Springer International Publishing: Cham, 2019; pp 431–436.
51. Venditti, A.; Piciocchi, A.; Candoni, A.; Melillo, L.; Calafiore, V.; Cairoli, R.; de Fabritiis, P.; Storti, G.; Salutari, P.; Lanza, F.; Martinelli, G.; Luppi, M.; Mazza, P.; Martelli, M. P.; Cuneo, A.; Albano, F.; Fabbiano, F.; Tafuri, A.; Chierichini, A.; Tieghi, A.; Fracchiolla, N. S.; Capelli, D.; Foà, R.; Alati, C.; La Sala, E.; Fazi, P.; Vignetti, M.; Maurillo, L.; Buccisano, F.; Del Principe, M. I.; Irno-Consalvo, M.; Ottone, T.; Lavorgna, S.; Voso, M. T.; Lo-Coco, F.; Arcese, W.; Amadori, S. GIMEMA AML1310 Trial of Risk-Adapted, MRD-Directed Therapy for Young Adults with Newly Diagnosed Acute Myeloid Leukemia. *Blood* 2019, 134 (12), 935–945.
52. Zhu, H.-H.; Zhang, X.-H.; Qin, Y.-Z.; Liu, D.-H.; Jiang, H.; Chen, H.; Jiang, Q.; Xu, L.-P.; Lu, J.; Han, W.; Bao, L.; Wang, Y.; Chen, Y.-H.; Wang, J.-Z.; Wang, F.-R.; Lai, Y.-Y.; Chai, J.-Y.; Wang, L.-R.; Liu, Y.-R.; Liu, K.-Y.; Jiang, B.; Huang, X.-J. MRD-Directed Risk Stratification Treatment May Improve Outcomes of t(8;21) AML in the First Complete Remission: Results from the AML05 Multicenter Trial. *Blood* 2013, 121 (20), 4056–4062.

■ Author

Lok Yin Kwan is a senior student at HKUGA College. She is an avid learner with a desire to acquire knowledge that is beyond her school curriculum. She hopes to pursue her passion in biomedical sciences and helping others by taking up medicine in university.

The Prevalence of Post-Traumatic Stress Disorder in Self-Identified South Asians

Sruthi K. Medepalli

Lynbrook High School, 1280 Johnson Ave, San Jose, CA, 95129, USA; sruthi.medepalli@gmail.com

ABSTRACT: Post-traumatic stress disorder (PTSD) is widely regarded as a post-war veteran's disease, a stereotype that this study aims to dispel. The goal of this study was to determine the prevalence of this disorder in understudied populations, specifically in the South Asian population. Firstly, the prevalence of post-traumatic stress disorder (PTSD) in various geographical areas was determined using existing datasets. This experimental approach to determining PTSD prevalence used the PCL-C self-assessment and scoring based on the Diagnostic and Statistical Manual of Mental Disorders (DSM-5) criterion. 40 adult subjects of South Asian descent living in the U.S., Canada, and India were randomly selected and their anonymous responses to the PCL-C questions were analyzed. The results showed that 37.5% of the subjects had moderate to very severe levels of PTSD. This suggests that there may be a higher percentage of PTSD in South Asians than previously recognized. This study was limited by the fact that the South Asians within this study were self-identified and that the study had a small sample. However, due to the inadequate amount of existing research on anxiety and trauma/stressor-related disorders in this subject population, it is highly recommended that a broader and deeper study of PTSD prevalence, causes, and treatment in this population be examined.

KEYWORDS: Behavioral and Social Sciences; Neuroscience; Mental Disorders; Post-Traumatic Stress Disorder; South Asia.

■ Introduction

One in eleven people will be diagnosed with PTSD at some point in their lives, and it affects about 8 million people per any given year.¹ Soldiers and veterans are most susceptible to trauma, and therefore, to PTSD. But this "soldier's disease" has been given multiple names in its past, including "shell-shock" during World War I and "combat fatigue" in the time of World War II. Although these descriptions corresponded to the same disease, the idea that PTSD only affected war veterans was erroneous.

Causes and Risk Factors:

Risk factors for PTSD include histories of substance abuse, mental illness, physical and sexual assault, high-stress level in daily life, lack of a support system, and poor coping mechanisms. Women are twice as likely to get PTSD simply for the reason that they are a more common target for sexual assault and rape.²

Family history is one of the biggest factors for mental illnesses and neurodegenerative disorders, and PTSD is no different. Susceptibility to PTSD also has genetic components and environmental effects as a result of trauma, that

leaves a chemical (epigenetic) mark on your genes, as illustrated in Figure 1.

Diagnosis and Brain Function:

When diagnosing patients for PTSD, clinicians often look for detachment, reexperiencing the traumatic event, emotional effects, avoidance, and sympathetic hyperactivity (hypervigilance), most of which must span a month or longer. More specifically, physicians often examine the amygdala, prefrontal cortex, and hippocampus. Indicators of PTSD come from immune, genetic, hormonal, and diagnostic factors. The amygdala is used for fear, and PTSD affected brains often over-panic and have heightened fear reactions. The prefrontal cortex processes and regulates the emotional reactions coming from the amygdala, and it often does not function well when a patient has PTSD because of their tendency to be over/under emotional. Finally, the hippocampus is the memory center of the brain, and the PTSD-affected brain has difficulty remembering the event and often constantly replays specific memories of the trauma.⁴

As with other psychological disorders, physicians often refer to the DSM-5. The manual, as written by the American Psychological Association, lists seven criteria that must be met in response to the first criteria, a stressor.⁵ Criterion A is arguably one of the most essential to be met, as most other criteria overlap with those of general anxiety disorders and phobias, as well as acute stress disorder. A stressor is defined as an event in which one has been exposed to death, threatened death, actual or threatened sexual violence. Criteria B and C include intrusion symptoms and avoidance, with at least one of each required. These are defined as the traumatic event being persistently reexperienced in memories, nightmares, flashbacks, emotional distress, physical reactivity to trauma

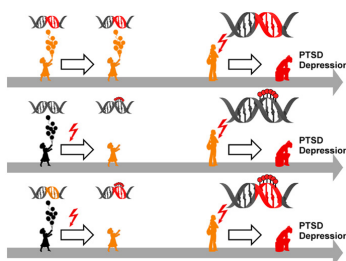


Figure 1: Diagram of Genetic PTSD.³

reminders respectively. Criterion D, or negative alterations in cognitions and mood, is negative thoughts/feelings that have worsened after trauma in inability to recall key features of the trauma, exaggerated blame, decreased interest, and isolation. Two of these are required for a patient to be properly diagnosed. Criterion E is closely related, being alternations in arousal and activity. This is shown through worsened behavior such as irritability, risky or destructive behavior, heightened startle reaction, difficulty sleeping and concentrating. Criteria F, G, and H are duration, exclusion, and distress. These require that symptoms last for more than a month, are not due to substance abuse, medication, or mental illness, and cause distress or functional impairment.

Screening and Treatment:

Current brain-screening techniques include Positron Emission Tomography (PET) scans of mGluR5 receptor availability, which is a type of brain cell receptor for the neurotransmitter glutamate, that is altered in PTSD patients. Figure 2 showcases the PET scan of a PTSD affected brain.

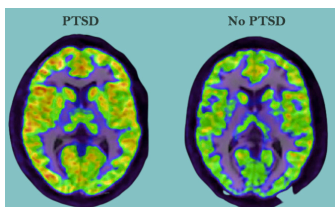


Figure 2: PET Scan of PTSD Afflicted Brain vs. Healthy Brain.⁶

Magnetic Resonance Imaging (MRI) scans assess the effects of stroke, trauma, and degenerative diseases and can be used on PTSD patients to reveal grey-matter reductions in certain parts of the brain, as demonstrated in Figure 3 (see scan on the left).

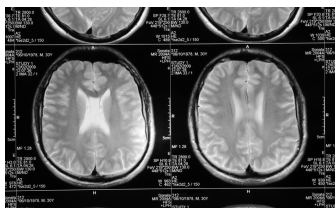


Figure 3: MRI Scan of Healthy Brain vs. PTSD Afflicted Brain.⁷

The current most productive treatment is therapy-based, specifically Cognitive-Behavioral Therapy (CBT) and Eye Movement Desensitization & Reprocessing (EMDR). Other common forms of psychotherapy include exposure therapy, cognitive restructuring therapy, and group therapy. Therapists employing CBT encourage patients to re-evaluate their thinking patterns and assumptions to identify unhelpful patterns in thought, like overgeneralizing bad outcomes, negative thinking, and expectations of catastrophic outcomes, into more positive and effective thinking patterns. CBT is meant to help the person rethink their understanding of traumatic experiences, themselves, and their ability to cope. The goal of exposure therapies for the patient will actively confront fears and emotions, learning along the way that anxiety and fear will lessen on their own. The goal is to eliminate avoidance and increasing quality of life. EMDR therapy accesses the traumatic memory network in order to enhance information

processing, forming new associations between the traumatic memory and more adaptive memories or information. Trauma is often stuck in the limbic system of the brain, consisting mainly of the hippocampus, amygdala, hypothalamus, and thalamus, and which is known as the emotional brain. EMDR focuses specifically on these areas. These result in elimination of emotional distress and development of cognitive insight.

Pharmacological treatments can also be effective, and usually aim to reduce specific symptoms. Symptoms of PTSD overlap with those of depression and anxiety; therefore, antidepressants and anti-anxiety medication are feasible for patients. Anti-depressants focus on the production of three chemicals in the brain- serotonin, norepinephrine, and oxytocin. Ongoing and completed clinical trials have investigated the effect that music therapy,⁸ cannabis,⁹ and medications including hydrocortisone, morphine, oxytocin, propranolol, and benzodiazepines.¹⁰ Understanding the differences in approaching trauma and targeting symptoms is vital to a full understanding of the disorder.

Geography:

Current research in PTSD based on geographic location shows a very limited reach, and studies generally only research into countries in Europe and the Americas. Countries like Canada show the highest PTSD-affected population, at 9.20%,¹¹ while China has the lowest rate, with only 0.30%¹² reported with PTSD. A geographical compilation of existing PTSD research is encapsulated in Figure 4. As seen there, the South Asian region has been greyed out, only limited studies have been done in the villages surrounding Pakistan, Bangladesh, and India investigating the effects of low natural resources and disasters on PTSD.¹³ In contrast, this research focuses on the prevalence of PTSD in the South Asian ethnic pool.

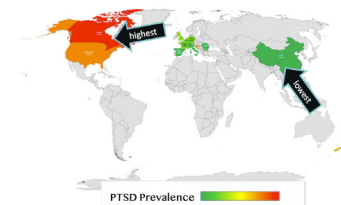


Figure 4: PTSD Prevalence.

■ Methods

The PCL-C self-assessment was used based on the DSM-5 PTSD symptom requirements. The exact measures and questions from the official assessment were entered onto an online form, allowing participants to be completely anonymous. Therefore, there was no requirement to submit the methods to a research review board. This study assumed the presence of a stressor, or Criterion A (Diagnosis and Brain Function) in each participant, given the variance in the answers received when asking for participants to recall a traumatic event. Hence, the eventual prognoses may lack certainty in associating stressor type and severity with a specific individual. The anonymous surveys were conducted from August 2020 to September 2020 by sending the online form to social media groups dominated by South Asians and a random pool of subjects voluntarily responded to it. The subjects

spread across the US, Canada and India (12 respondents were from US, 18 from Canada, 10 were from India). The subject age group were adults 18 and older. Due to the sensitive nature of this survey, the privacy of the subjects has been strictly enforced, hence no attempt has been made to correlate subjects with underlying health problems or genetic history. However, none of the subjects had prior diagnosis or awareness of PTSD. The 40 subjects were assigned patient numbers and each one was diagnosed. This was done by adding together their given responses from a range of 1-4 to 20 questions. From there, the percentage of subjects with mild, moderate, severe, and very severe PTSD were found.¹⁴ The control group was composed of subjects with scores from 21-29. Those who scored between 30-35 were diagnosed with mild PTSD, 36-45 was moderate, 45-55 was severe, and subjects who scored above 56 had very severe PTSD.

Results and Discussion

Table 1 summarizes the survey results grouped by PTSD severity. The most common group within our subjects was the control group, or individuals with no official PTSD diagnosis accounting for 37.5%. 15% were diagnosed with mild PTSD, 17.5% with moderate, 7.5% with severe PTSD, and an alarming 12.5% with very severe PTSD. This means that the percentage of subjects with severe and very severe PTSD was in total, 20%. Figure 5 graphs the severity of the subjects overall in order to gain a fuller understanding of the distribution of scores.

Table 1: PTSD Scores Received.

Control	Mild	Moderate	Severe	Very Severe
21	31	36	50	57
21	33	36	51	62
21	33	37	53	68
23	33	39		76
24	34	42		86
24	35	43		
24		43		
24				
24				
25				
25				
26				
26				
28				

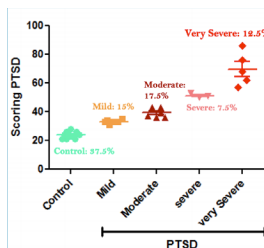


Figure 5: PTSD Scores Organized by Severity.

This experimental study also showed that although 3.5% of U.S. citizens experience PTSD, the average score of subjects in the U.S. was 38, indicating moderate to severe PTSD. Furthermore, past research shows that 9.20% of Canadian citizens have been diagnosed with PTSD, and in this study, it was observed that Canada had sufficiently lower scores than the average of the U.S. Figure 6 shows the geographical prevalence of PTSD in the subjects. Based on the data collected from every subject which self-identified as being of South Asian,

descent, the scores received were all sufficiently higher than the 5.2 percent average worldwide.¹⁵

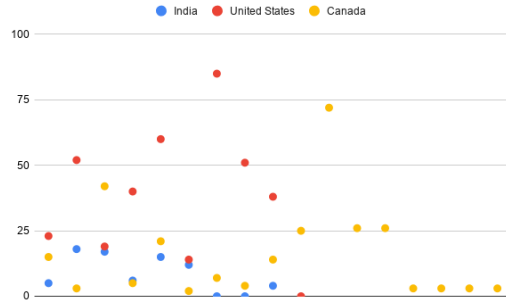


Figure 6: PTSD Scores Organized by Geographys.

These scores were potentially affected by the stress of the coronavirus pandemic, which gave families worldwide trauma from businesses closing, death of loved ones, and even having the virus themselves.

Conclusion

The prevalence of PTSD in the South Asian population and in the coronavirus-affected world is disproportionately large, indicating further studies into these particular subject groups. Having a realistic idea of how common trauma and mental disorders is necessary for the general public and for patients. With stress about working conditions, personal/family health, and online school, the entire population has become more susceptible to trauma. 20% of the subjects in this study were diagnosed with severe to very severe PTSD with no previous diagnosis or knowledge of PTSD, showing how often and undiscussed this disorder is. This 20% average, although within a relatively small sample size, shows a clear advance from the 5.2% of PTSD-affected people worldwide. Previous research focuses mainly on areas within Europe and North America, disregarding Asian countries, despite the level of PTSD there and the universal nature of PTSD exposure – PTSD can affect anyone. Hence, it is strongly recommended that future studies are conducted with a focus in this ethnic group. Larger sample sizes within these areas are highly encouraged in order to gain a better understanding. Finally, understanding the effect this pandemic has had on humans’ mental state and risk towards trauma is also essential to helping everyone recover from this past year – for example, repeating this survey with the same subjects after the COVID pandemic has ended globally.

Acknowledgements

I am incredibly grateful to my mentor, Dr. Shrivastava, for helping me through this process, to SkoolMentor for allowing me access to this opportunity, and to my entire family, for continuing to support me in my endeavors. I would also love to thank the reviewers, whose advice and comments contributed so much to the contents of this paper and to my own understanding of psychiatric disorders.

References

1. “What Is Posttraumatic Stress Disorder?” What Is PTSD?, American Psychiatric Organization, www.psychiatry.org/patients-families/ptsd/what-is-ptsd. “VA.gov: Veterans Affairs.”

2. How Common Is PTSD in Women?, U.S. Department of Veteran's Affairs, 18 Sept. 2018, www.ptsd.va.gov/understand/common/common_women.asp#:~:text=After%20a%20trauma%2C%20some%20women,likely%20to%20experience%20sexual%20assault.
3. Raabe, Florian & Spengler, Dietmar. (2013). Epigenetic Risk Factors in PTSD and Depression. *Frontiers in psychiatry*. 4. 80. 10.3389/fpsy.2013.00080.
4. Bremner JD. Traumatic stress: effects on the brain. *Dialogues Clin Neurosci*. 2006;8(4):445-461. doi:10.31887/DCNS.2006.8.4/jbremner.
5. Center for Substance Abuse Treatment (US). Trauma-Informed Care in Behavioral Health Services. Rockville (MD): Substance Abuse and Mental Health Services Administration (US); 2014. (Treatment Improvement Protocol (TIP) Series, No. 57.) Exhibit 1.3-4, DSM-5 Diagnostic Criteria for PTSD. Available from: https://www.ncbi.nlm.nih.gov/books/NBK207191/box/part1_ch3.box16/
6. Sophie E. Holmes^{a,b}, Matthew J. Girgentia^{b,c}, Margaret T. Davis^{a,b}, Robert H. Pietrzaka^{b,c}, Nicole DellaGioia^{a,b}, Nabeel Nabulsi^{a,b}, David Matuskeya^b, Steven Southwick^{a,b,c}, Ronald S. Dumana^{b,c}, Richard E. Carson^{a,b}, John H. Krystal^{a,b,c}, Irina Esterlisa^{b,c}, and the Traumatic Stress Brain Study Group, 2017 Altered metabotropic glutamate receptor 5 markers in PTSD: in vivo and postmortem evidence. *Proceedings of the National Academy of Sciences (USA)* 114: 8390-8395.
^aDepartment of Psychiatry, Yale University School of Medicine, New Haven, CT 06519;
^bDepartment of Radiology and Biomedical Imaging, Yale University School of Medicine, New Haven, CT 06519; and ^cNational Center for PTSD, Clinical Neurosciences Division, West Haven, CT 06515
7. Stoppelbein, L., Greening, L., & Fite, P. (2017). The role of cortisol in PTSD among women exposed to a trauma-related stressor. *Journal of Anxiety Disorders*, 26(2), 352–358. <https://doi.org/10.1016/j.janxdis.2011.12.004>
8. “Guitars for Vets: Evaluating Psychological Outcome of a Novel Music Therapy”, Sponsored by US Department of Veterans Affairs, 2015 April 7
9. Orsolini L, Chiappini S, Volpe U, Berardis D, Latini R, Papanti GD, Corkery AJM. Use of Medicinal Cannabis and Synthetic Cannabinoids in Post-Traumatic Stress Disorder (PTSD): A Systematic Review. *Medicina (Kaunas)*. 2019 Aug 23;55(9):525. doi: 10.3390/medicina55090525. PMID: 31450833; PMCID: PMC6780141.
10. Qi W, Gevonden M, Shalev A. Prevention of Post-Traumatic Stress Disorder After Trauma: Current Evidence and Future Directions. *Curr Psychiatry Rep*. 2016 Feb;18(2):20. doi: 10.1007/s11920-015-0655-0. PMID: 26800995; PMCID: PMC4723637.
11. Van Ameringen M, Mancini C, Patterson B, Boyle MH. Post-traumatic stress disorder in Canada. *CNS Neurosci Ther*. 2008 Fall;14(3):171-81. doi: 10.1111/j.1755-5949.2008.00049.x. PMID: 18801110; PMCID: PMC6494052.
12. Xi Y, Chen R, Yan F, Ma X, Rakofsky JJ, Tang L, Guo H, Wu X, Li X, Zhu H, Guo X, Yang Y, Li P, Cao X, Li H, Li Z, Wang P, Xu Q, Tang Y, Broome MR. Low post-traumatic stress disorder rate in Chinese in Beijing, China. *Asian J Psychiatr*. 2017 Dec;30:79-83. doi: 10.1016/j.ajp.2017.07.003. Epub 2017 Jul 4. PMID: 28837943.
13. MP. Shannon, CJ. Lonigan, et al. “Post-Traumatic Stress Disorder in Children and Adolescents One Year after a Super-Cyclone in Orissa, India: Exploring Cross-Cultural Validity and Vulnerability Factors.” *BMC Psychiatry*, BioMed Central, 1 Jan. 1998, bmcpsychiatry.biomedcentral.com/articles/10.1186/1471-244X-7-8.
14. “VA.gov: Veterans Affairs.” Adult PTSD Self-Report Measures, 24 Sept. 2018, www.ptsd.va.gov/professional/assessment/adult-sr/index.asp.
15. Hoppen, T. H., & Morina, N. (2019). The prevalence of PTSD and major depression in the global population of adult war survivors: a meta-analytically informed estimate in absolute numbers. *European journal of psychotraumatology*, 10(1), 1578637. <https://doi.org/10.1080/20008198.2019.1578637>

■ Author

Sruthi Medepalli is a sophomore at Lynbrook High School in San Jose, CA. Her interests include psychiatry, psychology, neuroscience, and journalism. Sruthi aims to bridge the gap between scientific research and common media in order to stop the spread of misinformation and wants to pursue a major in the brain sciences with a minor in literature or journalism.

Carbon-derived Substrate Accelerated the Biodegradation of Low-density Polyethylene

Crystal Radinski

Webber Academy, 1515 93 St SW, Calgary, AB T3H 4A8, Canada; cradinski@hotmail.com

ABSTRACT: Plastic is a commonly used carbon-based product that poses a major environmental pollution hazard due to its poor biodegradability. The natural environment is rich in organic carbon sources. Only few microorganisms have developed abilities to disintegrate heavy plastic molecules, and their lytic capabilities are generally poor. Microorganisms select carbon molecules that require less energy to digest. As bacteria are highly adaptable organisms, it is hypothesized that bacterial plastic biodegradation activity could be stimulated by limiting carbon sources to plastic and forcing bacteria to upregulate necessary metabolic pathways. Bacteria with natural abilities to decompose plastic from three different ecosystems in Alberta, Canada (forest, river, and farm) were cultured in an artificially created environment with limited carbon access. *Pseudomonas* sp. demonstrated the ability to accelerate LDPE biodegradation from 1.39% in carbon-saturated to 21.335% in carbon-restricted mediums in three months. The results of our study suggest that plastic pollution could be reduced by increasing its biodegradation in dedicated composters. Finding a solution to the overwhelming waste issue is critical to the planet's health.

KEYWORDS: Microbiology; Bacteriology; Biodegradation; *Pseudomonas*; Plastic.

■ Introduction

Plastic is a carbon-based polymer of high molecular mass, usually produced from petroleum. It is a very versatile modern material, widely used in the manufacturing of a large range of products from automobiles and buildings to toys and cosmetics.¹ Plastic poses a significant environmental pollution threat due to its resistance to biodegradation. In 2009, it was estimated that 10% of modern waste was in the form of plastics.² In marine areas, plastic debris reaches 50%-80% of total waste.³ Indeed, a study done in 2014 estimated that 245,000 tons of plastic waste were floating in the ocean.⁴ Plastic pollution has been described as the "single greatest threat" to marine animals and birds.⁵ Moreover, animals of different sizes are affected by plastic in a variety of ways. When consumed, plastic blocks digestion in animal's stomachs and can cause starvation. Large marine mammals can be killed by entanglement. Poisoned animals can harm human food supplies as well. Additionally, some additives may be cancerous to humans.⁵ Additives such as phthalates and BPA can provoke hormonal dysregulations like thyroid, fertility, and skin disorders.⁵

The disposal of plastics is extremely difficult. Despite being a carbon-based material, plastics are synthetically produced and, because of the high molecular weight of their hydrophobic long carbon chains, are not easily breakable by microbial enzymes. Several bacteria, yeast, and fungi have been identified to have a weak ability to breakdown plastic.⁶ Research has been done to create biodegradable plastics, but the resulting products are expensive.⁷ In a landfill, plastic becomes a carbon sink, and incineration increases carbon emissions.⁸ If the plastic is incinerated, it also increases carbon emissions and produces polychlorinated di benzo-p-dioxins, a carcinogen.⁹ Recycling is difficult and labor intensive. During 2008 in the US, only 6.5% of plastic waste were recycled, while 85.5% were discarded

in landfills.¹⁰ Because of plastic's intractable resistance to biodegradation, the disposal strategies are crucial and demand attention.

Low-density polyethylene (LDPE) is one of the most used plastics.¹ LDPE biodegradation, the safest way to treat waste, is limited by microbial abilities to break strong polymer chains. Several bacteria have demonstrated a natural ability to biodegrade plastics. *Ideonella sakaiensis* 201-F6 is able to use polyethylene terephthalate (PET) as its major energy and carbon source.¹⁴ *Bacillus brevis* showed ability to degrade polycaprolactone.¹⁶ *Streptomyces* can degrade PHB, poly(3-hydroxybutyrate-co-3-hydroxyvalerate), and polyester.¹⁷

This degradation occurs in sequential steps. Firstly, biodegradation alters the chemical and physical properties of the polymer before bio-fragmentation can use enzymatic cleavage to breakdown polymers to a simpler form. Then, in the assimilation phase, microorganism's uptake polymer molecules produce oxidized metabolites (CO₂, CH₄, H₂O). In the final step of degradation, mineralization occurs.¹⁸

Several natural metabolic pathways leading to plastic degradation were identified. *Ideonella sakaiensis* produces two enzymes, terephthalic acid and ethylene glycol allow it to efficiently convert PET into environmentally friendly monomers.¹⁷ *Rhodococcus ruber* uses copper-binding laccase in enzymatic degradation of polythene.¹⁹

However, the activity of enzymes participating in the synthetic polymer's fermentation has been shown to be weak. This could be possibly explained by the availability of other biopolymers, such as cellulose, requiring less energy to digest.¹¹ Nevertheless, since natural pathways for plastic fermentation exist, it might be possible to stimulate their activity to increase plastic natural and safe decay. It is possible that re

stricting bacterial sources of carbon to plastic will cause the microorganisms to adapt and naturally activate their plastic biodegrading ability. Providing synthetic polymers, like plastic, as a sole carbon source will stimulate bacteria to adapt to these carbon sources, forcing the upregulation of plastic-degrading enzymes to allow the metabolism of synthetic polymers and, therefore, help decompose plastic into environmentally neutral monomers faster.

■ Methods

In the first stage of this study, to obtain bacteria with natural plastic biodegradation ability, soils from three sources were utilized: an Alberta cattle farm, Elbow riverbed, and an Alberta mixed forest. It was previously demonstrated that biodegradation begins with the colonization of microorganisms on the surface of the material.¹² Soil microorganisms were cultured in nature-like landfill conditions, recreated in a miniature, enclosed ecosystem. Winogradsky columns containing the soil, rainwater, and 30 cm² LDPE strips were used. Plastic samples were incubated for three months in a room with indirect natural light and allowed temperature fluctuation consistent with the Alberta climate. This allowed the bacterial strains capable of using LDPE as a carbon source to colonize the plastic. After three months, biofilm was observed to form on the surfaces of the plastic. Three colonies formed on the plastic incubated in the forest ecosystem, three in the river and six in the farm Winogradsky columns. Bacterial samples were collected and cultured on agar in petri dishes to isolate monoclonal bacterial cultures with the presumed natural plastic-degradation ability. Twelve colonies were isolated and used as the study subjects in the second stage of the study.

In the second stage, to assess each isolate's plastic biodegradation activity (BA), two test groups were created with carbon-restricted and carbon-enriched media. Each bacterial culture was with an LDPE sample in two mediums for three months. In three months, the BA in the two groups was compared. Biodegradation is characterized by signs of disintegration such as a loss of weight, change in physical properties, carbon dioxide production etc. In this study, BA was monitored as a percentage of plastic weight loss after three months of incubation. BA in the control group served as an indicator of baseline biodegradation activity for a given bacterial strain.

Procedure:c

Twenty-five 15 ml test tubes were sterilized and filled with 10 ml sterile Bushnell-Haas medium (MgSO₄ - 0.2g, CaCl₂- 0.02g, KH₂PO₄- 1g, FeCl₂ - 0.05g, NH₄NO₃ - 1g, distilled water - 1000 ml, pH - 7.0) to provide necessary elements for bacterial growth other than carbon. Twenty-five strips of LDPE plastic (1x3cm) were prepared: washed with distilled water, sterilized with 70% ethanol for 5 minutes and subsequently dried in an incubator at 25°C for 24 hours. Plastic samples were then weighed with a Mettler Toledo model AL204 analytical balance and added to each test tube. In the carbon-restricted group, twelve monoclonal cultures were incubated in a medium where plastic was the only source of carbon. In the carbon-saturated test group, starch was added to the medium as a source of easy-to-digest carbon to

simulate a carbon-rich natural environment (soil). A colony representative of each isolate was inoculated into two test tubes (one in carbon-restricted and one in carbon-enriched groups). Three samples of bacteria were collected from the forest soil, three from the river soil and six from the farm soil agar dishes. A plastic strip was also added to one test tube with a carbon-deprived medium in the absence of inoculum to account for any abiotic losses. Tubes were labelled, and medium and soil type data was recorded in a corresponding logbook. Tubes were incubated for three months at 25°C. The inoculation and incubation were carried out under aseptic conditions. After three months, incubated plastic samples were removed and cleaned of the colonizing bacteria and their metabolism byproducts with water and 70% ethanol. Samples were air-dried for 24 hours before the weight was recorded.

Biodegradation activity, as a percent of LDPE weight loss, was measured for each test sample and compared between respective cultures in carbon-saturated and carbon-restricted mediums. Cultures (isolates) with the most accelerated biodegradation activities were identified following sample preparation using the polymerase chain reaction (PCR) of the 16S rRNA gene and subsequent DNA sequencing at the University of Calgary.

■ Results and Discussion

In the first stage of the study, LDPE samples with bacteria from three Alberta natural environments were colonized to isolate bacteria with presumed natural biodegrading abilities. Twelve bacterial cultures were isolated from colonies formed on LDPE.

A summarized weight loss of the plastic samples after three months of incubation in three natural soils was created to provide a better understanding of the rate of natural biodegradation (Table 1). In the first stage, the most active BA was detected in the soil collected from Alberta mixed forest at 6.01%, compared to farm soil at 3.13 % and from river at 1.27%.

Table 1: Weight (in grams) of plastic samples.

Soil source	initial weight (g)	weight in 3 months (g)	weight loss (g)	% weight at 3 months	BA %
Forest	0.2793	0.2625	0.0168	93.984	6.015
Farm	0.2617	0.2535	0.0082	96.866	3.133
Riverbed	0.2198	0.217	0.0028	98.726	1.273

In the second stage of the experiment, LDPE samples were submerged into carbon-deprived substrate and separately exposed to twelve bacterial isolates with presumed plastic degenerative abilities cultured in the first stage of the study. The results for the carbon-deprived group are summarised in Table 2 and for the carbon-enriched group in Table 3. In three months, all twelve cultures demonstrated an increase in biodegradation activity. A plastic strip incubated in the medium with no inoculum was compared to account for any abiotic losses that did not show any weight loss.

To determine statistical significance in the groups' BA differences, a student t-test was performed.

Twelve bacterial cultures demonstrated statistically significantly increased biodegradation activity in the carbon-deprived

group showed a statistically significant acceleration of biodegrading abilities of microbial cultures.

$$t\text{-value} = -2.92202$$

$$p\text{-value} = .003948$$

Table 2: Plastic weight loss in response to the exposure to monoclonal cultures in carbon-deprived medium.

culture#	source	initial wt./g	wt. at 3 mo./g	wt. loss/g	Wt. at 3 mo. (%)	BA (%)
1	forest	0.0989	0.0778	0.0211	78.6653	21.3346
2	farm	0.0669	0.0663	0.0006	99.1031	0.8968
3	farm	0.0675	0.0643	0.0032	95.2592	4.7407
4	farm	0.0625	0.0609	0.0016	97.44	2.56
5	farm	0.0535	0.0521	0.0001	97.3831	2.6168
6	riverbed	0.0575	0.0574	0.0001	99.826	0.1739
7	forest	0.0603	0.0519	0.0084	86.0696	13.9303
8	forest	0.0503	0.0449	0.0054	89.2644	10.7355
9	riverbed	0.0517	0.0506	0.0011	97.8723	2.1276
10	riverbed	0.0701	0.0685	0.0016	97.7175	2.2824
11	farm	0.0679	0.0624	0.0055	91.8998	8.1001
12	farm	0.0636	0.0605	0.0031	95.1257	4.8742

Table 3: Plastic weight loss in monoclonal culture in carbon-saturated medium (control).

culture#	source	initial wt./g	wt. at 3 mo./g	wt. loss/g	Wt. at 3 mo. (%)	BA (%)
1	forest	0.0789	0.0778	0.0011	98.60583	1.3941
2	farm	0.0769	0.0763	0.0006	99.2197	0.7802
3	farm	0.0647	0.0643	0.0004	99.3817	0.6182
4	farm	0.0602	0.0599	0.0003	99.5016	0.4983
5	farm	0.0759	0.0755	0.0004	99.4729	0.527
6	riverbed	0.0575	0.057	0.0005	99.1304	0.8695
7	forest	0.0601	0.0594	0.0007	98.8352	1.1647
8	forest	0.0872	0.0861	0.0011	98.7385	1.2614
9	riverbed	0.0517	0.0512	0.0005	99.0328	0.9671
10	riverbed	0.0701	0.0698	0.0003	99.572	0.4279
11	farm	0.0679	0.0671	0.0008	98.8217	1.1782
12	farm	0.0636	0.0632	0.0004	99.371	0.6289

The result of the study supported the hypothesis that providing plastic as the sole source of carbon stimulation or providing a way for mutating bacteria's natural metabolic pathways, allows digestion of synthetic polymers and acceleration of LDPE plastic biodegradation. The study showed a promising microorganisms' ability to decay LDPE at a faster rate than currently occur in nature.

Culture identification:

Four cultures with the greatest change in BA to be identified with PCR and DNA sequencing were selected. Three cultures isolated from forest originated sample (#1, #7, #8) showed accelerated activity at 21.33%, 13.93% and 10.73% compared to control bioactivity of respective cultures 1.39%, 1.16% and 1.26%. Fourth active sample collected from farmland (#11) demonstrated bioactivity of 8.1% compared to the control bioactivity of 1.17%.

A multitude of *Pseudomonas* species were identified in culture#1. *Comamonas*, *Rhizobium*, and *Agrobacterium* were identified in cultures # 7, #8 and #11 (Table 4).

Table 4: Top four cultures with the highest BA acceleration.

Soil source	Microbial strain	BA in carbon-deprived medium	BA in carbon-saturated medium
forest	<i>Pseudomonas</i>	21.34%	1.39%
forest	<i>Comamonas</i>	13.93%	1.16%
forest	<i>Rhizobium</i>	10.73%	1.26%
farm	<i>Agrobacterium</i>	8.1%	1.17%

All identified organisms are known soil organisms, some with pollutant-degrading metabolism (*Pseudomonas* and *Comamonas*). *Pseudomonas* have very simple nutritional require

ments. One of the most striking properties of *Pseudomonas* species is the ability to use a wide variety of organic carbon and energy sources. Some *Pseudomonas* species utilize over 100 different compounds, including many simple sugars, fatty acids, alcohols, glycolic, amino acids, and many other compounds not fitting in any other categories.¹⁴ *Pseudomonas* contain multiple different enzymes and capable of using multiple metabolic pathways to allow different types of carbon digestion. *Pseudomonas* are known for a weak lytic activity necessary to break down long polymers' chains. For example, *Pseudomonas* can degrade polythene, PVC, PHB, poly(3-hydroxybutyrate-co-3-mercaptopropionate), and poly(3-droxypropionate). Since *Pseudomonas* species possess such a wide variety of metabolic mechanisms, in order to survive, the bacteria can be highly adaptive and activate their lytic activity.

Study limitations:

Identification and isolation of bacteria with a natural ability to decompose plastic was a challenging process. There were billions of bacteria and millions of cultures in the original soil samples. The selection process was based on the assumption that bacteria would adhere/colonize plastic. Samples were collected from the plastic surface. However, it is possible that some active cultures were not captured. It does not change the outcome of this study as the focus was on a variety of bacteria with a different degree of enzyme activity. The focus of the study was to research the ability of bacteria to adapt in a carbon-restricted environment. Therefore, it is possible that even more active in lytic activity bacteria could exist in a natural environment.

Due to limited resources, it was not possible to replicate each test condition. In the future, a goal for this project would be to repeat the test with the study's most accelerated culture *Pseudomonas* sp. Creating three to five replicates would strengthen the statistical analysis of the study. Also, limited resources precluded the use of PCR to identify all 12 isolates. It would be interesting to know if other tests contained the same species but did not accelerate at the same rate.

Conclusion

Some bacteria's natural metabolic pathways could be stimulated to allow the digestion of synthetic polymers and accelerated biodegradation of LDPE plastic. The current LDPE recycle rate is very low (less than 10%) due to the labor-intensive recycling technique.¹³ The study showed a promising ability of the microorganisms to decay LDPE at a faster rate than it currently occurs in nature. To achieve that, synthetic polymers need to be treated as selective compost to stimulate the microorganism's lytic activity. A designated site for proper disposal of rejected recyclables could help reduce the planet's overall pollution.

Acknowledgements

I'd like to thank my mentor Dr. Lisa Geig and my parents for their endless support and encouragement.

References

1. Market Study: Polyethylene LDPE, 3rd edition; *Ceresana*, 2020.
2. Thompson RC, Swan SH, Moore CJ, vom Saal FS. Our Plastic Age. *Philos. Trans. R. Soc. Lond., B, Biol. Sci* 2009. 364 (1526): 1973–6.

3. Barnes DK; Galgani F; Thompson RC, Barlaz M. Accumulation and fragmentation of plastic debris in global environments. *Philos. Trans. R. Soc. Lond., B, Biol. Sci.* 2009, 364 (1526): 1985–98.
4. Laura Parker. Eight Million Tons of Plastic Dumped in Ocean Every Year. *National Geographic*. 2015.
5. Emily J. North, Rolf U. Halden. Plastics and Environmental Health: The Road Ahead. *Rev Environ Health*. 2013; 28(1): 1–8.
6. Cacciari I; Quatrini P; Zirletta G; Mincione E; Vinciguerra V; Lupattelli P; Giovannozzi Sermanni G. Isotactic polypropylene biodegradation by a microbial community: physicochemical characterization of metabolites produced. *Applied and Environmental Microbiology*. 1993.
7. Vink, E. T. H.; Rabago, K. R.; Glassner, D. A.; Gruber, P. R. Polymer Degradation and Stability. 2003, 80, 403-419.
8. Halden, R. Plastics and Health Risks. *Annual Review of Public Health*. 2010; 31:179-94.
9. Burd D. Plastic Not Fantastic. 2008 <http://wwsef.uwaterloo.ca/archives/2008/08BurdReport.pdf>
10. Margaret Weigel. Energy and Economic Value of Non-recycled Plastics and Municipal Solid Wastes. *The Journalist's Resource*. 2017.
11. M Madigan, J Martinko. *Brock Biology of Microorganisms*, 11th edition. International Microbiology. 2005.
12. Roy PK, Surekha P, Tulsi E, Deshmukh C, Rajagopal C. Degradation of abiotically aged LDPE films containing pro-oxidant by bacterial consortium. *Polym Degrad Stab*. 2008; 93:1917–1922.
13. Margaret Weigel. Energy and Economic Value of Non-recycled Plastics and Municipal Solid Wastes. *The Journalist's Resource*. 2011.
14. Shosuke Yoshida et al. A bacterium that degrades and assimilates poly (ethylene terephthalate). *Science* 11. 2016: 6278,1196-1199
15. Maria Jose Cardenas Espinosa et al. Toward Biorecycling: Isolation of a Soil Bacterium That Grows on a Polyurethane Oligomer and Monomer. *Pub Med*. 2020
16. Hadad D, Geresh S, Sivan A .Biodegradation of polyethylene by the thermophilic bacterium *Brevibacillus borstelensis*. *J Appl Microbiol*. 2005, 98(5):1093–1100
17. Lee et al. Biodegradation of degradable plastic polyethylene by Phanerochaete and Streptomyces species. *Appl Environ Microbiol*. 1991, 57(3):678-85.
18. Singh B, Sharma N. Mechanistic implications of plastic degradation. *Polym Degrad Stab*. 2008. 93:561- 584
19. Santo M, Weitsman R, Sivan A. The role of the copper-binding enzyme- laccase- in the biodegrading of polyethylene by the actinomycete *Rhodococcus ruber*. *Int Biodeterior Biodegrad* 2013. 84:204-210.

■ Author

Crystal Radinski began her scientific problem-solving experiments at the age of twelve and presented her successful work at several international competitions. Crystal enjoys equestrian show jumping, traveling, and spending time with friends. She hopes to make a positive difference in our society by pursuing her interests in mental health and psychology.

The Effects of Hybrid Fertilizer on Plant Life

Eva Saramya

Forsyth Country Day School, 5501 Shallowford Rd, Lewisville, North Carolina, USA; esaramya@gmail.com

ABSTRACT: Current research suggests that roughly 50% of all food that is produced around the world is wasted. Finding a sustainable solution to the global compost waste issue was the primary motivation for this study. This analysis encompasses the first-ever quantitative data sought for “Soil Sauce”, an organic-compost based liquid fertilizer. To understand the impact(s) of fertilizer on the efficacy of plant growth, a lab analysis - Procedure I - along with a fertilizer test - Procedure II - were conducted to gain more insight into the product's ability to aid in plant growth and reduce food waste. The lab analysis involved observing the properties of soil sauce under a microscope using the Gram's sample staining method. Procedure II involved applying quantities ranging from 2-6 drops of soil sauce into distinct plant groups to test product efficiency.

A basic understanding of fertilizer, what it possesses, differences between commercial and compost-based fertilizers, and fundamental knowledge of bacterial shapes were needed as a foundation to thoroughly comprehend the different parts of this study thoroughly. The main conclusions from this experiment were that “Soil Sauce” is, in fact, extremely beneficial for plant growth. The results showed that the plant group with the most drops of “Soil Sauce” grew significantly better compared to its counterparts, the plant groups with less drops of soil sauce and the control group.

KEYWORDS: Earth and Environmental Sciences; Hybrid Fertilizer; Soil Sauce; Bacterial Ecology; Environmental Effects on Ecosystems.

■ Introduction

“Soil Sauce” is a hybrid fertilizer made in Pittsburg, Pennsylvania by the Ecotone Renewables Team. The fertilizer is described as “hybrid” due to its unique combination of properties from both compostable and chemicalized fertilizers. The process to make “Soil Sauce” involves taking leftover vegetables and fruits and putting the scraps through a manufacturing process involving an anaerobic digester. Anaerobic digestion is the process in which organic matter is broken down to produce biogas or biofertilizer. This process occurs in the absence of oxygen in a sealed oxygen-free tank known as an anaerobic digester.¹

Fertilizer is a solution composed of essential elements and nutrients needed to make plants grow rapidly and healthier. Important elements such as nitrogen, phosphorus, potassium, magnesium, sulfur, and calcium are all needed in successful plant growth. Nitrogen (nitrate) strengthens foliage during the critical development stage. Nitrate also contributes to chlorophyll production, responsible for creating the signature green color commonly seen in many plants. Phosphorus aids in root growth and offers protection to plants against harmful environmental stresses and factors.² Potassium helps in water retention, contributes to early plant growth, and protects against insects and diseases. Magnesium aids in chlorophyll production by absorbing sunlight during photosynthesis. Magnesium is also critical to plant organisms for cell division, protein/enzyme formation, cell membrane stabilization, and metabolic functions in the plant.³ Sulfur aids in protecting the plant organism from disease and helps with the production of amino acids, enzymes, proteins, and vitamins. Calcium contributes to the growth and development of the cell wall, which

is critical as the cell wall is the first line of defense for the plant organism in withstanding harmful diseases.⁴

One of the objectives of this study was to classify where “Soil Sauce” fits in the spectrum of fertilizers. This research was critical in understanding how exactly “Soil Sauce” works. Roughly 50% of all food that is produced around the world is wasted.⁵ By understanding Soil Sause proper classification, in terms of fertilizer, it distinguished how exactly “Soil Sauce” aids in plant enrichment whilst potentially reducing global waste and improving soil health through utilization of natural, reusable compostable waste. By understanding where “Soil Sauce” fits within fertilizer classification, it can be distinguished how this plant-enriching product can potentially reduce global waste and improve soil health by utilizing natural, reusable, compostable waste. Additionally, we can understand how the use of “Soil Sauce” can contribute to regenerative agriculture and preserve vital soil nutrients.

The spectrum of fertilizers, ranging from compost-based to chemicalized, entails a variety of options to enrich plant life. Fertilizer provides the vital nutrients plants need to regenerate and grow effectively. The creation of fertilizer is to bring back the nutrients the soil loses through the previous plant cycle continuing the food production process effectively. The broad types of fertilizers include mineral rich, nutrient rich, and chemicalized fertilizers. These fertilizers tend to capitalize on specific vital nutrients, such as calcium, phosphorus, magnesium, to promote plant growth. Mineral-based fertilizers transform naturally occurring, geologically derived raw materials into plant nutrients. Conversely, there are organic fertilizers typically comprised from cow manure, left over crop yield, or compost. These fertilizers, unlike their chemicalized

counterparts, depend on their composition by way of regional resources. Organic fertilizers are ambiguous in terms of consistent nutrient compounds. As resources and crop yields change the organic fertilizer, the makeup adheres to the change as well, providing different nutrient compositions per each batch. This does not take away from its ability to benefit plant growth and proves to be just as effective as its chemicalized counter parts.⁶ Nevertheless, both organic and inorganic nutrients are important to sustainable crop productivity and soil health.⁷

A compost-based fertilizer is composed primarily of compost consisting of natural ingredients such as leftover fruits and vegetable scraps. Compost has notably assisted in plant growth due to its soil-enriching properties. It is associated with improving texture and aiding in creating a healthier environment for plant life due to its composition. Organisms found in compost such as bacteria, fungi, redworms, and dung beetles replenish and provide nutrients to the soil, correlating with successful and healthy plant growth. Commercial fertilizer is mostly, if not entirely, chemical-based. The vitamins and minerals needed are chemically processed and manufactured from raw elements and compounds such as ammonia (NH₃). The elements are broken down chemically or manually with machinery to make the process of absorbing the vital nutrients easier for the soil.⁸

The main gap found throughout prior research was the lack of proper classification for what "Soil Sauce" is in terms of fertilizers on the market today. "Soil Sauce" is classified as a chemicalized fertilizer made out of compost; it combines elements from both the compost-based and commercially chemicalized fertilizers, placing the product within its own hybrid classification. Since this category of hybrid fertilizer hasn't been researched in detail, it made distinguishing "Soil Sauce" as a proper fertilizer cumbersome and made finding information on its properties difficult.

Understanding the basic bacterial shapes, arrangements, sizes, and organisms found in many fertilizers is beneficial. It offers reference and a basic framework on what needed to be looked for and observed, especially during Procedure I, to be detailed later in this paper.

The three shapes that were looked at were cocci, spirilla, and bacilli cells. Coccus (single cell) is a round, spherical shaped cell. Spirilla cells (spirillum for single cells) are bacteria with a distinct curve range varying from gently curved to tight corkscrews. Spirilla cells are rigid and capable of movement. Bacilli (bacillus for single cell) are rod-shaped bacteria.⁹ Soil enriching organisms such as gastrotrichs were also looked for and observed.

The objectives of this study were to measure and establish concrete quantitative data for "Soil Sauce" as this fertilizer had no data previously. Objective 1 was to collect data points to see if "Soil Sauce" had the capabilities to accelerate plant growth. Objective 2 involved seeing if "Soil Sauce" could potentially be an alternative needed to minimize global compost waste whilst helping and nourishing the environment.

■ Methods

Measurements (Variables):

The independent variable was the amount of fertilizer in each batch of mustard plant samples. The dependent variable was how tall the mustard plants grew. The constants included the experimental material, procedures, and the amount of water, sunlight, and soil each plant received.

Design:

The procedures were critical in analyzing and understanding "Soil Sauce" from all perspectives and finding the information needed to test and prove its efficiency. Procedure I involved evaluation and observation of chemical and bacterial make-ups. Procedure I was also crucial in comparing "Soil Sauce" to fertilizers on the market today for possible correlations. Procedure II directly tested "Soil Sauce" on plant life. Procedure II was vital in testing the efficiency of the fertilizer.

The experimental design involved growing mustard plants and observing growth rate after the addition of Soil Sauce. Thus, the execution of the procedures was critical in data identification. The aim was to take the growth rate into account and gain calculations to support the research hypothesis: the plant group with the most soil sauce will thrive the best. The results and data were then placed in charts and analyzed. Data for each group was reported separately. The data compiled the growth rates of each plant group per day for approx. 1 week. The data helped identify patterns, correlations, and constancies in plant growth. A chart of growth throughout the week, the averages for each day, and a visual data curve were created based on each group.

Procedure I:

Procedure I involved testing, analyzing, and observing the bacterial and chemical compositions of "Soil Sauce" using the Gram's Staining Method; a process of finding bacteria involving a methodical repetition of staining and washing until a final stained product is achieved. The materials used were microscope slides, matches, alcohol lamps, crystal violet stain, safranin stain, isopropyl alcohol, gram's iodine stain, agar plates, loop, and tryptic soy broth cultures. The alcohol lamps were heated to sterilize the loop after each use to avoid contamination from sample to sample. The heated loop was then put into "Soil Sauce" and then placed onto a labeled agar plate. The samples were then incubated with the broth cultures at 37°C to develop over 24 hours. After the incubation period, the samples were subjected to the Gram's Staining method. The sterilized loop was then used to scrape off a part of the incubated sample and was placed on a microscope slide with a drop of water. The water was combined with the scraped sample to create a homogenous mixture. The slide was then placed on and off an open fire, fueled by the alcohol lamps, until the water and excess liquid evaporated. What was left was the evaporated residual sample of "Soil Sauce" on the microscope slide. Crystal violet was then applied onto the cooled sample for 20 seconds. It was rinsed off with water, which was then followed up with gram's iodine for 1 min. The isopropyl alcohol was then used to decolorize the gram's iodine after 1 min. The isopropyl alcohol was then washed off with water and was followed by the safranin for 20 seconds.

The final wash of water was then used to rinse off the excess stain and the slide was blot dried until no water or liquids were left. Since 5 samples of “Soil Sauce” were taken, this process was repeated 5 times. Finally, each of the 5 samples were put under the microscope to be observed.

Procedure II:

Procedure II involved actively testing “Soil Sauce” on plant life and recording the data accumulated. The hypothesis “the plants with the most fertilizer will thrive the best” guided this part of the experiment. Some materials used included egg cartons as planters, tray, eyedropper, “Soil Sauce” fertilizer, cups, soil, and mustard seeds. This experiment was set up and split into 4 main groups. The first group was the control group with no fertilizer, labeled and marked with the blue popsicle stick. The second, third, and fourth groups all contained varying amounts of soil sauce. Group 2 had the least amount of fertilizer (1-2 drops) represented by the red popsicle stick. Group 3 contained 3-4 drops of fertilizer, represented by the yellow popsicle stick. Group 4 had the most amount of fertilizer (5-6 drops) and was represented by the green popsicle stick. All groups received equal amounts of soil, water, sunlight, and seeds. The tray was placed near a window for a consistent, adequate source of sunlight. The egg cartons were then placed onto the tray along with the dampened soil within them. The popsicle sticks were then cut and labeled with a color and placed into its allotted group to keep data collection organized. 14 ml (approx. 1 tsp) of seeds were added to each big group (each big group was comprised of four mini-groups) and then covered up with the remaining soil. 14 to 28 ml of water along with the specific amounts of “soil sauce” per group were added every day for 5 days until the experiment concluded. Data was recorded and accumulated through measuring each plant individually, consistently every day until the conclusion of the experiment.

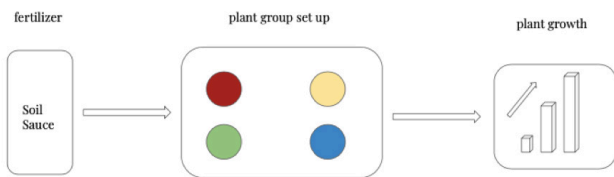


Figure 1: Experiment schematic design. The varying quantities of soil sauce on plant growth are represented through the final factor of growth.

The schematic above outlines how Procedure II was conducted. The varying quantities of soil sauce on plant growth are represented through the final factor of growth.

Results and Discussion

The samples included bacillus cells while others contained cocci. Some samples contained both cell types while others only had one or the other. None of the samples consisted of spirilla cells. The bacteria range observed depended on the specific sample taken. Each sample had a very different chemical and bacterial composition, thus making “Soil Sauce” an extremely complex and multilayered product. A soil organism known as a gastrotrich was also found among one of the samples. Gastrotrichs are common aquatic detritivores, that help break down complex organic material, found usually in the liquid compost (refer to Appendix for details).

The overall growth average (OGA), took the average of the averages from each day (refer to Table 6), was also determined for all plant groups (refer to the Tables 1-4 & Figures 2 - 5 below). Table 2 focuses on the plant group data with the least “low” amount of fertilizer (red group). Table 3 contains the data for the yellow group; the group contained the “medium” amount of fertilizer. Table 4 covers the data of the green group; the plants that received the most drops of fertilizer (“high”). The blue group was the control group. No fertilizer was added to this group. All plants (regardless of grouping) received the same amount of sunlight, water and were subjected to the same temperature. The data recorded for all plants was over a 5-day period and was recorded down at the same time every day.

Table 1: Data for red batch samples. Active, consistent growth starts at day 3 and progresses throughout the experiment.

red sample (1-2 drops of fertilizer)	plant 1	plant 2	plant 3	plant 4
day 1	0 cm	0 cm	0 cm	0 cm
day 2	0 cm	0 cm	0 cm	0 cm
day 3	1 ½ cm	½ cm	1 ½ cm	1 cm
day 4	1 ¾ cm	1 ½ cm	3 cm	2 cm
day 5	2 cm	2 cm	3 ½ cm	2 ½ cm

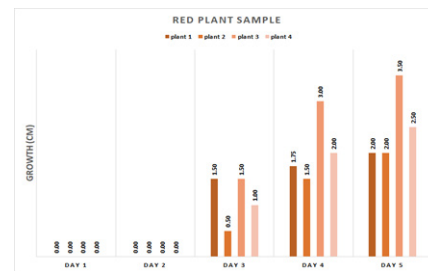


Figure 2: Data chart for red batch samples. The data in day 4 mirrors that of day 5 showing the consistent upward trend in plant growth.

Table 2: Data for yellow batch samples. All plants started growing at day 4 and continued to show promising growth onwards.

Yellow sample (3-4 drops of fertilizer)	plant 1	plant 2	plant 3	plant 4
day 1	0 cm	0 cm	0 cm	0 cm
day 2	0 cm	0 cm	0 cm	0 cm
day 3	0 cm	1 ½ cm	0 cm	1 cm
day 4	2 cm	2 cm	1 cm	2 cm
day 5	2 ½ cm	2 ¾ cm	1 ½ cm	2 ½ cm

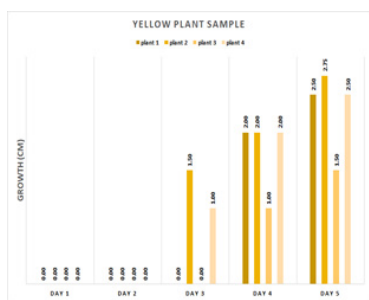


Figure 3: Data chart for yellow batch samples. The data in days 4 and 5 is mostly consistent within the plants with 3 out of 4 plants having close growth rates.

Table 3: Data for green batch samples. All plants grew consistently from day 2.

Green sample (5-6 drops of fertilizer)	plant 1	plant 2	plant 3	plant 4
day 1	0 cm	0 cm	0 cm	0 cm
day 2	1 ½ cm	1 ½ cm	1 cm	3 cm
day 3	3 cm	2 cm	3 cm	3 cm
day 4	4 cm	3 cm	4 ½ cm	5 cm
day 5	5 cm	4 cm	5 ½ cm	5 ½ cm

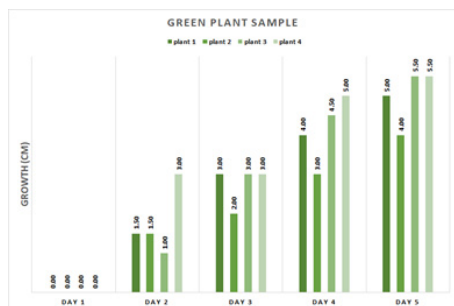


Figure 4: Data chart for green batch samples. Growth data appears in a steady upward progression from day 2 onwards.

Table 4: Data for blue batch samples. Plants start growing from day 2.

Blue sample (control group)	plant 1	plant 2	plant 3	plant 4
day 1	0 cm	0 cm	0 cm	0 cm
day 2	½ cm	½ cm	1 cm	½ cm
day 3	1 ½ cm	2 cm	3 cm	1 ½ cm
day 4	3 ½ cm	3 ½ cm	3 cm	4 cm
day 5	3 ¾ cm	4 cm	4 cm	4 ½ cm

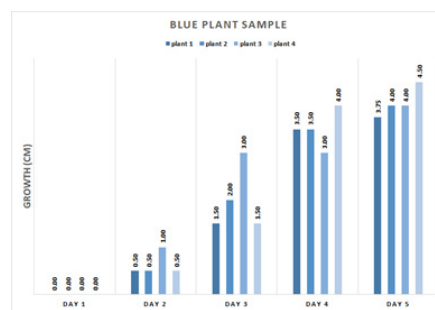


Figure 5: Data chart for blue batch samples. Plant Data has a significant jump from day 2 to 3. From Day 3 onwards data has a steady, consistent upward trend.

Table 6: OGA Chart. The purpose of the chart is to show the overall average of growth per each plant group. The data present supports that the plant group that received the most fertilizer (group green) grew exponentially well overall compared to the other plant groups recorded.

Plant Group Name	Overall Growth Average (OGA)
red	1.1375 cm
yellow	0.9375 cm
green	2.725 cm
blue	1.9875 cm

Table 6a: OGA data probability distribution.

	Plant Growth	Probability Distribution
Yellow	0.9375	0.3173
Red	1.1375	0.4114
Blue	1.9875	0.5152
Green	2.725	0.1977

Mean	1.70
Standard Deviation	0.71

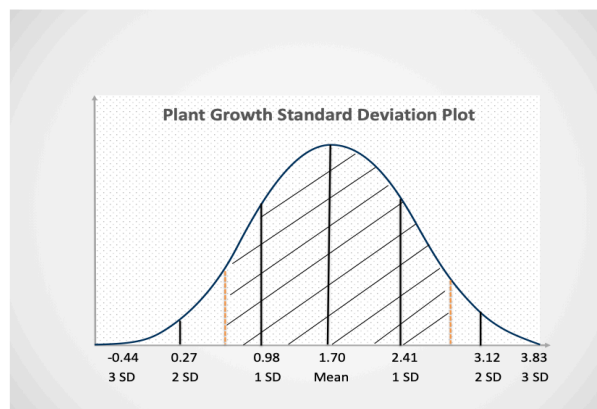


Figure 6: Standard deviation plot.

The plot displays the average standard deviation for overall plant growth represented by the calculated overall growth average (OGA). The chart shows that about 90% of the study

data falls within 2 standard deviations from the mean, represented between the two orange lines. This shows that the sample data used lies within the statistically significant range.

Observations:

Some observations to note from Procedure II were that all the plants that received “Soil Sauce” appeared to look healthier, with a darker, richer green pigment, especially compared to the control group. The control group plants look quite malnourished, underdeveloped, and were lacking in the rich healthy color, instead a pale whitish green, compared to their fertilized counterparts. From this alone, it can be concluded that “Soil Sauce” not only accelerates plant growth but also promotes healthier, well-nourished plant life.

Discussion

From what was analyzed, “Soil Sauce” does have all the elements and resources needed to potentially be a successful fertilizer. The efficiency in plant growth throughout the experiment supports this conclusion. Testing different fertilizers on a common plant group and comparing it with “Soil Sauce’s” efficacy rates could provide more insight and better understanding of soil sauces’ abilities, especially when compared to its commercial and organic counterparts. Note that the quantities of soil sauce put into the red, yellow and green plant groups were relatively minimal. Experimenting with different quantities of “Soil Sauce” could lead in finding the optimal amount for the most substantial plant growth. The experiment did lack in variety because only one plant type was tested. Testing “Soil Sauce” on plants in addition to mustard seed could be integral in understanding the range of “Soil Sauce’s” benefits and limitations. Manipulating the time of the conducted experiment could also observe if “Soil Sauce” is consistently effective long term. Overall, the efficacy of compost-based fertilizer is very promising and could potentially revolutionize the agricultural industry.

Conclusion

In conclusion, both procedures suggest that the hybrid fertilizer “Soil Sauce” is promising for excellent plant growth. The most conclusive and promising data included the green group - the plant group that received the most fertilizer - which generated healthy plant life exponentially well at a consistent rate compared to the other groups tested. The groups fertilized at lower amounts did show growth, but not at the rate the green groups growth. Practical applications with the data collected from this experiment could revolutionize the agricultural industry greatly and in a positive way, especially with the high and popular demand for organic food. From a financial standpoint, if “Soil Sauce” was in retail, more farmers could grow their crops organically, leading to more income for farmers and customer satisfaction for consumers. This research could potentially help the environment by limiting chemical runoff into water areas, eliminating the risk of water contamination, and providing safety assurance for marine life.¹⁰ On a smaller note “Soil Sauce” could also help the avid home gardeners with their plants. Since “Soil Sauce” is made up of liquid compost the waste from compostable foods would also go down tremendously. According to Ecotone Renewables “Globally, 30-40 % of all food that is produced is wasted”.¹¹ This experiment suggests that “Soil Sauce” could potentially reduce global waste

by utilizing natural, reusable, compostable surplus. The uses for this multipurpose fertilizer are endless and could change the world for the better one day.

Acknowledgements

I wish to thank both Dr. Peter Kish and Dr. Gabriella Dee for all their help and support. Dr. Kish for providing the lab facility to guide me through the lab procedures and Dr. Dee for providing access to soil sauce. I would also like to thank Dr. Saravana “Samy” Govindasamy for help in editing and polishing the paper.

References

1. Interdirect. What is anaerobic digestion? <http://www.biogen.co.uk/Anaerobic-Digestion/What-is-Anaerobic-Digestion> (accessed Feb 28, 2021).
2. <https://www.holganix.com/blog/why-your-plants-need-phosphorus-advantages-and-disadvantage> (accessed Feb 28, 2021).
3. <https://www.gardeningknowhow.com/garden-how-to/soil-fertilizers/fixing-magnesium-deficiency> (accessed Feb 28, 2021).
4. Ersek, K. The 6 essential nutrients for healthy plants <https://www.holganix.com/blog/the-6-essential-nutrients-for-healthy-plants> (accessed Feb 28, 2021).
5. Smithers, R. Almost Half of the World’s Food Thrown Away, Report Finds. The guardian. January 10, 2013.
6. Types of fertilizer - fertilizers Europe <https://www.fertilizerseurope.com/fertilizers-in-europe/types-of-fertilizer> (accessed Feb 28, 2021).
7. Mahmood, F.; Khan, I.; Ashraf, U.; Shahzad, T.; Hussain, S.; Shahid, M.; Abid, M.; Ullah, S. Effects of Organic and Inorganic Manures on Maize and Their Residual Impact on Soil Physico-Chemical Properties. *J. soil sci. plant nutr.* 2017, 17 (ahead), 0–0.
8. How fertilizer is made - material, production process, making, history, used, components, composition, product <http://www.madehow.com/Volume-3/Fertilizer.html> (accessed Feb 28, 2021).
9. Aryal, S. Different Size, Shape and Arrangement of Bacterial Cells <https://microbiologyinfo.com/different-size-shape-and-arrangement-of-bacterial-cells> (accessed Feb 28, 2021).
10. Espinoza, R. Chemical waste that impact on Aquatic Life or Water Quality <https://blog.idrenvironmental.com/chemical-waste-that-impact-on-aquatic-life-or-water-quality> (accessed Feb 28, 2021).
11. About <https://ecotonerenewables.com/About> (accessed Feb 28, 2021).

Author

Eva Saramya is a senior in high school and is interested in the field of medical/health sciences. She is planning to major in microbiology, immunology and/or environmental sciences. She’s loved gardening from a young age and looking into the microbial aspects of plant life further has amplified her love not only for ecology but for microbiology as well.

Appendix

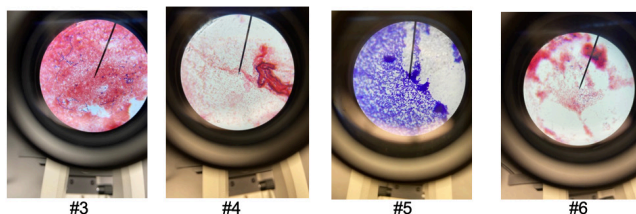
A. BACTERIAL SAMPLES (PROCEDURE I)

#1



#2





#1: shows the incubated soil sauce samples

#2: gastrotrichs found in drop sample of soil sauce under microscope (no incubation or gram's staining process)

#3 – 6: taken from incubated samples of soil sauce, put through grams' staining method and observed under microscope. All pictures contain cocci (red) and bacilli cells (blue). Through this process it was concluded that the composition of soil sauce remains to be complex and somewhat ambiguous. Within one batch itself that composition varied greatly from each sample.

Note: All samples were collected from 1 batch of soil sauce.

B: PLANT GROUP SET UP (PROCEDURE II)



- Each highlighted big group is comprised of 4 mini-groups
- Control group (top right, highlighted with blue square) - each mini group received no fertilizer
- Red group (bottom left, highlighted with red square) - each mini group received smallest amount of fertilizer (1-2 drops)
- Yellow group (top left, highlighted with yellow square) - each mini group received median amount of fertilizer (3-4 drops)
- Green group (bottom right, highlighted with green square) - each mini group received the highest amount of fertilizer (5-6 drops)

C: ECOTONE RENEWABLES TEAM

(GROUP RESPONSIBLE FOR CREATING "SOIL SAUCE")

- o Sasha Cohen Ioannides (CEO)
- o Kareem Rabbat (CIO)
- o Dylan Lew (CTO)
- o Kyle Wyche (COO)
- o Rob Davis (Nutrient Specialist)

An Analysis of Advantage Factors in Men's Tennis – Handedness, Age, Height, and Rank

Shreyes Sridhara

Stonehill International School, Tarahunise Post, Bangalore, Karnataka (KA), 562157, India; shreyesXsridhara@gmail.com

ABSTRACT: This study takes the discussion of the handedness advantage in men's tennis further and analyzes whether it has increased or decreased over the years as playing styles, racket technology, training, and diets of tennis athletes have changed, and as new players have entered the circuit. The results confirm that this advantage favoring left-handed tennis players has indeed diminished over the years to favor right-handers, and this shift was more conspicuous in the highest tier of men's professional tennis than it was in the second and third tiers. I found that the lower the tennis tier, the lower the probability of a shift in the handedness-related advantage over time. In addition to this, other features like age, height, and rank of competing players were investigated to observe whether they too displayed a trend or another advantage. In the higher tennis tiers, younger players had the advantage over their older counterparts while, quite surprisingly, the opposite was true in the lowest tier. Height was only a significant match-determinant in the lower tiers. Furthermore, higher-ranked tennis players were more likely to win against lower-ranked players in descending order of tier.

KEYWORDS: Robotics and Intelligent Machines; Machine Learning; Logistic Regression; Sports Analytics; Left-handedness in ATP.

■ Introduction

In Open Era tennis (began in 1968), it has long been conjectured that there is a handedness-related advantage – that being left-handed is a match determinant in the interactive sport. This claim has been backed by numerous studies. For example, one study by Hagemann divided 54 left-handed and right-handed players from different domains of tennis expertise into three groups and asked them “to predict the subsequent direction of an opponent's temporally occluded tennis strokes on a computer screen”.¹ The results demonstrated that regardless of skill, both right-handed and left-handed tennis players were better at predicting the trajectory of strokes coming from right-handed tennis players. Another study proved the handedness advantage through statistical analysis of a database of tennis matches.² Left-handers comprise approximately 10% to 13% of the world's population; however, they seem to be over-represented in interactive sports, such as tennis and combat sports like boxing and wrestling.^{3,4} Hagemann and Faurie & Raymond suggest two hypotheses to explain the reason behind this overrepresentation seen in tennis: (a) the innate superiority hypothesis and (b) the negative frequency hypothesis.^{1,5}

The innate superiority hypothesis elaborates on the neuropsychological advantages that left-handers possess. For instance, according to Geschwind and Galaburda, regions present in the right hemisphere of the brain are larger for left-handers, serving as an explanation for why left-handers might be better than right-handers at performing tasks that require the right side of the brain (such as attentional and spatial imagery tasks).^{1,6} In addition to this, the results of other studies assert that left-handers possess better anticipation skills and a quicker reaction time with their left hand than right-handers do.⁷⁻¹⁰ Furthermore, as a result of the weaker lateralization

of the brain hemispheres for left-handers, “the stronger non-dominant side or the superior interplay between the two sides could then lead to better overall performance” in motor tasks that demand both hands (such as playing tennis with a double-handed backhand).¹

Referred to by numerous research papers as the negative frequency hypothesis,¹⁻⁵ this hypothesis states that since left-handers are a minority in the world population, left-handed tennis players will play a more significant number of matches against right-handed tennis players, while right-handed tennis players will encounter more tennis players of the same handedness.^{11,12} Therefore, the lack of exposure to the playing style of a left-hander takes the right-handed player by surprise when the latter encounters a left-hander. The ball coming from the opposite side of the court, the topspin on the ball, and the ball's trajectory as it moves through the air all take some time for a right-hander to adjust to. In her autobiography, Monica Seles, a former world number one tennis player on the WTA tour, wrote, “It's strange to play a lefty because everything is opposite and it takes a while to get used to the switch. By the time I feel comfortable, the match is usually over”.² Thus, the motor skills of right-handed tennis players required to address the attack coming from the opposite side of the court are underdeveloped and unpretentious, prompting weaker and less effective responses to these attacks. The notion of negative frequency demonstrates how left-handers can also capitalize on “the movement information” and “anticipate an opponent's intentions” earlier and better than right-handers can, allowing them to distinguish the groundstrokes, the racket speed, and the ball trajectory when it comes off the racket of right-handed tennis players more accurately than right-handed tennis players can distinguish these features from left-handed tennis players.¹

It is evident from the studies conducted (that elaborate on and confirm the existence of a handedness-related advantage for left-handers in an interactive sport like tennis) and the prior research on the topic of handedness and its impact as a match determinant that this is a topic that has been thoroughly addressed. However, I wish to add value to this discussion by shedding new light on and analyzing whether the influence of handedness as a match determinant has changed over the years.

Handedness: I hypothesize that the influence of handedness as a match determinant has waned over the time period I am considering (Open Era tennis) in the highest tier of men's tennis – ATP (Association of Tennis Professionals); on the contrary, I believe that it still remains a prevalent and prominent factor in lower-tier tournaments, such as ATP Challengers (a tier below the ATP) and Futures tournaments on the ITF tour (International Tennis Federation and the third tier of tennis competition). The lower the tier, the lower the probability of a shift in the handedness-related advantage over time.

My theory is predominantly based on the negative frequency hypothesis. In lower-tier tournaments, left-handed tennis players should win more matches against their right-handed counterparts due to right-handers not having much experience playing against lefties to be able to consistently anticipate the left-hander's movements and the ball trajectory when it comes from the opposite side of the court. In addition to this, new tennis players (with limited tennis-related strengths) enter the circuit all the time allowing left-handers to constantly be at an advantage. Hence, in these situations, left-handedness proves to be a prominent match determinant. However, in the ATP level tournaments, the right-handers have played a number of matches against left-handers to reach the level at which they are at and may even train purposefully with opposite-handed players on a regular basis. This means that at the highest level of the sport, tennis becomes more of a game of skills rather than one of advantages; players that enter this circuit must already have a strong and highly-developed game. Also, interestingly, an analysis of the dataset utilized in this study revealed that since the 2000s, the percentage of left-handers on the ATP Tour has been about 12.3%, while this number increases to 13.8% on the Challenger Tour and 12.8% on the Futures Tour. The hypothesis is also in line with the argument that Breznik makes – that the advantage of left-handedness as a match determinant is more noticeable “in the less important types of professional tournament, Challengers and Futures tournaments”.²

I also wanted to investigate whether characteristics like age, height, and rank showed a trend over the years that I could interpret as an advantage.

Age: I expect juvenile tennis players to perform better than older players due to their better fitness and energy levels.

Height: I believe that tall tennis players have an advantage over their shorter peers since their height should help them serve at faster speeds (as they have more body mass), and at sharper angles (giving them a bigger margin for error).

Rank: Finally, higher-ranked players are believed to be more successful against their lower-ranked rivals because they must

be better tennis players (to have reached the rank at which they are at). It is to be noted that all of my claims on age, height, and rank are based on priori reasoning.

The goal of the study is to validate my main hypothesis based on handedness and my other claims on age, height, and rank statistically by constructing a machine learning model over a dataset of tennis matches and then interpreting the results.

■ Methods

Database:

The data utilized for this study was obtained from Jeff Sackmann's "tennis_atp" GitHub repository.¹³ The repository contains datasets of tennis stats, ranking, and results of men's singles tennis matches from different tiers – ATP Tour, ATP Challenger Tour, ITF Futures Tour – from 1968 to 2020. Each dataset comprises all the matches that occurred for each year in the respective tier along with 49 features, including the handedness, the age, the height, and the ranking of both winner and loser, the surface played on, the draw size of tournaments, and the match date.

For this analysis, I considered the handedness (principal), the age, the height, and the rank of the competing tennis players and investigated how the coefficients of these variables changed with time. The other features in the datasets, like the draw size and the match date, were rejected since they wouldn't have been helpful for modeling the winner. The features I chose are also displayed alongside tennis players on the ATP official website and those that have been speculated to affect the result of a tennis match.

Materials and Tools:

I performed the modeling and the analysis using Python. Python is a general-purpose, high-level object-oriented, programming language and one of the benefits of this programming language is the variety of libraries that can be accessed through the language, such as pandas, matplotlib, and sklearn. I used pandas for data manipulation, sklearn to train and test the logistic regression model and make further predictions using the model, and matplotlib to depict the results obtained through the model in a more perceptible manner.

Modelling Handedness:

I used machine learning to train models from the vast dataset and analyze the results. Machine learning algorithms (systems of instructions or procedures to solve problems) build models from data. In today's modern world, machine learning is used in built speech recognition software on smartphones, product recommendations, social media, and cybersecurity to prevent online fraud. For this study, I used supervised learning so that errors with the output of the model can be compared to the expected output data, thereby adjusting and improving the model. In supervised learning, an algorithm is provided with labeled examples or training data. Subsequently, the program learns how to map the input data supplied to the desired output to then be able to make predictions of similar future events.¹⁴ This study is an example of a binary classification problem as there are only two possible outcomes – loss or win; the intention is to use handedness, age, height, and rank to predict which player will either win or lose.

Using Logistic Regression :

I used logistic regression since this was a binary classification problem. In logistic regression one or a set of predictor variables ('x') are used to estimate a binary output variable ('y'); simply put, it will help us estimate the probability of label 'y' when a feature 'x' is inputted. In my analysis, I computed the differences in handedness, age, height, and rank between the two competing players of each match. Table 1 below summarizes this process.

Table 1: Table demonstrating the difference method used to obtain the 4 predictor variables. The significance of a positive coefficient for each variable is also shown.

Determinant	Difference Between	Significance of a positive coefficient
Handedness	right (which is taken as 1) & left (which is taken as 0)	Right-handed tennis players have an advantage
Age	older player age & younger player age	Older tennis players have an advantage
Height	taller player height & shorter player height	Taller tennis players have an advantage
Rank	lower ranked player rank (larger number) & higher ranked player rank (smaller number)	Lower-ranked tennis players have an advantage

I then used these differences as the predictor variables to estimate the probability of a player with a particular feature winning.

Before building the model, I had to make a few modifications to the data frames. I replaced the missing values with the mean value of the respective columns and normalized the difference columns. These were done to ensure I didn't have NaN values in the dataset before I computed the differences in the features and implemented my logistic regression model.

In logistic regression, the beta coefficients (represented using the symbol 'β') of the equation inform us by how much the outcome variable changes with every unit change in the predictor variable, provided that the other variables in the equation are held constant.¹⁵ Positive coefficients imply a higher probability of the event occurring, negative coefficients imply the opposite, and coefficients near zero signify that the feature is of less significance.

Logistic regression uses the logit function, which can be represented as

$$\text{logit}(p) \text{ or } \ln\left(\frac{p}{1-p}\right) = \beta_0 + \beta_1x_1 + \beta_2x_2 + \beta_3x_3 + \beta_4x_4 + \dots + \beta_kx_k$$

Since I only consider four features in this study, my logit function will be

where p is the probability of the winner label occurring

$$\ln\left(\frac{p}{1-p}\right) = \beta_1x_1 + \beta_2x_2 + \beta_3x_3 + \beta_4x_4$$

(win or loss), x_1 represents the difference in handedness, x_2 represents the difference in age, x_3 represents the difference in height, and x_4 represents the difference in rank; $\beta_1, \beta_2, \beta_3, \beta_4$ are their respective coefficients. On a further note, it is important to understand that when focusing on a certain predictor variable – for example, the difference in age of the two competing players – I am keeping every other feature, including random effects like luck in a tennis match, constant.

To name a few such random effects, sometimes net cord balls drop in and bad calls made by umpires require the point to be replayed when clearly one player was in control of the point. This means that (using the same example) I am only trying to see the effect of being a year older or younger (the two players are hypothetically of the same handedness, height and rank) on the result of the match. Therefore, the differences in handedness, height and rank are 0, which also means that I consider the two of them to have equal amounts of luck by taking the constant term as 0. This paper also does not capture the impacts of such random effects on a match; hence, β_0 is always taken as 0 and can therefore be omitted. Furthermore, the logistic regression model was run with every match between opponents of opposite handedness, and adding a constant term would be similar to a priori reasoning that one of the players in the match-up has an advantage over the other from the get-go in a case where every other variable is controlled. I also randomized the side of the court and so, by symmetry, β_0 will be 0 once again.

Procedure:

Since I only considered matches with opposite-handed tennis players (a right-hander and a left-hander), the other handedness combinations, including the 'U' values for handedness (the undefined or unknown values for handedness in the datasets) were dropped.

I discovered that on the ATP Tour (Tier 1), on average, left-handed tennis players won 52.4% of the time when playing against right-handers; this percentage drops to 51.4% for Challengers (Tier 2) and Futures (Tier 3).

The breakdown of the matches above shows that left-handed tennis players won a greater percentage of matches against the more prevalent right-handed players on average. These results confirm the work of other prior studies that showed a handedness-related advantage exists in tennis, even at the highest level of the sport.¹⁻⁵ However, I was curious if the influence of this handedness-related advantage on the different tennis circuits changed over time.

Statistical Analysis using Scikit-learn (sklearn):

I ran models for every year in each tennis tier and plotted the output variable coefficients of the respective features over the time period considered. Additionally, I performed loess smoothing on all curves to help see the trends and relationships better.

Results and Discussion

Handedness:

In Figure 1, the general trend of the ATP shows that left-handers had an advantage in the 1970s until the 1990s; now right-handed tennis players do. On the Challenger Tour, the handedness advantage prevailed during the 1980s but became less and less important afterward. A quick analysis of the dataset explains a possible reason behind this. The percentage of left-handed tennis players on the Challenger Tour went from 14.6% at the start of the 80s to an astounding 21.6% at the end of the decade. Therefore, according to the negative frequency hypothesis, right-handed tennis players were challenged more often by left-handed tennis players as the decade progressed, and this constant exposure would have helped

them get used to the different trajectories and the top spin that left-handers induce on the ball. Thus, the left-handedness advantage diminished during this decade.

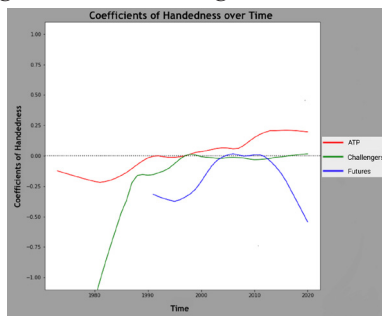


Figure 1: Graph of the coefficients of right-handedness on the ATP Tour, Challenger Tour, and Futures Tour over time.

Handedness seems to have had the least importance on the Challenger Tour over the last two decades, suggesting that it might be an even fight between players of different handedness. This once again can be explained by the fact that the percentage of left-handed tennis players on the Challenger Tour since the 1990s has stayed between 20% and 21%; hence the exposure to left-handers has more or less stayed the same on the tour.

In the Futures, handedness was important in the 1990s and in the 2010s (and continues to follow an increasing trend) but hardly showed any relevance during the middle years. Over the course of the last decade, the percentage of left handers on the Futures Tour fell from 13.6% to 11.9%. Therefore, in line with the negative frequency hypothesis, right-handers on the Futures Tour would have had limited exposure to playing tier level matches against their left-handed counterparts, creating a left-handed advantage.

I can deduce that currently, handedness is a salient factor in the Futures and in the ATP: the left-handedness advantage continues to increase on the Futures, while right-handedness prevails in the ATP. The handedness-related advantage did not shift over the period considered on the Challenger Tour and Futures Tour (lower-tier tournaments); however, this observation was more significant on the Futures graph. This aligns with my theory: the lower the tier, the lower the probability of a shift in the handedness-related advantage over time.

Figure 1 is in support of the hypothesis that the influence of handedness as a match determinant has waned over the time period considered on the ATP Tour – the highest tier of men’s professional tennis. The coefficient did not go below zero at all during the last two decades, demonstrating that the leftie advantage was no longer as influential or prevalent in the top tier of tennis as it was during the 90s, the 80s, or the 70s. I can confirm that right-handed tennis players had a greater probability of winning matches after the 21st century compared to the years before using the logit function.

In order to compare two players of different handedness, I controlled the age, the height, and the rank by keeping them constant. As a result, the input variables other than the difference in handedness (difference in age, difference in height, difference in rank of the two players) were zero.

$$\ln\left(\frac{p}{1-p}\right) = \beta_1 x_1 + \beta_2 x_2 + \beta_3 x_3 + \beta_4 x_4$$

$$\begin{aligned} \ln\left(\frac{p}{1-p}\right) &= \beta_1 * (\text{difference in handedness}) + \beta_2 * (\text{difference in age}) + \beta_3 \\ &\quad * (\text{difference in height}) + \beta_4 * (\text{difference in rank}) \\ &= \beta_1 * (1) + \beta_2 * (0) + \beta_3 * (0) + \beta_4 * (0) \end{aligned}$$

$$\ln\left(\frac{p}{1-p}\right) = \beta_1$$

Hence,

For handedness, the difference was always one.

When one of the beta coefficients of the difference in handedness from the results is entered, it gives us the probability of a certain handedness (either right or left depending on whether the coefficient is positive or negative) winning.

For instance, when I consider two players with the same age, height, and rank, and take the beta coefficient of 0.2 (which

$$\ln\left(\frac{p}{1-p}\right) = \beta_1$$

$$\ln\left(\frac{p}{1-p}\right) = 0.2$$

$$\therefore p = 0.550$$

lies on the ATP curve after the 2000s),

According to the model, right-handers had a 55% chance of winning against lefties.

On the other hand, when I take the coefficient -0.2 (which lies on the ATP curve between 1970 and 1990)

$$p=0.450$$

We see that right-handed tennis players only had a 45% chance of winning.

At the start of the 1980s, on the Challenger Tour, left-handed tennis players had a massive advantage over right-handers.

$$p=0.269$$

Left-handed tennis players had a 73.1% chance of winning.

The curve representing the Futures Tour was never over the x-axis for a significant amount of time, therefore, suggesting that the probability of winning would be in favor of the left-handers. The coefficients between (approximately) 2003 and 2015 illustrate that the advantage had lessened during this time period compared to previous and future years; however, the coefficients post 2015 and prior to 2000 were large negative values and demonstrate a convincing left-handed advantage.

An intriguing matter to investigate is how prevalent the left-handed advantage would be if Nadal’s match data is removed from the data set. Nadal has spent more than 800 weeks in the top 10, and continues to beat top right-handed players. For instance, Roger Federer is considered as one of the best players against left-handers, and poses a 125-36 (win-loss) record against lefties on the ATP Tour. However, 23 of those 36 losses have come just against Nadal.

It’s possible that Nadal’s dominance on the ATP Tour skews the left-handed advantage in its favor. But by exactly how much?

Upon removing Nadal's record and considering the time frame in which he has played,

$$\ln\left(\frac{p}{1-p}\right) = 0.4$$

$$p=0.60$$

According to the model, right-handers would have had a 60% chance of winning against lefties, if Nadal never played on ATP tour. This demonstrates that without Nadal, the right-handed advantage on the ATP Tour increases by 5%: being left-handed, is a clear disadvantage in this case.

Similarly, to find the chance of winning with the other coefficients, I kept the remaining features of the two players constant and followed the same process.

Age:

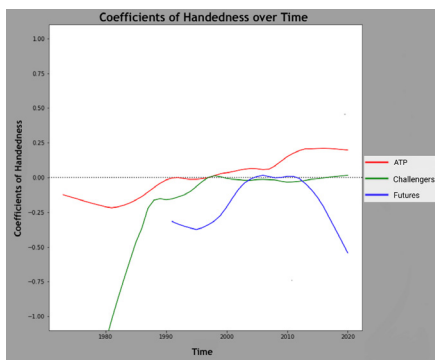


Figure 2: Graph of the coefficients of age on the ATP Tour, Challenger Tour, and Futures Tour over time.

Figure 2 shows that age has different impacts on the tiers. The ATP and Challengers graphs align with my claim that younger tennis players tend to perform better and defeat the older players. This juvenile advantage was more pronounced on the Challenger Tour than on the ATP Tour only prior to 1990. Post 1990, younger tennis players had a higher probability of winning on the ATP Tour than on the Challenger Tour. By contrast, older tennis players were better on the Futures Tour circuit, but this advantage favoring older players has decreased over the last couple of years. Older tennis players are better on the Futures Tour since they are likely to have more match experience. The level of tennis on the Futures Tour is not as great as that on the ATP Tour since it is the lowest rung of men's professional tennis. Often, matches involve taking advantage of the opponent's weakness. For instance, some players might have a weaker backhand compared to their forehand and their opponents will simply target their backhand side throughout the match. Older players are more likely to have had more time to work on bettering their overall game, giving these men an edge over the young teenagers who usually enter Futures tournaments. However, the last few years have seen the likes of Felix Auger Aliassime and Jannik Sinner; prodigies like these two have beat numerous older players in the lower tier tournaments like the Futures, before they advanced to the ATP Tour. On the contrary, to even be on the ATP Tour, players must have almost no weaknesses. At that level, the game becomes more of a mental, physical, and tactical sport rather than one that involves targeting weaknesses.

When I consider two players who are one year apart in age, I get the normalized difference in age from my training set to be 0.0272.

On the Challenger Tour during the 1980s,
 $p=0.483$

The chance of winning when being one-year younger was 51.7%.

However, on the Challenger Tour during the 2010s,
 $p=0.501$

It shows that the chance of winning for a younger player was 49.9%. The numbers show how the chance of winning for younger players and therefore their advantage diminished over time on the Challenger Tour.

On the ATP tour, 55 of the last 64 Grand Slams have been won either by Roger Federer, Novak Djokovic, or Rafael Nadal, who are collectively known as "The Big Three". These three tennis players have continued to dominate the top tournaments despite the numerous young talents that have emerged over the last few years and despite the fact that they are all in their 30s (Federer will turn 40 in August 2021). Over the last couple of years, the age-related advantage has not only reduced on this tour, but has also become positive – in support of older players.

Building the same logistic regression model without "The Big Three" in the data set would reveal the extent to which the previous model had been biased towards older tennis players in recent years on the ATP Tour.

$$p=0.489$$

Interestingly, the chance of winning for a younger player would have been 51.1% if "The Big Three" didn't compete on the ATP Tour. Although not a salient advantage, the age-related advantage would have been in favor of younger players over older players.

Height:

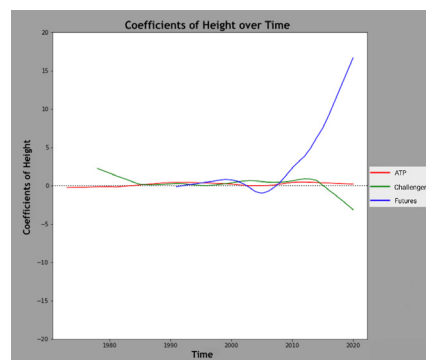


Figure 3: Graph of the coefficients of height on the ATP Tour, Challenger Tour, and Futures Tour over time.

Figure 3 demonstrates that taller tennis players on the Challenger circuit had a slightly higher probability of winning against shorter players in the late 1970s and early 1980s. Now, shorter players have the advantage. On the ATP tour, no certain height-related advantage could be deciphered as the curve constantly hugged the x-axis, suggesting that height hasn't had much importance on this tour. On the other hand, being taller than the opponent on the Futures Tour was a significant advantage. The dataset reveals that on the Futures Tour, the mean winning player height was 182.6 cm during

the 90s as compared to 188.1 cm during the 2010s. Taller tennis players on this tour serve better and faster for the following reasons: their heights provide a larger margin for error and a greater angle to serve out wide. In addition to this, they are more likely to exert a larger force on the ball (more body mass, which correlates to a greater change in momentum). The lack of experience in playing against taller players means that height is a significant match determinant on the Futures Tour. This puts shorter tennis players, who have a smaller wingspan and racket-arm extension, on the Futures Tour at a huge disadvantage. And since the mean height of tennis players has increased on this tour, this advantage has surged.

When I take two players who only differ by 1 cm in height, I get the normalized difference in height from my training set to be 0.0349. This predictor variable was plugged into the logit function.

During the 1980s on the Challenger Tour,
 $p=0.517$

This implies that the chance of winning for a player who was a centimeter taller than the opponent was 51.7% during the 1980s.

And as stated above, this chance of winning shifted to favor the shorter players during the last couple of years.

$p=0.474$

A shorter player on the Challengers had a 52.6% chance of winning.

On the Futures tour, taller players had a significantly higher chance of winning than on the other two tiers during the 2010s.

$p=0.612$

A 61.2% chance of winning for a taller player.

Rank:

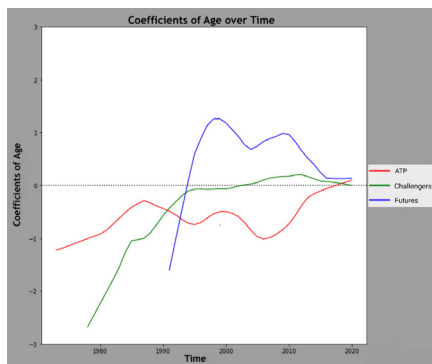


Figure 4: Graph of the coefficients of rank on the ATP Tour, Challenger Tour, and Futures Tour over time.

In Figure 4, all three curves on the graph show that higher-ranked tennis players have always had the advantage in a tennis match when playing against a lower-ranked opponent, supporting my claim that higher-ranked players had the upper hand between the two. Between the 1970s and the early 1980s, the probability of higher-ranked tennis players being more successful against their lower-ranked counterparts decreased on the ATP tour. Around the mid-1980s, the curves for both the ATP and Challengers started to plateau, suggesting that the advantage has had the same importance on the respective tours for a while. However, the ATP curve plateaued

lower than the Challenger curve implying that the advantage is more prominent on the ATP Tour and that the probability of a higher-ranked player defeating a lower-ranked player is higher on the ATP Tour than on the Challenger Tour. Since the Futures curve is above the other two and has a general negative trend, it implies that upsets are more likely to happen on the ITF Futures Tour and that this advantage is less salient on this tour compared to the other two circuits; however, the negative trend suggests that it is slowly becoming more relevant and important.

To quantify the advantage seen above, I chose two players who only differ by 1 ranking position, and got the normalized difference in height from my training set to be 0.111.

On the Futures Tour during the 1990s,
 $p=0.418$

When a player faced an opponent who was 1 rank below him during the 1990s, he had a 58.2% chance of winning against his opponent. I also know from the graph that the advantage of being higher-ranked in the Futures slowly increased with time; this can be confirmed by taking a coefficient from the 2010s.

$p=0.315$

When a player faced an opponent who was 1 rank below him during the 2010s, he had a 68.5% chance of beating his opponent.

■ Conclusion

I study how the handedness-related advantage develops over time on three consecutive tiers of men's tennis. The results agree that the influence of handedness as a match determinant has waned over time on the ATP Tour, but is still a prevalent factor on the ITF Futures Tour, while the ATP Challenger Tour seems to be an unbiased ground now.

This study substantiates my belief that younger players have a higher probability of beating older players. This claim holds true on the ATP Tour and Challenger Tour, but not on the Futures Tour. With rank, I confirm that higher-ranked players perform better, and that lower-ranked players have a better chance at winning against their counterparts on the Futures Tour than on the other two tiers. With height, the Futures Tour shows that this feature was important; on the contrary, shorter players have the advantage in Challenger matches.

A limitation of the study is the incomplete datasets on the GitHub repository during the first couple of years of Open Era tennis. The unavailability of data meant I couldn't get to use the exact values for those four features for my logistic regression model. I had to settle with the mean values of the columns they belonged to instead. Future work could undertake the same approach in women's, doubles, and mixed doubles tennis and their respective tiers; the findings should then be compared to the ones in this study.

Implications: From a tennis player's perspective:

As a tennis player and a right-hander who has played the sport for the last 8 years, I have first-hand experience of playing against left-handers and also evidence to support my main hypothesis. Having played low-tier tennis tournaments, such as AITA (All India Tennis Association), I can say that lefties have an advantage in this circuit, once again due to the negative frequency hypothesis. Righties like myself (who don't get

a chance to practice or play with left-handers often) struggle against left-handed tennis players during these tournaments due to lack of experience of playing against lefties and due to psychological influences (it's common for tennis coaches to constantly label left-handers as difficult opponents). More often than not, the left-handed tennis player will control and dictate the majority of points in such a matchup, and will end up winning the match.

■ Acknowledgements

I would like to thank my mentor Patrick Chao, who is a statistics Ph.D. student at the University of Pennsylvania, for his guidance during the research and writing processes. Furthermore, I would like to thank the faculty at Lumiere Education for providing me with the resources to make this project successful.

■ References

1. Hagemann, N. The advantage of being left-handed in interactive sports. <https://link.springer.com/article/10.3758/APP.71.7.1641> (accessed Apr 21, 2021).
2. Breznik, K. On the gender effects of handedness in professional tennis. <https://www.ncbi.nlm.nih.gov/pmc/articles/PMC3761843/> (p.72) (accessed Apr 21, 2021).
3. AP, R. M. P. D. D. A. B. M. Frequency-dependent maintenance of left handedness in humans. <https://pubmed.ncbi.nlm.nih.gov/9025310/> (accessed Apr 21, 2021).
4. Richardson, T.; Gilman, R. T. Left-handedness is associated with greater fighting success in humans. <https://www.ncbi.nlm.nih.gov/pmc/articles/PMC6817864/> (accessed Apr 21, 2021).
5. Faurie, C.; Raymond, M. Handedness, homicide and negative frequency-dependent selection. <https://www.ncbi.nlm.nih.gov/pmc/articles/PMC1634940/> (accessed Apr 21, 2021).
6. Norman Geschwind, M. D. Cerebral Lateralization. <https://jamanetwork.com/journals/jamaneurology/article-abstract/584161> (accessed Apr 21, 2021).
7. PMC, E. <http://europepmc.org/article/med/11104547> (accessed Apr 21, 2021).
8. P., B. S. B. Manual reaction time asymmetries in human subjects: the role of movement planning and attention. <https://pubmed.ncbi.nlm.nih.gov/11711210/> (accessed Apr 21, 2021).
9. APA PsycNet. <https://psycnet.apa.org/record/2006-03817-005> (accessed Apr 21, 2021).
10. Vasconcelos, O.; Barreiros, J.; Barbosa, R.; Trifilio, F. Functional asymmetry in a simple coincidence-anticipation task: Effects of handedness. <https://www.tandfonline.com/doi/abs/10.1080/17461390802603903> (accessed Apr 22, 2021).
11. Akpınar, S.; Bicer, B. Why Left-handers/footers are overrepresented in some sports? . http://mjssm.me/clanci/MJSSM_Sept_2014_Akpınar_33-38.pdf (accessed Oct 2020).
12. Loffing, F.; Hagemann, N.; Strauss, B. Left-Handedness in Professional and Amateur Tennis. <https://journals.plos.org/plosone/article?id=10.1371/journal.pone.0049325> (accessed Apr 21, 2021).
13. JeffSackmann. JeffSackmann/tennis_atp. https://github.com/JeffSackmann/tennis_atp (accessed Apr 22, 2021).
14. Joseph A. Cruz, D. S. W. Applications of Machine Learning in Cancer Prediction and Prognosis - Joseph A. Cruz, David S. Wishart, 2006. <https://journals.sagepub.com/doi/full/10.1177/117693510600200030> (accessed Apr 21, 2021).
15. Shewchuk, J. R. Concise Machine Learning. <http://people.eecs.berkeley.edu/~jrs/papers/machlearn.pdf> (accessed Oct 2020).

■ Author

Shreyes Sridhara is an IB student in his junior year at the Stonehill International School in Bangalore, India. He enjoys using statistical analysis to analyze and extract practical information from large-scale data, and hopes to major in Computer Science in college.

The Risk Factors of Adolescent Depression

Sia Agarwal

Valley Christian High School, 100 Skyway Dr #130, San Jose, CA 95111, USA; sia1991agarwal@gmail.com

ABSTRACT: The identification of potent risk factors is crucial to potentially prevent and intervene in adolescent depression. Conducting a literature search about the risk factors for adolescent depression in Google Scholar, BioMed Central, Nature, Pubmed, APA PsycNet, Science Direct, I included articles if the study discussed or measured risk factors of depression in a sample of individuals ages 10 to 19. The genetic, sex, stress, cognitive, gender, and interpersonal risk factors of adolescent depression are reviewed. Certain genetic mutations, negative inferential style, having a depressed parent, being a girl, and experiencing a recent stressful life event emerged as the most potent risk factors of adolescent depression. Understanding these risk factors and targeting them could lead to more effective adolescent depression prevention and interventions.

KEYWORDS: Behavioral and Social Sciences; Clinical and Developmental Psychology; Adolescent Depression; Depression Interventions.

■ Introduction

Because adolescents, who are individuals ages 10 to 19, are especially vulnerable to the risk of depression, identifying risk factors – characteristics often correlated with depression – will lead to more efficient interventions.¹ Intervention can be most effective when risk factors are appropriately identified and targeted.²

This paper discusses the gender, cognitive, interpersonal, and chronic and acute stress factors of adolescent depression. The review concludes with a proposal of methods to target the strongest predictors of adolescent depression.

■ Discussion

What is Depression?:

The American Psychiatric Association defines depression as a medical disorder that affects an individual's thinking, feelings, and behavior. Loss of enjoyment in usually enjoyable activities along with prolonged feelings of low mood constitutes the nature of depression.³ A doctor must note that a patient exhibits at least five symptoms out of Diagnostic and Statistical Manual of Mental Disorders (DSM-5) to diagnose the individual with depression. To fulfill the requirements of a diagnosis of depression, symptoms must persist for at least two weeks.⁴ Symptoms of depression include dejected mood, prolonged feelings of sadness, frequent feelings of lethargy, sleeping problems, loss in interest in usually enjoyable activities, and difficulties in concentrations and making decisions.⁵

Researchers and doctors use screening scales to effectively measure and identify symptoms of depression in individuals.⁶ Scales include the Beck Depression Inventory (BDI), the Center for Epidemiological Studies Depression Scale for Children (CES-DC), Centers for Epidemiologic Study Depression (CESD) Scale, Hamilton Depression Rating Scale (HAM-D), the Children's Depression Inventory (CDI), and the Behavior Assessment System for Children (BASC).⁷

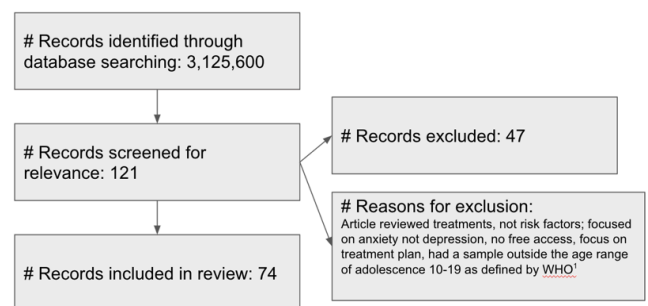
■ Methods

To determine which risk factors to discuss, I reviewed literature from Google Scholar, BioMed Central, Nature Journal, Pubmed, APA PsycNet, Science Direct, and Google searches. Some of the search terms I used were the following: 'genetic influences depression in adolescents', 'genetic predisposition to depression intervention', 'individual sex risk factor adolescent depression', 'biological sex risk factor adolescent depression', 'gender stereotypes effect on adolescent depression', 'negative attributional style adolescent depression', 'family functioning adolescent depression', 'peer relationships adolescent depression', and 'exposure to stress depression adolescents'.

Because the study of emotional disorders involves biological, psychological, and social influencing factors, I included risk factors from each of these categories; these decisions were supported by their prevalence in existing scientific literature.² I included articles on risk factors if the article studied individuals ages 10 to 19 and examined adolescent depression.

Prisma:

PRISMA (Preferred Reporting Items for Systematic Reviews and Meta-Analyses) is a set of items reported in a systematic review. Below is a modified version of the PRISMA set. This review is not systematic.



Biological Factors:

Sex and genetics are the biological factors most associated with adolescent depression in existing scientific literature. I chose to review these two factors as risk factors based on their prevalence in the literature review.

Psychological Factors:

I included gender due to the extensively researched difference in depression rates between boys and girls. I also included a range of interpersonal factors; the condition of social relationships is an indicator of psychological well-being.⁸

Risk Factors of Adolescent Depression:

1. Biological Factor – Genetics:

Research estimates that 40% of adolescent depression is related to inherited genes.⁹

5-HTT:

The 5-HTT gene codes for a serotonin transporter.¹⁰ The short allele, or the S allele, of 5-HTT is related to depression in adolescents.¹¹ Hankin et al. found that individuals with the s/s genotype tested for the highest scores of depression in a sample of 220 adolescents as they experienced external stressors, interacted with external stressors.¹² Another study, Benjet et al., found that the interaction between the 5-HTT gene and peer stress predicted for higher levels of depressive symptoms in adolescent girls.¹³ It was further concluded that adolescent girls with the s/s genotype were the most vulnerable to depressive symptoms because of peer stress. Girls with two short alleles and experiences of bullying scored higher on the study's depression screening measure than girls who had the same genotype but no experiences of peer stress.

To understand the strength of 5-HTT as a risk factor of adolescent depression, it is necessary to consider the frequency of 5-HTTLPR genotypes in the adolescent population. In a sample of 309 adolescents from Wisconsin, Pries-Groben and Hyde found "[f]requencies of 5-HTTLPR...were 34.6 % long/long, 46.8 % long/short, and 18.6 % short/short".¹¹ In another sample, genetic frequencies of "5-HTTLPR were 33% L/L, 46% S/L, and 21% S/S".¹²

Brain-derived neurotrophic factor (BDNF):

The Brain-derived neurotrophic factor (BDNF) gene codes for the protein that maintains neuron survival by regulating growth, maturation, and cell repair/maintenance.¹⁴ The BDNF Val66Met gene is a polymorphism where valine (Val) is replaced with methionine (Met) at codon 66 in the genetic sequence. Emotional and cognitive dysfunction is associated with this polymorphism; the polymorphism causes alterations in grey matter and modifies glutamate receptor activities.¹⁵ The average frequency of this polymorphism across a sample of populations in one study was 19.6%.¹⁶ Comasco et al. observed the interaction effect of 5-HTTLPR, negative early life events, and BDNF Val66Met in a sample of 1393 adolescents and found that adolescents with the ss/sl+Val/Val or the ll+Met genotypes had more depressive symptoms than those without.¹⁷

2. Biological Factor – Sex:

Biological sex can be observed at the genetic, hormonal, anatomical and behavioral levels. As sex differentiation occurs in adolescence, it can lead to the risk of depressive disorders.¹⁸

Hormones :

The HPA axis (hypothalamic-pituitary-adrenal axis) is a neuroendocrine system that consists of the hypothalamus, the pituitary gland, and the adrenal glands. It serves the key role in the body's reaction to stress.¹⁹ As the HPA axis develops during adolescence, certain pathways begin to produce hormones, such as estrogen and testosterone.¹⁸

Estrogen increases the transport and uptake of serotonin. During puberty, the homeostasis of estrogen is disrupted. Due to the consequential disruption of estrogen levels, adolescent girls are more vulnerable to mood disorders such as depression. Low levels of estrogen are related to depression.²⁰

On the other hand, the hormone testosterone functions in both males and females.²¹ However, the effects of testosterone for boys and girls differ. For girls, high levels of testosterone are correlated with depression; for boys, low levels of testosterone are correlated with depression.²²

3. Psychological factor – Stress :

Stress can trigger the onset of depression, according to the Hopelessness Theory of Depression. There are different types of stressors: acute, episodic acute, and chronic stressors.²³

Acute stress occurs after a single particularly stressful event; symptoms of acute stress develop in a short time period (minutes to hours) after the individual experiences the stressor.²⁴ Episodic acute stressors are several, continued experiences of acute stressors, resulting in episodes of acute stress over a period of time.²³ Chronic stress is stress that persists over time; because of its unrelenting nature, many people acclimate themselves to the symptoms of chronic stress, especially if the stress is a result of the individual's mindset or strenuous circumstances.²³ This section discusses stressful life events, which can be acute stressors or episodic stressors, and daily life or chronic stressors.

Stressful Life Events :

Stressful life events (SLEs) can trigger the onset of adolescent depression. Severely stressful life events include physical abuse, assault, and emotional abuse. Other stressful life events are parents' divorce or moving to a new home or school.²⁵ Since "approximately 70% of first depressive episodes and 40% of recurrent episodes of depression are preceded by a severe stressful life event"²⁶, SLEs should be seriously considered as a risk factor for adolescent depression. Interventions can screen for SLEs to identify those at a greater risk for adolescent depression.

One type of SLE is an adverse childhood experience (ACE). The CDC states that ACEs "are potentially traumatic events that occur in childhood (0-17 years)".²⁷ In a sample of 288 Native American adolescents and young adults (sample mean age = 19.25), Brockie et al. measured ACEs and depressive symptoms via a 189-question questionnaire.²⁸ The questionnaire assessed six childhood traumatic events: "physical abuse, emotional abuse, sexual abuse, emotional neglect, physical neglect, and witnessing violence against mother." An assessment of depressive symptoms associated with racial discrimination and historical loss were also included in this questionnaire.²⁸ Based on the questionnaire's results, the researchers found that with every additional instance of an ACE, there was a

57% increase of depressive symptoms. Not including sexual abuse, the ACEs measured predicted for depressive symptoms. Out of the six ACEs assessed, physical abuse correlated most strongly with depressive symptoms. Those with experiences of 3-6 ACEs had four and half times chances of depressive symptoms compared to those experiences of 0-2 ACEs.²⁸ Another study, Schilling et al., measured ACEs and depressive symptoms in a sample of 1093 high school seniors using a modified version of the CESD and a series of questions to assess ACEs.²⁹ Similar to Brockie et al., Schilling et al. concluded that depressive symptoms increased with each additional ACE.²⁹

Chronic Stressor: Daily Stressors and Common Life Difficulties:

A 2014 APA survey of 1018 adolescents, ages 13-17, reported that 30% of surveyed adolescents felt depressed due to stress; additionally, 31% of surveyed individuals also reported that their stress levels have increased in the past year and that they feel stress will continue to increase.³⁰

Daily or common stressors for adolescents usually include school, extra-curriculars, and family responsibilities. Overloading of assignments, social pressure, academic performance pressure, and peer competition contribute to school-related stress. One study, Jayanthi et al., found that adolescents who reported academic stress were at a 2.4 higher risk of depression than those who did not report academic stress.³¹ Low et al. studied associations between common stressors and mental health impacts in a sample of 1025 adolescents, ages 11 to 15, and found similar results in the relationship between depressive symptoms and stress from school work.²⁵ These studies suggest that chronic academic stress could be a risk factor in adolescent depression.

4. Psychological factor - Cognitive Style:

A cognitive style is a pattern of thinking that deals with attention, memory, and other vital cognitive functions. In childhood, cognitive styles begin to form, stabilizing and influenced by external factors during adolescence.³²⁻³⁴ A negative cognitive style, also called a negative attributional or inferential style, refers to how individuals continually assign the cause of negative events to internal, stable, and global causes.^{33,35} Three dimensions constitute an attributional style: "internal vs. external (whether attributions relate to causes inside or outside the self), stable versus unstable (whether attributions are for causes that persist with time or not), and global versus specific (whether attributions affect many or few situations)".³⁶ Individuals with a negative inferential style assume that their personal characteristics are negative and unfixable because of these attributions.³⁷ Individuals whose attributional styles are internal, stable, and global are more likely to be at risk to depression.³⁶

An example of a negative inferential style can operate like so: An individual attributes the cause of the end of a friendship to their own fault (self). They then infer that all this circumstance will always be the case for their friendships (stability). Finally, they infer that this would affect their future and all relationships of this nature (global).

Research suggests that a negative cognitive style is a strong predictor of adolescent depression. Rohde et al. tested several

risk factors of adolescent depression ("depressive symptoms, past MDD, hopelessness, negative cognitions, negative attributional style, poor self-esteem, loneliness, low social support, negative life events, poor social adjustment, substance use, low motivation to reduce depression, sex, race/ethnicity, age, and socioeconomic status") and found that the strongest predictor of adolescent depression in that sample was a negative inferential style. The group of adolescents with high negative inferential style scores were at four times more risk of depression than those who did not have negative attributional styles.³⁸ Muris et al. supports the correlation between a negative attributional style and adolescent depression with a model that showed negative attributional styles as the main source of depression in their sample.³⁹

Negative attributional style coupled with other cognitive vulnerabilities can also cause risk of adolescent depression. One study, Southall and Roberts, found that self-esteem moderates the degree to which an adolescent with a negative attributional style is at risk of depression.⁴⁰ A moderate correlation was discovered between low self-esteem and a negative attributional style, putting adolescents with both at a greater risk for depression than adolescents without either.⁴⁰ High self-esteem could act as a protective factor against the effects of a negative attributional style on depression because it prevents the spiraling towards general hopelessness. High esteem provides resilience against times of stress for individuals with negative attributional style. The development of depressive symptoms is avoided in this manner. This combination of high self-esteem with a negative attributional style may be a result of an unconditional positive self-regard.⁴¹ The protective nature against depression of high self-esteem could be explored in cognitive behavioral therapies for depression interventions.

Cognitive Style and Stress:

When a negative cognitive style interacts with stress, it can contribute to depression, as put forth by the cognitive-diathe-sis stress model.³⁷ The Hopelessness Theory of Depression adds to this model by proposing that individuals with negative inferential styles react to negative life events with hopelessness.¹⁹ These kinds of attributions, especially if repeated due to multiple occurrences of the stressful event, increase risk of depression.³³

Hankin et al. tested the Hopelessness Theory by observing the interactions of different negative inferential styles with stress and comparing the resulting depressive symptoms.³⁴ In a sample of 350 adolescents, the researchers measured negative inferential styles and depressive symptoms with the Adolescent Cognitive Style Questionnaire (ACSQ); stressful life events were also recorded. The study found that for individuals with highly negative inferential styles, levels of depressive symptoms increased as stress increased. Those who did not have negative inferential styles coped better with stress and did not have high levels of depressive symptoms as a result of their inferential style.³⁴

While some do not, some adolescents may actively contribute to the amount of stress in their life. The stress generation framework posits that adolescents actively contribute to the amount of stress in their life due to specific types of behavior.⁴² Before the beginning of a stressful event, pre existing

frameworks of thinking, such as an adolescent's expectations, perceptions, and interpretations influence the reaction to stress. These cognitive styles are established more firmly during adolescence.³⁴ Furthermore, adolescents with higher levels of cognitive vulnerability, such as negative cognitive style, self-criticism, and dependency, contribute to more stress in their life, which in turn means higher levels of depressive symptoms.⁴³

Interpersonal stress and cognitive styles:

A negative cognitive style can also affect how an individual perceives interpersonal interactions. Lee *et al.* concluded adolescents who possessed a negative cognitive style were more affected by negative parental interactions in terms of depression levels.⁴⁴ Ongoing negative interactions in relationships, coupled with negative perceptions of life situations, can put an adolescent at risk to depression.⁴⁴

Peer relationships can also influence who has a negative attributional style. In friendships, adolescents whose close friends had negative attributional styles were more likely to have negative attributional styles, and subsequently, were more likely to exhibit depressive symptoms.⁴⁵

Identifying the types of stress that exacerbate the use of negative attributional styles, and therefore increase risk to depression, may be useful in the construction of effective depression interventions.

Gender differences in negative cognitive styles and implications for depression:

For both female and male adolescents, depression is correlated with higher levels of a negative attributional style. However, research suggests that girls and boys differ in their types of attributional styles. Gladstone *et al.* found that boys were more likely to have depressogenic attributions in the stable dimension; this means that boys were more likely to attribute the cause of a negative event to stable causes than girls.⁴⁶ On the other hand, girls were more likely to have depressogenic attributions in the global dimension, meaning that the cause of a negative event would affect all situations of a similar nature. Girls made more internal attributions than boys; this behavior correlated with their overall lower self-esteem compared to boys. As mentioned before, lower self-esteem is also correlated with adolescent depression. The gender differences in types of negative attributions may relate to the differences in depression rates between boys and girls.⁴⁶

In summary, negative cognitive styles can interact with stress to form cognitive vulnerabilities to depression in adolescents. Identifying individuals with negative attributional styles, perhaps by using the Adolescent Cognitive Style Questionnaire, could prove useful in interventions that target cognitive styles. Cognitive behavioral therapies focus on negative inferential styles, which are a strong predictor of depression, and they are effective at shifting these styles to more positive patterns of thinking. Thus, interventions should consider targeting cognitive styles for efficacy in reducing adolescent depression levels.

5. Social factor – Gender:

Gender is defined as the social constructs of the characteristics of girls and boys. Behaviors and roles are associated with

certain genders, affecting how individuals view themselves and experience the world.⁴⁸

Boys and girls are at different levels of risk of depression and experience depression differently. Girls are twice more likely to develop depression in adolescence than boys.⁴⁹

Boys and girls exhibit depression differently. In a sample of 383 adolescents, Bennett *et al.* measured depressive symptoms with the Childhood Version of the Schedule for Affective Disorders and Schizophrenia and the BDI.50 From their trial, they concluded that girls' depressive symptoms could be described by higher levels of excessive guilt, self-blame, dissatisfaction, "self-disappointment, feelings of failure, concentration problems, difficulty working, sadness or depressed mood, sleep problems, fatigue".⁵⁰ Depression in boys appeared as symptoms of "anhedonia, depressed morning mood, and morning fatigue".⁵⁰ Another study, Khesht-Masjedi *et al.*, measured depressive symptoms in a sample of 191 adolescents and found similar results.⁵¹ In this sample, depressed girls experienced more guilt, self-blame, and dissatisfaction whereas boys experienced more trouble sleeping and fatigue.⁵¹ Seeley *et al.* screened for a number of risk factors for depression (parent and peer support, negative life events, attributional style, emotionality, perfectionism, body dissatisfaction, bulimic symptoms, physical activity, social adjustment, delinquency, substance use) in a sample of 479 adolescent girls.⁵² They found that the strongest predictors of depression in this sample were delinquency, poor school and familial functioning, subclinical depressive symptoms, minimal parental support, and symptoms of bulimia. The highest risk group were girls who had both elevated depressive symptoms and poor academic performance; they marked a 40% incidence of major depression.⁵²

The stress of social pressure that girls and boys face to conform to gender roles may be a risk factor to depression. As they move into adolescence, girls may face real or perceived reduction in choices or opportunities. Reports from adolescents show that girls perceive more expectations and restrictions from their parents as compared to boys. Girls also may feel restricted by the types of activities and preferences that are deemed 'suitable' for girls by social norms. Such restrictions could be a source of chronic stress for adolescent girls.⁵³ The mediational--stress exposure model posits that girls' rates of depression are higher due to their greater exposure of stress compared to boys.⁵⁴ Girls experience greater exposure to interpersonal stress from peers, romantic partners, and family members. Reports of higher stress are not limited to the interpersonal domain.⁵⁵

In addition to the differences in exposure to stress, girls and boys react differently to stress. The moderation--stress model posits that girls react more strongly to stressors in a way that puts them at a greater risk for depression.⁵⁶ For example, girls are more likely to respond to stress with rumination, meaning they are more likely to dwell on the stressful situation without taking steps to relieve or eliminate stress.⁵³ Rumination is a type of thinking pattern that focuses on negative content from the past and present. This type of thinking can be a cognitive vulnerability to adolescent depression.⁵⁷

Depression in parents, especially mothers, is associated with negative parenting styles including rejection, high levels of criticism, and minimal acceptance, comfort, and/or warmth. These types of parenting styles strongly correlate with depression in their adolescents.⁶¹ Weissman *et al.* found that adolescents of depressed parents are three times more likely to develop depressive and anxiety disorders than those of non-affected parents.⁶² Between ages 15-20, adolescents of depressed parents were more likely to experience the onset of depression.⁶² Rice *et al.* found similar results: Children of depressed parents are at three to four times more risk of depression than children of healthy parents.⁹

Depression in parents is correlated with cognitive vulnerabilities to depression in adolescents. This includes higher levels of self-blame, usage of a negative attributional style, and lower self-worth. While each of these behaviors by themselves might not automatically lead to depression, they can be risk factors to developing depression later on. Depression in parents has also been correlated with poor interpersonal functioning, which in itself can be a risk factor to adolescent depression. Finally, depression in parents can also be a risk for the following: earlier age of onset, longer duration, greater functional impairment, higher likelihood of recurrence.⁶¹

Family relationships:

Parents play a vital role in an adolescent's development.⁶³ Conflict within the parent-adolescent relationship and in the family may become a stressor for adolescents. Specifically, it may become a chronic stressor due to adolescent's inability to remove themselves from their family environment.⁶⁴

The state of family functioning can also be a risk to adolescent depression. Family functioning can be described as composed of elements such as family structure, family communication, adaptability and cohesion, and problem solving.⁶⁵

Rawatlal *et al.*, found that adolescents who reported high levels of family dysfunction were more likely report depressive symptoms.⁶⁶ Certain behaviors of the adolescent and parents may worsen the risk of depression. Constrained parental aggressiveness is correlated with adolescent depression. For girls, maternal submissiveness is correlated with depression.⁶⁴ On the other hand, there are also positive behaviors that can act as a buffer against depression. One example is emotional clarity, which is defined as the ability of an individual to accurately identify and understand their emotions. Over an observation period of 2 years, Freed *et al.* found that emotional clarity in adolescents acted as a protective factor against depressive symptoms and poor family functioning.⁶⁷ The relationship that exists between depression and family functioning could be explained by the degree to which adolescents are able to exercise emotional clarity. A cycle may occur when poor emotional clarity degrades family relationships, which may subsequently cause depressive symptoms over an extended period of time. The study suggested that "it is possible that poor family functioning exacerbates depression and impaired emotion regulation for youth who already experience these deficits".⁶⁷

Peer relationships:

Adolescents put more importance on peer relationships than any others, which sets the stage for greater exposure to inter-

personal incidents and possible higher levels of reactivity to such stressors.⁶⁸

Peer relationships can vary from dyadic relationships, a small group, or a large group of peers. These function as different social units. The dimensions of a social unit include social interactions, social support, and liking. Difficulties in peer relationships can include rejection, lack of perceived support from friends, and lack of popularity.⁶⁹ Dysfunction in peer relationships may put an adolescent at risk to depression. In a sample of 143 adolescents, ages 13-14, Allen *et al.* found that "behavior undermining relatedness with close friends, calls for emotional support from close friends, and social withdrawal" strongly correlated with future depressive symptoms.⁶⁹ Social withdrawal may be a particularly potent risk factor to depression because withdrawal isolates the adolescent from getting help they need to navigate changing relationship expectations. Withdrawal also causes long term effects when the individual does not know how to cope with new interpersonal changes or is left out interpersonal interactions entirely due to previous absence. For adolescents already diagnosed with depression, Armsden *et al.* supported the finding that depression is related to less secure peer attachment.⁷⁰ Another study, Joiner, found a similar result that higher levels of depression in adolescents are correlated with higher levels of social withdrawal.⁷¹ Undermining behaviors of anger and hostility that are related to adolescent depression could provide a starting point for interventions for depression.

Peer relationships:

Peer victimization, consistent exposure of negative behaviors from peers, is associated with adolescent depression.⁷² Klomek *et al.* measured the relationship between depressive symptoms and peer victimization in 2,342 high school students, ages 13 to 19, using the BDI and a peer victimization questionnaire.⁷³ They found that as rates of types of peer victimization increased, those individuals' depression rates increased. For male participants who experienced 5-6 types of victimization, there was a 29.7% prevalence of depression; for female participants who experienced 5-6 types of victimization, there was a 65.0% prevalence of depression. The more types of peer victimization a participant experienced, the more at risk they were to depression.⁷³

■ Conclusion

The findings of this paper suggest that the strongest indicators and risk factors of adolescent depression are genetics, being a girl, a negative inferential style, having a depressed parent, and experiencing a recent stressful life experience. First, 40% of depression cases can be linked to genetics. Second, girls are 2 times more likely to develop depression in adolescence. Second, an adolescent with a depressed parent is 3 to 4 times more likely to develop depression compared to children with healthy parents. Third, having a highly negative inferential style puts an adolescent at four times the risk of depression than an adolescent with a healthy inferential style. Finally, "approximately 70% of first depressive episodes and 40% of recurrent episodes of depression are preceded by a severe stressful life event", making SLEs a significant risk factor to adolescent depression.²⁷ These five make up the risk factors that are the most

correlated with adolescent depression based on this literature review.

An effective intervention for adolescent depression could screen for four identified risk factors: female gender, a negative inferential style, having a depressed parent, and recent SLEs. Genetic screening is still possible, but it is more expensive. The intervention could resemble a psychoeducational intervention, such as the Coping with Depression Course, with modifications.⁷⁴ First, a participant would be taken through a screening process; then, they would be directed to a risk-factor specific course that would help them with their specific issues. This way, high-risk groups could be identified by the screening measures and be given problem-specific skill training to help them prevent future depression or cope with current depressive symptoms. Future research could determine whether screening for risk factors before treatment is effective in reducing depressive symptoms or preventing depression. Future research could also look at whether an electronic delivery or an in-person of this program is more effective; electronic deliveries of interventions may be worthwhile researching because of global circumstances such as COVID-19.

■ Acknowledgements

I want to thank Dr. Ethan Hutt for his guidance and support through the research process. Thank you for reviewing multiple drafts of my paper, encouraging me to keep researching and writing, and providing valuable feedback.

■ References

- Adolescent health. (n.d.). Retrieved November 1, 2020, from Who.int website: <https://www.who.int/southeastasia/health-topics/adolescent-health>
- Risk and Protective Factors <https://www.samhsa.gov/sites/default/files/20190718-samhsa-risk-protective-factors.pdf> (accessed Oct 26, 2020).
- Depression (major depressive disorder) <https://www.mayoclinic.org/diseases-conditions/depression/symptoms-causes/syc-20356007> (accessed Oct 26, 2020)
- Depression Diagnosis <https://www.webmd.com/depression/guide/depression-diagnosis> (accessed Oct 26, 2020).
- Torres, F. What Is Depression? <https://www.psychiatry.org/patients-families/depression/what-is-depression> (accessed Oct 26, 2020).
- Vahle, V. L. Depression Measures in Outcomes Research. *Physical Medicine* 2000, 81, S53–S62. <https://doi.org/10.1053/apmr.2000.20625>.
- Depression Assessment Instruments <https://www.apa.org/depression-guideline/assessment> (accessed Oct 26, 2020).
- Majd Ara, E.; Talepasand, S.; Rezaei, A. M. A Structural Model of Depression Based on Interpersonal Relationships: The Mediating Role of Coping Strategies and Loneliness. *Noro* 2017, 54 (2), 125–130. <https://doi.org/10.5152/npa.2017.12711>.
- Rice, F.; Harold, G.; Thapar, A. The Genetic Aetiology of Childhood Depression: A Review. *J. Child Psychol. Psychiatry* 2002, 43 (1), 65–79.
- Bernaras, E.; Jaureguizar, J.; Garaigordobil, M. Child and Adolescent Depression: A Review of Theories, Evaluation Instruments, Prevention Programs, and Treatments. *Frontiers in Psychology* 2019, 10.
- Priess-Groben, H. A.; Hyde, J. S. 5-HTTLPR X Stress in Adolescent Depression: Moderation by MAOA and Gender. *Journal of Abnormal Child Psychology* 2012, 41 (2), 281–294.
- Hankin BL, Jenness J, Abela JR, Smolen A. Interaction of 5-HTTLPR and idiographic stressors predicts prospective depressive symptoms specifically among youth in a multiwave design. *J Clin Child Adolesc Psychol.* 2011;40(4):572–585. doi:10.1080/15374416.2011.581613
- Benjet C, Thompson RJ, Gotlib IH. 5-HTTLPR moderates the effect of relational peer victimization on depressive symptoms in adolescent girls. *J Child Psychol Psychiatry.* 2010;51(2):173–179. doi:10.1111/j.1469-7610.2009.02149.x
- BDNF gene: MedlinePlus Genetics. <https://medlineplus.gov/genetics/gene/bdnf/> (accessed Apr 8, 2021).
- Park, C.-hyun; Kim, J.; Namgung, E.; Lee, D.-W.; Kim, G. H.; Kim, M.; Kim, N.; Kim, T. D.; Kim, S.; Lyoo, I. K.; Yoon, S. The BDNF Val66Met Polymorphism Affects the Vulnerability of the Brain Structural Network. *Frontiers in Human Neuroscience* 2017, 11.
- Vulturar, R.; Chiş, A.; Hambrich, M.; Kelemen, B.; Ungureanu, L.; Miu, A. C. Allelic Distribution of BDNF Val66Met Polymorphism in Healthy Romanian Volunteers. *Translational Neuroscience* 2016, 7 (1), 31–34.
- Comasco, E.; Åslund, C.; Orelund, L.; Nilsson, K. W. Three-Way Interaction Effect of 5-HTTLPR, BDNF Val66Met, and Childhood Adversity on Depression: A Replication Study. *European Neuropsychopharmacology* 2013, 23 (10), 1300–1306.
- Naninck, E. F.; Lucassen, P. J.; Bakker, J. Sex Differences in Adolescent Depression: Do Sex Hormones Determine Vulnerability? *Journal of Neuroendocrinology* 2011, 23 (5), 383–392.
- Heaney, J. Hypothalamic-Pituitary-Adrenal Axis. *Encyclopedia of Behavioral Medicine* 2013.
- Halbreich, U.; Kahn, L. Role of Estrogen in the Aetiology and Treatment of Mood Disorders. *CNS Drugs* 2001, 15, 797–817.
- Testosterone: Functions, deficiencies, and supplements. <https://www.medicalnewstoday.com/articles/276013> (accessed Apr 8, 2021).
- Granger, D.; Shirtcliff, E.; Zahn-Waxler, C.; Usher, B.; Klimes-Dougan, B.; Hastings, P. Salivary Testosterone Diurnal Variation and Psychopathology in Adolescent Males and Females: Individual Differences and Developmental Effects. *Development and Psychopathology* 2003, 15, 431–449.
- Ehrenfeld, T. The Three Types of Stress. *Psychology Today.* December 7, 2018.
- Knott, D. L. Acute Stress Reaction <https://patient.info/mental-health/stress-management/acute-stress-reaction> (accessed Oct 26, 2020).
- Low NC, Dugas E, O'Loughlin E, D. Rodriguez, G. Contraras, M. Chaiton, and J. O'Loughlin. Common stressful life events and difficulties are associated with mental health symptoms and substance use in young adolescents. *BMC Psychiatry.* 2012; 12:116. Published 2012 Aug 17. doi:10.1186/1471-244X-12-116
- Mufson, L.; Dorta, K. P.; Wickramaratne, P.; Nomura, Y.; Olfson, M.; Weissman, M. M. A Randomized Effectiveness Trial of Interpersonal Psychotherapy for Depressed Adolescents. *Arch. Gen. Psychiatry* 2004, 61 (6), 577–584.
- Stroud, K. *Stressful Life Events and Major Depression.*
- Brockie, T. N.; Dana-Sacco, G.; Wallen, G. R.; Wilcox, H. C.; Campbell, J. C. The Relationship of Adverse Childhood Experiences to PTSD, Depression, Poly-Drug Use and Suicide Attempt in Reservation-Based Native American Adolescents and Young Adults. *Am. J. Community Psychol.* 2015, 55 (3–4), 411–421.
- Schilling, E. A.; Aseltine, R. H., Jr; Gore, S. Adverse Childhood Experiences and Mental Health in Young Adults: A Longitudinal

- Survey. *BMC Public Health* 2007, 7 (1), 30.
30. Bethune, S. American Psychological Association Survey Shows Teen Stress Rivals That of Adults <https://www.apa.org/news/press-releases/2014/02/teen-stress> (accessed Oct 26, 2020)
31. Jayanthi, P.; Thirunavukarasu, M.; Rajkumar, R. Academic Stress and Depression among Adolescents: A Cross-Sectional Study. *Indian Pediatr.* 2015, 52 (3), 217–219.
32. Cole, D. A.; Ciesla, J. A.; Dallaire, D. H.; Jacquez, F. M.; Pineda, A. Q.; Lagrange, B.; Truss, A. E.; Folmer, A. S.; Tilghman-Osborne, C.; Felton, J. W. Emergence of Attributional Style and Its Relation to Depressive Symptoms. *J. Abnorm. Psychol.* 2008, 117 (1), 16–31.
33. Hankin, B. L. Stability of Cognitive Vulnerabilities to Depression: A Short-Term Prospective Multiwave Study. *J. Abnorm. Psychol.* 2008, 117 (2), 324–333.
34. Hankin, B. L.; Oppenheimer, C.; Jenness, J.; Barrocas, A.; Shapero, B. G.; Goldband, J. Developmental Origins of Cognitive Vulnerabilities to Depression: Review of Processes Contributing to Stability and Change across Time. *J. Clin. Psychol.* 2009, 65 (12), 1327–1338
35. Abramson, L. Y.; Seligman, M. E.; Teasdale, J. D. Learned Helplessness in Humans: Critique and Reformulation. *J. Abnorm. Psychol.* 1978, 87 (1), 49–74.
36. Hu, T.; Zhang, D.; Yang, Z. The Relationship Between Attributional Style for Negative Outcomes and Depression: A Meta-Analysis. *Journal of Social and Clinical Psychology* 2015, 34 (4), 304–321.
37. Abramson, L. Y. Hopelessness Depression: A Theory-Based Subtype of Depression. *Psychological Review* 1989, 96 (2), 358–372. <https://doi.org/10.1037/0033-295X.96.2.358>.
38. Rohde, P.; Stice, E.; Gau, J. M. Effects of Three Depression Prevention Interventions on Risk for Depressive Disorder Onset in the Context of Depression Risk Factors. *Prev. Sci.* 2012, 13 (6), 584–593.
39. Muris, P.; Schmidt, H.; Lambrichs, R.; Meesters, C. Protective and Vulnerability Factors of Depression in Normal Adolescents. *Behaviour Research and Therapy* 2001, 39 (5), 555–565.
40. Southall, D.; Roberts, J. E. Attributional Style and Self-Esteem in Vulnerability to Adolescent Depressive Symptoms Following Life Stress: A 14-Week Prospective Study. *Cognitive Therapy and Research* 2002, 26 (5), 563–579.
41. Rogers, C. R. *On becoming a person* 1961.
42. Alloy, L. B.; Liu, R. T.; Bender, R. E. Stress Generation Research in Depression: A Commentary. *International Journal of Cognitive Therapy* 2010, 3 (4), 380–388.
43. Auerbach RP, Ho MH, Kim JC. Identifying cognitive and interpersonal predictors of adolescent depression. *J Abnorm Child Psychol.* 2014;42(6):913-924. doi:10.1007/s10802-013-9845-6
44. Lee A, Hankin BL, Mermelstein RJ. Perceived social competence, negative social interactions, and negative cognitive style predict depressive symptoms during adolescence. *J Clin Child Adolesc Psychol.* 2010;39(5):603-615. doi:10.1080/15374416.2010.501284
45. Stevens, E. A.; Prinstein, M. J. Peer Contagion of Depressogenic Attributional Styles Among Adolescents: A Longitudinal Study. *Journal of Abnormal Child Psychology* 2005, 33 (1), 25–37.
46. Gladstone, T. R.; Kaslow, N. J.; Seeley, J. R.; Lewinsohn, P. M. Sex Differences, Attributional Style, and Depressive Symptoms Among Adolescents. *Journal of Abnormal Child Psychology* 1997, 25 (4), 297–306.
47. Hankin, B. L.; Abramson, L. Y. Measuring Cognitive Vulnerability to Depression in Adolescence: Reliability, Validity, and Gender Differences. *Journal of Clinical Child & Adolescent Psychology* 2002, 31 (4), 491–504.
48. Gender and health. https://www.who.int/health-topics/gender#tab=tab_1 (accessed Apr 8, 2021).
49. Mood disorders: Depression and anxiety in teen girls <https://childmind.org/article/mood-disorders-and-teenage-girls/> (accessed Oct 26, 2020).
50. Bennett, D. S.; Ambrosini, P. J.; Kudes, D.; Metz, C.; Rabinovich, H. Gender Differences in Adolescent Depression: Do Symptoms Differ for Boys and Girls? *J. Affect. Disord.* 2005, 89 (1–3), 35–44.
51. Khesht-Masjedi, M. F.; Shokrgozar, S.; Abdollahi, E.; Golshahi, M.; Sharif-Ghaziani, Z. Comparing Depressive Symptoms in Teenage Boys and Girls. *J. Family Med. Prim. Care* 2017, 6 (4), 775–779.
52. Seeley, J. R.; Stice, E.; Rohde, P. Screening for Depression Prevention: Identifying Adolescent Girls at High Risk for Future Depression. *J. Abnorm. Psychol.* 2009, 118 (1), 161–170.
53. Nolen-Hoeksema, S. Gender Differences in Depression. *American Psychological Society* 2001.
54. Hankin, B. L.; Abramson, L. Y. Development of Gender Differences in Depression: Description and Possible Explanations. *Annals of Medicine* 1999, 31 (6), 372–379.
55. Hankin, B. L.; Mermelstein, R.; Roesch, L. Development of Gender Differences in Depression: Description and Possible Explanations. *Child Development* 2007, 38 (1), 279–295.
56. Rudolph, K. D. Gender Differences in Emotional Responses to Interpersonal Stress during Adolescence. *Journal of Adolescent Health* 2002, 30 (4), 3–13.
57. Sansone RA, Sansone LA. Rumination: relationships with physical health. *Innov Clin Neurosci.* 2012;9(2):29-34.
58. Kato, T. Assessing Coping With Interpersonal Stress: Development and Validation of the Interpersonal Stress Coping Scale in Japan. *International Perspectives* 2013, 2 (2), 100–115. <https://doi.org/10.1037/ipp0000002>.
59. Kobak, R.; Ferenz-Gillies, R. Emotion Regulation and Depressive Symptoms during Adolescence: A Functionalist Perspective. *Development and Psychopathology* 1995, 7 (1), 183–192.
60. Avison, W. R.; Turner, R. J. Stressful Life Events and Depressive Symptoms: Disaggregating the Effects of Acute Stressors and Chronic Strains. *Journal of Health and Social Behavior* 1988, 29 (3), 253.
61. National Research Council (US) and Institute of Medicine (US) Committee on Depression, Parenting Practices, and the Healthy Development of Children; England, M. J.; Sim, L. J. *Associations between Depression in Parents and Parenting, Child Health, and Child Psychological Functioning*; National Academies Press: Washington, D.C., DC, 2009.
62. Weissman, M. M.; Wickramaratne, P.; Nomura, Y.; Warner, V.; Pilowsky, D.; Verdelli, H. Offspring of Depressed Parents: 20 Years Later. *Am. J. Psychiatry* 2006, 163 (6), 1001–1008.
63. Steinberg, L. We Know Some Things: Parent-Adolescent Relationships in Retrospect and Prospect. *Journal of Research on Adolescence* 2001, 11 (1), 1–19.
64. Sheeber, L.; Hops, H.; Davis, B. Family Processes in Adolescent Depression. *Clinical Child and Family Psychology Review* 2001, 4 (1), 19–35.
65. COMBRINCK-GRAHAM, L. E. E. Developments in Family Systems Theory and Research. *Journal of the American Academy of Child & Adolescent Psychiatry* 1990, 29 (4), 501–512.
66. Rawatlal, N.; Kliewer, W.; Pillay, B. J. Adolescent Attachment, Family Functioning and Depressive Symptoms. *South African Journal of Psychiatry* 2015.
67. Freed RD, Rubenstein LM, Daryanani I, Olinio TM, Alloy LB. The Relationship Between Family Functioning and Adolescent Depressive Symptoms: The Role of Emotional Clarity. *J Youth Adolesc.* 2016;45(3):505-519. doi:10.1007/s10964-016-0429-y

68. Shih, J. H.; Eberhart, N. K.; Hammen, C. L.; Brennan, P. A. Differential Exposure and Reactivity to Interpersonal Stress Predict Sex Differences in Adolescent Depression. *Journal of Clinical Child & Adolescent Psychology* 2006, 35 (1), 103–115.
69. Allen, J. P.; Insabella, G.; Porter, M. R.; Smith, F. D.; Land, D.; Phillips, N. A. Social-Interactional Model of the Development of Depressive Symptoms in Adolescence. *J. Consult. Clin. Psychol.* 2006, 74 (1), 55–65.
70. Armsden, G. C.; McCauley, E.; Greenberg, M. T.; Burke, P. M.; Mitchell, J. R. Parent and Peer Attachment in Early Adolescent Depression. *Journal of Abnormal Child Psychology* 1990, 18 (6), 683–697.
71. Joiner, T. E. Depression's Vicious Scree: Self-Propagating and Erosive Processes in Depression Chronicity. *Clinical Psychology: Science and Practice* 2000, 7 (2), 203–218.
72. Bowes, L.; Joinson, C.; Wolke, D.; Lewis, G. Peer Victimization during Adolescence and Its Impact on Depression in Early Adulthood: Prospective Cohort Study in the United Kingdom. *BMJ* 2015, 350, h2469.
73. Klomek, A. B.; Marrocco, F.; Kleinman, M.; Schonfeld, I. S.; Gould, M. S. Peer Victimization, Depression, and Suicidality in Adolescents. *Suicide Life Threat. Behav.* 2008, 38 (2), 166–180.
74. Cuijpers, P. A Psychoeducational Approach to the Treatment of Depression: A Meta-Analysis of Lewinsohn's "Coping With Depression" Course. *BEHAVIOR THERAPY* 1998, 29.

■ Author

Sia is a senior at Valley Christian High School in San Jose, California. She is interested in understanding how mental health affects youth. Through her website and magazine, Decompress, Sia learns alongside her users about mental wellbeing. She aims to study environmental science in the future.

Reduction of Heat Resistance of *Campylobacter jejuni* Using D-limonene from Calamansi Rinds Extract

Trinity Bjork M. Coduco, Bea Nicole S. Gacayan, Mary Danielle M. Estrada

Quezon City Science High School, Misamis St. corner Golden Acres. Road, Bago Bantay, Quezon City, 1105, Philippines; coduco.trinitybjork@gmail.com; nicole.gacayan@gmail.com; estradadanielamary@gmail.com

ABSTRACT: *Campylobacter jejuni* (*C. jejuni*) is a gram-negative bacterium. It induces several bacterial effects, such as extra-gastrointestinal manifestations. Its ubiquity and heat-resistance make it hard to control and eliminate. D-limonene is a monocyclic monoterpene found in citrus fruits. It constitutes 94% of the essential oil from calamansi (*Citrus microcarpa Bunge*) rinds. Reducing the heat resistance of *C. jejuni* using D-Limonene from Calamansi rinds extract is the main objective of this study. D-limonene extracted from calamansi rinds was dissolved in ethanol and used to create a mixture with *C. jejuni* ATCC 29428 with a ratio 1:3. Two triplicates were made and placed inside a water bath under temperatures of 50°C and 55°C for six minutes, then plated on Mueller-Hinton agar with 5% lysed horse blood under 24-hour incubation in a microaerophilic environment. The results show that D-limonene from calamansi rinds has a significant effect on reducing the heat resistance of *C. jejuni* and was more evident at 50°C than at 55°C. The negative controls showed too numerous to count (TNTC) colonies (approximately 30-300), while treated replicates showed an average of 15.7 for 50°C and 51 for 55°C. This study shows that D-limonene from calamansi rinds can decrease the heat resistance of *C. jejuni*.

KEYWORDS: Microbiology; Bacteriology; *Campylobacter jejuni*; Calamansi; D-limonene; Heat-resistance.

■ Introduction

Campylobacter jejuni (*C. jejuni*) is a gram-negative bacterium that is one of the most prevalent reported bacterial causes of campylobacteriosis in humans.¹ *C. jejuni* is more likely to cause cases of gastroenteritis than *Salmonella* or *Shigella* species.² This bacterium has optimum growth at 37°-42°C and can survive at temperatures up to 55°C.³ *Campylobacter* can also survive in water around 15°C for a few days, and can be inactivated through heat at 85°C for 1 minute.⁴ Various species of *Campylobacter* were long-assumed to be associated with warm-blooded animals only. They were unidentified as human pathogens for decades due to the lack of methods in detecting the bacteria.⁵ Reservoirs of *Campylobacter* contamination are mainly poultry products, water, unpasteurized milk, mushrooms, and pets which are considered the sources of sporadic infections in humans, but cross-contamination, improper handling, and cooking of foods of animal origin account for the majority of the diseases.⁶

Campylobacter has a commensal relationship with an extensive range of birds and mammals, such as domestic animals used for food production and pets. This bacterium lives in the intestinal tract of its host, leading to various ways of infecting humans.⁵ The organisms have the ability to survive in the environment for several weeks at temperatures around 4°C, and cause infections as a result of consuming untreated water and milk.⁷ Direct contact with infected animals can also transmit infection, which puts those who work in specialized occupations which require exposure and contact with animals such as veterinarians, animal husbandry personnel, butchers, meat inspectors, and animal caretakers at high risk of infection.⁵ Moreover, there are records that show 80% of all *Campylobacter*

infections are affiliated with chickens, mainly in their cecum and feces where the bacterium is frequently found.⁸ Poultry is also heavily contaminated in the course of mass processing. In the event of the processing of chicken carcasses, spreading of the organisms may occur either from the large number of bacteria within the intestinal tract or from the presence of *C. jejuni* from the birds' feathers and skin. This enormous number of bacteria results in substantial contamination of processed carcasses. In a recent study, findings show that there were very low levels of *C. jejuni* (1.7%) in the feces of broilers at 4-5 weeks of age. However, at the time of slaughter (ca. 6-7 weeks of age), the ceca of birds yielded a higher incidence of *C. jejuni* (24%).⁵ *C. jejuni* is considered ubiquitous, therefore making it difficult to control and to prevent its spread.⁹ A study conducted in the laboratory, had indicated that birds already colonized with *C. jejuni* can expeditiously transmit the bacterium to the majority of its hatch mates as fast as 3 days or even less.⁵ Infection with this bacterium may cause a variety of diseases such as acute enteritis, extraintestinal infections, postinfectious complications, and more.² This pathogen has also been recorded to be affiliated in extra-gastrointestinal manifestations, which include lung infections, bacteremia, meningitis, brain abscesses, and reactive arthritis.¹

Campylobacter is becoming progressively resistant to clinically essential antibiotics, which is a major problem for public health.¹⁰ Due to the indiscriminate use of antibiotics, there is a rising number of human infections caused by antimicrobial resistant strains of the bacterium. The chronic continuation of this practice makes clinical management of campylobacteriosis cases more difficult to handle. Antimicrobial resistance can lengthen the period of the illness and compromise treatment

of patients with bacteremia. The rate of antimicrobial-resistant enteric infections is highest in developing countries, where the use of antimicrobial drugs in humans and animals is relatively unrestricted.⁵ A study in the Philippines showed that *C. jejuni* found in chicken carcasses bought around Metro Manila have now developed strains resistant to antibiotics such as clindamycin (98.6%), erythromycin (98.6%), nalidixic acid (98.1%), tetracycline (94.2%), gentamicin (65.2%), and chloramphenicol (52.7%).¹¹ In the management of campylobacteriosis, fluid therapy is highly recommended. However, it must be remembered that antimicrobial treatment is only prescribed to patients with severe cases or if they are immunocompromised. It is also not advisable to inject antibiotics that can stop the bacterium from transmitting to consumers. Several side effects and new diseases are potential hazards that are likely to occur.¹²

Aside from using antibiotics, another solution is disinfection and cleaning programs. These programs include dry and wet cleaning, along with the application of two detergents (one basic and one acid) and two disinfectants (250 g/L glutaraldehyde and 185 g/L formaldehyde at 0.5% and 210 g/L para-chloro-meta-cresol at 4%) which are to be used for disinfection and that were evaluated to be effective in eliminating *C. jejuni* and other bacteria such as the *Salmonella* sp.¹³ Since the bacteria spreads fast in chicken flocks and fecal-oral spread is also possible because chickens are coprophagic,⁵ both the producers and consumers are not able to guarantee that this program is effective enough to eliminate the bacteria completely.¹³

Calamansi (*Citrus microcarpa Bunge*) is native to the Philippines and is predominantly cultivated in the country, making it abundant and easily accessible in terms of obtaining. D-Limonene is identified as a primary component in a Calamansi rinds and constitutes 94% of the *Citrus oil*.¹⁴ D-limonene, a naturally occurring hydrocarbon, is a cyclic monoterpene commonly found in the rinds of citrus fruits.¹⁵ Generally regarded as safe (GRAS) status,¹⁶ it is commonly used in insecticide formulation and medicinal purposes, such as bronchitis treatment, weight loss, and cancer prevention.¹⁷

D-limonene is a vital component in citrus essential oils and has an exceptional antimicrobial property compared to other essential oils, especially when combined with thermal treatments.^{16,18-21} Several researchers have studied the synergistic effect of a heat treatment, which resulted in a 100-times reduction of the thermal resistance of *Listeria monocytogenes* (*L. monocytogenes*) and an essential oil nano-emulsion led to a reduction of the heat resistance of *Salmonella senftenberg* (*S. senftenberg*) of 50 times. These studies show the most dramatic decrease in microbial heat resistance when the heat has combined with natural antimicrobials.¹⁹⁻²¹

This study aims to reduce the heat resistance of *C. jejuni* by using D-limonene from calamansi (*Citrus microcarpa Bunge*) rinds extract. Specifically, it (1) aims for the D-Limonene from calamansi (*Citrus microcarpa Bunge*) rinds to have a significant effect on the heat resistance of *C. jejuni*. The authors of this study also (2) aim to know at which temperature (50°C or 55°C) will the extract be most effective in reducing the heat

resistance of the bacteria. In addition, the authors of this study (3) aim to know to what extent can the heat resistance of *C. jejuni* be reduced by the D-Limonene content from calamansi rinds.

The results of this study will help lessen the contamination of poultry as well as, reduce the risks of contracting campylobacteriosis and diseases caused by this pathogen. The results of this study can also be used in food processing companies since D-limonene can be an alternative for several treatments of processed foods. The results will also be used as a reference for improving studies related to heat-resistant bacteria and a solution for the continuous growth of several other bacteria.

■ Methods

Bacterial Strains:

C. jejuni ATCC 29428 was purchased from Fil-Anaserve Inc. The preparation of the bacterial culture was performed in a biosafety cabinet and all laboratory equipment used were sterilized to avoid contamination. The *C. jejuni* ATCC 29428 was grown and maintained in Mueller-Hinton Broth tubes and incubated at 42°C for 48 hours under microaerophilic conditions – 85% N₂, 10% CO₂, and 5% O₂.²²

Preparation of D-limonene:

For the collection of calamansi rinds, 6 kg of calamansi were purchased from a supermarket and were authenticated in University of the Philippines Diliman-Institute of Biology. The calamansi were rinsed before the rinds were aseptically separated from its components by squeezing out the juice and taking out the remaining parts in the albedo, the inner white part, until it became hollow. The rinds were then air-dried for 3 days, and then cut into smaller pieces. A Soxhlet extractor was used to obtain D-Limonene from the rinds with a ratio of 1:3 with ethanol as solvent.²³ To separate the solvent from the solution, a rotary evaporator set at 60°C was used and pure calamansi rinds extract was acquired.²⁴

Preparation of Campylobacter jejuni Inoculum:

Using a 0.5 McFarland Standard as a basis for their turbidity to acquire bacterial inoculum, a desired bacterial concentration of 1,300 µL of freshly cultured bacteria was added in each 3 double-strength Mueller-Hinton broth tubes.²⁵

The equipment needed and the double-strength Mueller-Hinton broth was prepared following the manufacturer's instructions and sterilized through autoclaving at 121°C for 30 minutes.²⁶ After the broth had cooled down, 8 test tubes with 3mL of double-strength Mueller-Hinton broth were prepared. 3mL of the bacterial culture was then added into each tube. The negative control set-up consisted of two test tubes containing 3mL of double-strength Mueller-Hinton broth and 3mL of the bacterial culture. Subsequently, the formulation of the D-limonene and *C. jejuni* inoculums included the addition of 3mL of calamansi rinds extract to the remaining 6 test tubes.

Experimentation Using Water Bath and Plate Count Method:

After preparing the samples, 3 test tubes along with a control, a total of 4 test tubes, were placed in a water bath at 50°C for 6 minutes. This was also done to the remaining 4 test tubes, at 55°C.²⁷ The samples were cooled shortly after the

process. Using a 10 μL inoculating loop, 10 μL of each sample was placed onto Petri dishes containing Mueller Hinton Agar supplemented with 5% lysed horse blood, lysed following Clinical and Laboratory Standards & Institute Guideline,²⁸ by streak plating using quadrant method.²⁹ The plates were then inverted and incubated at 37°C for 24 hours under microaerophilic conditions.³⁰

Data Gathering:

After a 24-hour incubation, the bacterial colonies were counted using a manual colony counter. Results showed that the colonies of the negative controls, plates 1 and 2, were considered too numerous to count (TNTC) therefore, the value used to represent the controls is 300.³¹ In contrast to that, definite number of colonies were recorded in both triplicates. Data collected from the triplicates of 55°C was 0 colonies in plate A, 40 colonies in plate B, and 113 colonies in plate C. 15 colonies in plate D, 15 colonies in plate E, and 17 colonies in plate F were recorded from the triplicates for 50°C.

Statistical Analysis:

The data, specifically the difference between the bacterial inoculums with the extract and without the extract, were analyzed using the statistical test “ANOVA: Two-way Factor with Replication”. The statistical test was used to determine whether there are any statistically significant differences between the means of the two independent groups which were the bacterial inoculums with calamansi rinds extract and the bacterial inoculums without the extract. The independent variables of this study were the presence of the extract in the inoculum, and the dependent variable was the reaction of *C. jejuni* on the treatment.

Results and Discussion

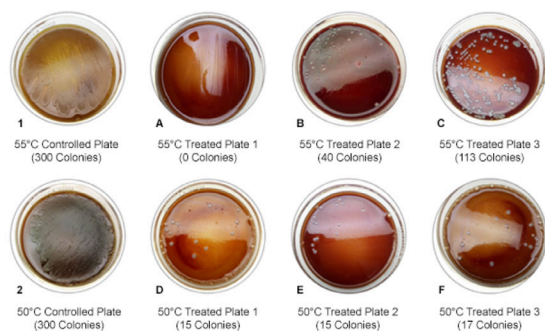


Figure 1: The results of the plates after a 24-hour incubation. (1) 55°C Controlled plate, (2) 50°C Controlled plate. (A-C) Treated plates under 55°C, and (D-F) Treated plates under 50°C.

Figure 1 shows the effect of D-limonene added directly on the thermal resistance of *C. jejuni* at two different temperatures, 50°C and 55°C, after a 24-hour incubation time. Results showed a dramatic difference between the number of bacterial colonies between the treated and untreated bacterial inoculums. The negative controls' bacterial colonies were considered too numerous to count (TNTC) therefore, the value used is 300.³¹ In contrast to that, definite number of colonies were recorded for both triplicates being 0, 40, and 113 for the 55°C, and 15, 15, and 17 for the 50°C. The average number of colonies at 50°C is 15.7, with a 94.766% decrease from the negative

control's bacterial colonies, while the average number of colonies at 55°C is 51, with an 83% decrease. The statistical analysis of the treatments was done using ANOVA: Two-Factor with replication. As shown in Table 1, there is a significant difference between the treatments. The p-value shows a lower value than the level of significance ($\alpha = 0.05$). Therefore, the null hypothesis should be rejected, which means that D-limonene from calamansi rinds extract can reduce the heat resistance of *C. jejuni*.

Table 1: ANOVA: Two-Factor with Replication. There is a significant difference between the treatments therefore, the null hypothesis should be rejected.

Anova: Two-Factor with Replication

SUMMARY	50	55	Total
WITH			
Count	3	3	6
Sum	47	153	200
Average	15.667	51	33.333
Variance	1.3333	3283	1688.3
WITHOUT			
Count	3	3	6
Sum	900	900	1800
Average	300	300	300
Variance	0	0	0
Total			
Count	6	6	
Sum	947	1053	
Average	157.833	175.5	
Variance	24254.2	19913.5	

ANOVA

Source of Variation	SS	df	MS	F	P-value	F crit
Sample	213333	1	213333	259.819	2.203E-07	5.317655
Columns	936.33	1	936.33	1.14036	0.316737	5.317655
Interaction	936.33	1	936.33	1.14036	0.316737	5.317655
Within	6568.7	8	821.08			
Total	221775	11				

D-limonene as an antimicrobial combined with heat has been tested by a number of authors, displaying promising results. Based on the study of Ros-Chumillas *et al.*, *S. senftenberg* is the most heat-resistant among the bacteria that can be found in the guts of a chicken and a gram-negative bacterium like *C. jejuni*.²¹ In the said study, using nanoemulsified D-limonene showed a dramatic decrease in the heat-resistance of *S. senftenberg*. The same results were seen in multiple studies conducted by Maté *et al.*¹⁸⁻²⁰ in using nanoemulsified D-limonene to reduce the heat-resistance of the bacteria, *L. monocytogenes*. These bacteria are also ubiquitous and contaminates an extensive amount of food just like *C. jejuni*.

In this study, a higher concentration of D-limonene was used, and similar results were recorded and observed by the researchers. The studies mentioned showed an average decrease of three times in the thermal resistance of various cells when antimicrobials are added to the heating medium.³² Different cell structures are injured when exposed to heat, but heat alone could not inactivate these damaged cells. However, antimicrobials, combined with heat, would aid in inactivating these cells.³³ This report confirms that antimicrobials reduce heat resistance when added directly, depending on the heating temperature.²⁰ D-limonene, an essential oil with antimicrobial properties, can help in inactivating the damaged cells with

heat. Thus, it might reduce the heat resistance of bacteria at a greater level in higher temperatures.^{16,18-20}

Therefore, several medications can use D-limonene, specifically for poultry. D-limonene could aid in reducing the heat resistance of the bacteria living in the intestinal tract of chickens since they have a high body temperature and might prevent the spread of pathogens from one another. Food processing companies can also use D-limonene to serve as an alternative for several treatments for processed foods. Furthermore, this study could be a reference for improving and investigating studies related to heat-resistant bacteria.³⁴

■ Conclusion

In conclusion, D-limonene from calamansi (*Citrus microcarpa Bunge*) rinds extract had a significant effect in reducing the heat resistance of *C. jejuni*. This research contributes to the potential of using D-limonene as an antimicrobial when combined with thermal treatments which have been previously shown in studies on *L. monocytogenes* and *S. senftenberg*.¹⁸⁻²¹

The researchers suggest further research to test the effect of the D-limonene extract in the form of nanoemulsion on the heat resistance of *C. jejuni*. Based on published studies where in nano-emulsified D-limonene is used in decreasing the heat resistance of *L. monocytogenes* and *Salmonella senftenberg*, nano-emulsified D-limonene showed a higher rate of decrease in the heat resistance of the bacteria compared to when D-limonene is introduced to the strain directly.¹⁸⁻²¹ It also indicates that using nano-emulsified D-limonene would be beneficial for food processing as it only uses a low concentration of the extract, and companies could save more.³⁴

Different compounds, such as fat and fiber, should also be taken into consideration if it will interfere with the effectiveness of D-limonene in reducing the heat resistance of *C. jejuni* when applied to food products. The interference of these compounds is seen in a study conducted by Maté *et al.* in where compounds such as, but not limited to fat and fiber; hinder the effectiveness of nano-emulsified D-limonene.¹⁸

Additional studies are also needed to determine the effect of D-limonene under non-isothermal conditions, for it to be applied in actual food processing in where microorganisms respond differently due to the dynamic conditions.³⁵ Microbial cells may develop a physiological response that can increase their resistance against heat due to certain treatments. Several studies observed that an increased rate of heating in cells may result in higher sensitivity, which would decrease their resistance to underlying stresses.³⁶⁻⁴² Although active in the research field, further studies are required to understand these mechanisms at a molecular level.^{4,41,43}

■ Acknowledgements

The student researchers would like to extend their gratitude and appreciation to the following individuals and institutions that helped in the completion of this study: Ms. Sheila Marie R. Serrano and Ms. Ruth Paulynn M. Grulla, research assistants, for helping the researchers inside the laboratories. BGR Hydrolab Testing Center and Diamond Laboratories Inc. for accommodating the researchers and providing other materials that were used during the experiment. Mrs. Remedios P. Dano and Mrs. Cecilia Cauguiran, the Quezon City Science High

School principal and Science Department Head respectively, for the support that the researchers received throughout the conduct of the study. Mr. Earl Francis C. Merilles, the research adviser, gave the researchers his full support and knowledge that helped in this experiment. Ms. Genevieve Vasquez, the researchers' grade 9 teacher, who assisted in the research plan while the research adviser was not available. Mr. Dan Allen Q. Nuesca, the researchers' statistician who helped and guided the researchers in making and interpreting the results. For the researchers' parents for the unfailing support and guidance throughout the experiment.

■ References

1. Kaakoush, N. O., Castaño-Rodríguez, N., Mitchell, H. M., & Man, S. M. (2015). Global Epidemiology of *Campylobacter* Infection. *Clinical Microbiology Reviews*, 28(3), 687-720. doi:https://doi.org/10.1128/CMR.00006-15.
2. Acheson, D., & Allos, B. (2001, April 15). Trends, *Campylobacter jejuni* Infections: Update on Emerging Issues and Trends. *Clinical Infectious Diseases*, 32(8), 1201-1206. doi:https://doi.org/10.1086/319760.
3. Haddad, N., Burns, C. M., Bolla, J., Prévost, H., Fédérighi, M., Drider, D., & Cappelier, J. (2009, November). Long-Term Survival of *Campylobacter jejuni* at Low Temperatures is Dependent on Polynucleotide Phosphorylase Activity. *Applied and Environmental Microbiology*, 75(23), 7310-7318. doi:10.1128/AEM.01366-09.
4. de Jong, A. E., van Asselt, E. D., Zwietering, M. H., Nauta, M. J., & de Jonge, R. (2012). Extreme Heat Resistance of Food Borne Pathogens *Campylobacter jejuni*, *Escherichia coli*, and *Salmonella typhimurium* on Chicken Breast Fillet during Cooking. *International Journal of Microbiology*. doi:https://doi.org/10.1155/2012/196841
5. Bungay, A. C., de los Reyes, C. S., & Estacio, M. J. (2005, June). The Zoonotic Potential of *Campylobacteriosis* and its Implication to Human Health. *Philippine Journal of Science*, 134(1), 69-77. Retrieved from https://philjournalsci.dost.gov.ph/home-1/21-vol-134-no-1-march-2005/304-the-zoonotic-potential-of-campylobacteriosis-and-its-implication-to-human-health
6. Workman, S. N., Mathison, G. E., & Lavoie, M. C. (2005). Pet dogs and chicken meat as reservoirs of *Campylobacter spp.* in Barbados. *Journal of Clinical Microbiology*, 43(6), 2642-2650. doi:https://doi.org/10.1128/JCM.43.6.2642-2650.2005
7. Trigui, H., Thibodeau, A., Fravallo, P., Letellier, A., & Faucher, S. (2015). Survival in water of *Campylobacter jejuni* strains isolated from the slaughterhouse. *SpringerPlus*, 4(1), 799. doi:https://doi.org/10.1186/s40064-015-1595-1
8. Bahrndorff, S., Rangstrup-Christensen, L., Nordentoft, S., & Hald, B. (2013). Foodborne Disease Prevention and Broiler Chickens with Reduced *Campylobacter* Infection. *Emerging infectious diseases*, 19(3), 425-430. doi:https://doi.org/10.3201/eid1903.111593
9. Cody, A. J., Colles, F. M., Sheppard, S. K., & Maiden, M. C. (2010). Where Does *Campylobacter* Come From? A Molecular Odyssey. *Advances in Experimental Medicine and Biology*, 659, 47-56. doi:https://doi.org/10.1007/978-1-4419-0981-7_4
10. Luangtongkum, T., Jeon, B., Han, J., Plummer, P., Logue, C. M., & Zhang, Q. (2009). Antibiotic resistance in *Campylobacter*: emergence, transmission and persistence. *Future Microbiology*, 4(2), 189-200. doi:https://doi.org/10.2217/17460913.4.2.189
11. Lim, P. W., Tiam-Lee, D. C., Paclibare, P. A., Subejano, M. S., Cabero-Palma, J. A., & Penuliar, G. M. (2017). High Rates of Contamination of Poultry Meat Products with Drug-Resistant

- Campylobacter in Metro Manila, Philippines. *Japanese Journal of Infectious Diseases*, 70(3), 311-313. doi:https://doi.org/10.7883/yoken.JJID.2016.309
12. Wiczorek, K., & Osek, J. (2013). Antimicrobial Resistance Mechanisms among Campylobacter. *BioMed Research International*, 2013, 12. doi:https://doi.org/10.1155/2013/340605
 13. de Castro Burbarelli, M. F., do Valle Polycarpo, G., Deliberali Lelis, K., Granghelli, C. A., Carão de Pinho, A. C., Ribeiro Almeida Queiroz, S., . . . de Albuquerque, R. (2017). Cleaning and disinfection programs against Campylobacter jejuni for broiler chickens: productive performance, microbiological assessment and characterization. *Poultry Science*, 96(9), 3188-3198. doi:3188-3198. https://doi.org/10.3382/ps/pex153
 14. Othman, S., Hassan, M. A., Nahar, L., Basar, N., Jamil, S., & Sarker, S. D. (2016). Essential Oils from the Malaysian *Citrus* (Rutaceae) Medicinal Plants. *Medicines*, 3(2), 13. doi:https://doi.org/10.3390/medicines3020013
 15. Burnham, P. M. (2017, September 22). LIMONENE - The industrial degreasing agent found in orange peel. *Molecule of the Month* - March 2008. doi:10.6084/m9.figshare.5427154
 16. Sun, J. (2007, September). D-Limonene: safety and clinical applications. *Alternative Medicine Review*, 12(3), 259-64. Retrieved from https://pubmed.ncbi.nlm.nih.gov/18072821/
 17. Karr, L. L. (1989). Toxic properties of d-limonene in insects and the earthworm *Eisenia fetida*. *Retrospective Theses and Dissertations*, 9057. doi:https://lib.dr.iastate.edu/rtd/9057
 18. Maté, J., Periago, P. M., & Palop, A. (2016, March). Combined effect of a nanoemulsion of D-limonene and nisin on *Listeria monocytogenes* growth and viability in culture media and foods. *Food Science Technology International*, 22(2), 146-52. doi:10.1177/1082013215577034
 19. Maté, J., Periago, P. M., Ros-Chumillas, M., Grullón, C., Huertas, J. P., & Palop, A. (2017, April). Fat and fibre interfere with the dramatic effect that nanoemulsified d-limonene has on the heat resistance of *Listeria monocytogenes*. *Food Microbiology*, 62, 270-274. doi:10.1016/j.fm.2016.10.031
 20. Maté, J., Periago, P. M., & Palop, A. (2016). When nanoemulsified, d-limonene reduces *Listeria monocytogenes* heat resistance about one hundred times. *Food Control*, 59, 824-828. doi:https://doi.org/10.1016/j.foodcont.2015.07.020
 21. Ros-Chumillas, M., Garre, A., Maté, J., Palop, A., & Periago, P. M. (2017). Nanoemulsified D-Limonene Reduces the Heat Resistance of *Salmonella* Senftenberg over 50 Times. *Nanomaterials*, 7(3). doi:https://doi.org/10.3390/nano7030065
 22. Davis, L., & DiRita, V. (2008, August). Growth and laboratory maintenance of Campylobacter jejuni. *Current Protocol Microbiology*. doi:10.1002/9780471729259.mc08a01s10
 23. Park, S., Park, K., Kwan, & Kim. (2015). Optimization of d-limonene Extraction from Tangerine Peel in Various Solvents by Using Soxhlet Extractor. *Korean Chemical Engineering Research*, 53, 717-722. doi:10.9713/kcer.2015.53.6.717
 24. Nichols, L. (2021, March 5). Overview of Rotary Evaporation. *Chemistry LibreTexts*. Retrieved from https://chem.libretexts.org/go/page/95729
 25. Hombach, M., Maurer, F. P., Tamara, P., Böttger, E. C., & Furrer, R. (2015, November). Standardization of Operator-Dependent Variables Affecting Precision and Accuracy of the Disk Diffusion Method for Antibiotic Susceptibility Testing. *Journal of Clinical Microbiology*, 53(12), 3864-3869. doi:10.1128/JCM.02351-15
 26. Lerouge, S. (2010). Sterilisation and cleaning of metallic biomaterials. *ScienceDirect*, 303-326. doi:https://doi.org/10.1533/9781845699246.3.303
 27. Close, A. J., Jones, T., Williams, N. J., Rushton, S. P., & Humphrey, T. J. (2015, March 31). Development of accurate predictive models for the assessment of the survival of *Campylobacter jejuni* and *C. coli* under food-relevant conditions. *Food Standards Agency*. Retrieved from https://www.food.gov.uk/sites/default/files/media/document/fs241040execsumm.pdf
 28. CLSI. (2007, December). Methods for Dilution Antimicrobial Susceptibility Tests for Bacteria That Grow Aerobically. *Clinical and Laboratory Standards Institute*. Retrieved from https://www.eurl-ar.eu/CustomerData/Files/Folders/25-resourcer/330_lysis-of-blood-17-12-07-4.pdf
 29. Tankeshwar, A. (2016, July 16). Streak plate method: Principle, Purpose, Procedure, and results. *Learn Microbiology Online*. Retrieved from https://microbeonline.com/streak-plate-method-principle-purpose-procedure-results/
 30. Duffy, L., & Dykes, G. A. (2006, December). Growth temperature of four Campylobacter jejuni strains influences their subsequent survival in food and water. *Letters in Applied Microbiology*, 43(6), 596-601. doi:10.1111/j.1472-765X.2006.02019
 31. Sivasankar. (2017, January 3). TNTC and TFTC. *Pharmaceutical Microbiology*. Retrieved from http://pharmaceuticalmicrobiologi.blogspot.com/2017/01/tntc-and-tftc.html
 32. Cherrat, L., Espina, L., Bakkali, M., García-Gonzalo, D., Pagán, R., & Laglaoui, A. (2014, April). Chemical composition and antioxidant properties of *Laurus nobilis* L. and *Myrtus communis* L. essential oils from Morocco and evaluation of their antimicrobial activity acting alone or in combined processes for food preservation. *Journal of the Science of Food and Agriculture*, 94(6), 1197-1204. doi:10.1002/jsfa.6397
 33. Espina, L., Gelaw, T. K., de Lamo-Castellví, S., Pagán, R., & García-Gonzalo, D. (2013). Mechanism of bacterial inactivation by (+)-limonene and its potential use in food preservation combined processes. *PLoS ONE*, 8(2). doi:10.1371/journal.pone.0056769
 34. Cole, M. B., Augustin, M. A., Robertson, M. J., & Manners, J. M. (2018). The science of food security. *npj Science of Food*, 1-8. Retrieved from https://www.nature.com/articles/s41538-018-0021-9
 35. Dolan, K. D., Valdramidis, V. P., & Mishra, D. K. (2013). Parameter estimation for dynamic microbial inactivation: which model, which precision? *Food Control*, 29(2), 401-408. doi:https://doi.org/10.1016/j.foodcont.2012.05.042
 36. Hassani, M., Cebrián, G., Mañas, P., Condón, S., & Pagán, R. (2006, December). Induced thermotolerance under nonisothermal treatments of a heat sensitive and a resistant strain of *Staphylococcus aureus* in media of different pH. *Letters in Applied Microbiology*, 43(6), 619-624. doi:10.1111/j.1472-765X.2006.02014.x
 37. Garre, A., Egea, J. A., Iguaz, A., Palop, A., & Fernandez, P. S. (2018, July). Relevance of the Induced Stress Resistance When Identifying the Critical Microorganism for Microbial Risk Assessment. *Frontiers in Microbiology*, 9, 1663. doi:10.3389/fmicb.2018.01663
 38. Garre, A., Huertas, J. P., González-Tejedor, G. A., Fernández, P. S., Egea, J. A., Palop, A., & Esnoz, A. (2018, February). Mathematical quantification of the induced stress resistance of microbial populations during non-isothermal stresses. *International Journal of Food Microbiology*, 266, 133-141. doi:10.1016/j.ijfoodmicro.2017.11.023
 39. Garre, A., González-Tejedor, G. A., Aznar, A., Fernández, P. S., & Egea, J. A. (2019, December). Mathematical modelling of the stress resistance induced in *Listeria monocytogenes* during dynamic, mild heat treatments. *Food Microbiology*, 84. doi:10.1016/j.fm.2019.06.002
 40. Stasiewicz, M. J., Marks, B. P., Orta-Ramirez, A., & Smith, D. M. (2008, February). Modeling the effect of prior sublethal thermal history on the thermal inactivation rate of *Salmonella*

in ground turkey. *Journal of Food Protection*, 71(2), 279-285.
doi:10.4315/0362-028x-71.2.279

41. Huertas, J. P., Aznar, A., Esnoz, A., Fernández, P. S., Iguaz, A., Periago, P. M., & Palop, A. (2016, August). High Heating Rates Affect Greatly the Inactivation Rate of *Escherichia coli*. *Frontiers Microbiology*, 11(7), 1256. doi:10.3389/fmicb.2016.01256
42. Hassani, M., Mañas, P., Pagán, R., & Condón, S. (2007, May). Effect of a previous heat shock on the thermal resistance of *Listeria monocytogenes* and *Pseudomonas aeruginosa* at different pHs. *International Journal of Food Microbiology*, 116(2), 228-238. doi:10.1016/j.ijfoodmicro.2007.01.010
43. Yi-Der, L., & Cheng-Chun, C. (2004). Effect of heat shock on thermal tolerance and susceptibility of *Listeria monocytogenes* to other environmental stresses. *Food Microbiology*, 21(5), 605-610. doi:https://doi.org/10.1016/j.fm.2003.10.007

■ Author

Trinity Bjork M. Coduco was born in 2003 and a student at Quezon City Science High School. She is in her 11th grade, taking the STEM strand. Trinity aspires to discover new things and learn more about human behavior. She wants to take a B.S. in Psychology in college and be a Psychiatrist.

Bea Nicole S. Gacayan was born in 2004 and is currently an 11th grade student from Quezon City Science High School taking up STEM. Bea wants to major in subjects related to medicine and biomedical sciences. She intends to pursue a research-based science career which focuses on medical microbiology.

Mary Danielle M. Estrada, born in 2003, is an 11th-grade student taking up the STEM strand at Quezon City Science High School. She would love to travel around the world and learn about different cultures. She wants to take Biology in college and hopes to be a successful doctor someday.

Geometric Interpretation of Best Rational Approximation and Simple Continued Fractions

William Li

Delbarton School, 230 Mendham Road, Morristown, NJ 07960, U.S.A.; liwilliam2021@gmail.com

ABSTRACT: The best approximation of an irrational number by rational numbers has been a well-studied mathematical problem for centuries. In this paper we present a geometric interpretation of best approximation, discover a few interesting properties, and connect best approximations and simple continued fractions.

KEYWORDS: Mathematics; Algebra; Best Approximation; Continued Fractions.

Introduction

A rational number can be expressed as a fraction p/q , where p and q are integers. An irrational number α is a real number that is not a rational number. In practical applications, α is often approximated by a rational number. As an example, the ratio of a circle's circumference to its diameter is an irrational number, $\pi=3.14159265\dots$ Some rational approximations discovered in early history are 258 (Babylonian, 19th century B.C.), 227 (Archimedes, 3rd century B.C.), 377/120 (Ptolemy, 2nd century A.D.), 3927/1250 (Liu Hui, 3rd century A.D.) and 355/113 (Zu Chongzhi, 5th century A.D.).¹

Many rational approximations exist for α , but what is the "best" approximation? Conventionally, the best approximation is derived algebraically using continued fractions.² A drawback of this approach is that it uses one arithmetic equation after another, and the reader may lose sight of where the equations are leading. Inspired by the ideas by Irwin and Davenport,^{3,4} this paper takes a geometric approach to provide a geometric interpretation of the best approximation and connect the ideas of the best approximations and simple continued fractions. The geometric treatment may be of some help by providing more clear mathematic intuition.

Definition of Best Approximation:

Define p/q to be the best rational approximation of α if,

$$|p-\alpha q| < |p'-\alpha q'| \quad (1)$$

for any $p'/q' \neq p/q$ with $0 < q' \leq q$. One may replace (1) with

$$|p/q-\alpha| < |p'/q'-\alpha| \quad (2)$$

The inequality in (2) can be rewritten as

$$\frac{|p-\alpha q|}{q} < \frac{|p'-\alpha q'|}{q'}$$

which is equivalent to adding a weight (q or q') to the metric ($|p-\alpha q|$ or $|p'-\alpha q'|$) used in (1). We claim that (2) is weaker than (1) in the sense that some approximation p/q may be qualified as a best rational approximation, not because $|p-\alpha q|$ is the smallest, but because q is large. A best approximation under (1) is always a best approximation under (2), but the reverse is not true. Consider an example of approximating π . The best approximations under (1) are

$$\frac{3}{1}, \frac{22}{7}, \frac{333}{106}, \frac{355}{113}, \dots$$

which are a subset of those under (2) given by

$$\frac{3}{1}, \frac{13}{4}, \frac{16}{5}, \frac{19}{6}, \frac{22}{7}, \frac{179}{57}, \frac{201}{64}, \frac{223}{71}, \frac{245}{78}, \frac{267}{85}, \frac{289}{92}, \frac{311}{99}, \frac{333}{106}, \frac{355}{113}, \frac{52163}{16604}, \dots$$

Not only the definition of (1) is stronger, it also nicely connects to continued fractions, as explained later. Next, we next focus on the definition (1).

A Geometric Interpretation:

Consider a coordinate plane on which lattice points (q,p) are defined for all integers q,p . Imagine standing at the origin of the plane and shooting out a ray whose slope is α . For the sake of showing the geometric property, we assume $\alpha > 0$. The ray goes into the first quadrant, as depicted in Figure 1. Because the slope is irrational, the ray will not hit any lattice point. A lattice point is a rational approximation of α where the horizontal axis (q) represents the denominator and the vertical axis (p) is the numerator. The vertical distance of every point (q,p) to the ray is $|p-\alpha q|$.

As the ray travels, i.e., as q increases, keep track of the best

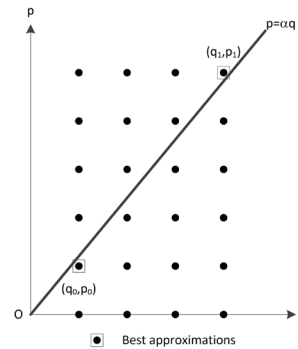


Figure 1: Definition of best approximation.

approximations as the lattice points closest to the ray: $p_0/q_0, p_1/q_1, \dots$. By definition, of the very first best approximation, $q_0=1$. Given p_0/q_0 , where will p_1/q_1 be?

Suppose that $p_0 < \alpha$ (the case of $p_0 > \alpha$ can be addressed similarly). $p_0 + 1 > \alpha$. As depicted in Figure 2, draw two lines from the origin to $(1, p_0)$ and $(1, p_0 + 1)$ respectively. By definition, (q_1, p_1) cannot be in the two grey closed areas in the following figure. The remaining points on the plane are the lattice formed by $i(1, p_0) + j(1, p_0 + 1)$ with positive integers i, j .

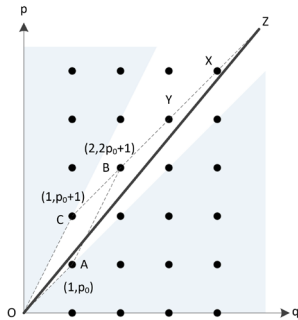


Figure 2: Determination of (q_1, p_1) .

Denote $O=(0,0)$, $A=(1, p_0)$, $B=(2, 2p_0+1)$, $C=(1, p_0+1)$. Draw parallelogram $OABC$. Since p_0 , not p_0+1 , is the best approximation, it follows that $(p_0+1) - \alpha > \alpha - p_0$. Thus, $2\alpha < 2p_0+1$. The ray intersects the line segment AB and meets the extension of the line segment CB at Z . Denote X the farthest lattice point on the extension of CB before Z . We claim the following.

Lemma 1. X is (q_1, p_1) .

Proof. We must show two statements:

1. The vertical distance of X to the ray is the smallest for any point whose horizontal coordinate does not exceed that of X , and
2. There is no best approximation between A and X .

X is the closest to the ray among all the lattice points on CB and its extension before Z . To show the first statement, it suffices to note that X is closer to the ray than A is because $XZ \parallel OA$ and $|XZ| < |OA|$. The second statement holds because for another lattice point on CB and its extension before Z , say Y , $YZ \parallel OA$ and $|YZ| > |OA|$.

From the above construction of (q_1, p_1) , the following corollary can be immediately obtained.

Corollary 2. If p_0/q_0 is a lower best approximation, then p_1/q_1 is an upper one.

We can apply a similar construction to locate any subsequent p_n/q_n as depicted in Figure 3.

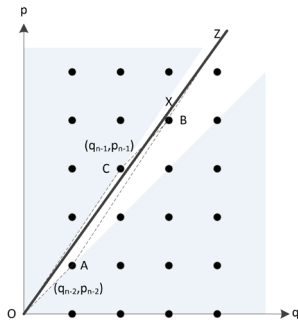


Figure 3: Determination of (q_n, p_n) .

Specifically, start from $A=(q_{n-2}, p_{n-2})$ and $C=(q_{n-1}, p_{n-1})$, where one of them (say A) is a lower and the other one, C , is an upper best approximation. Thus, $p_{n-1} - \alpha q_{n-1} < \alpha q_{n-2} - p_{n-2}$.

Denote $B=(q_{n-2}+q_{n-1}, p_{n-2}+p_{n-1})$. (q_n, p_n) cannot be in the two grey closed areas in the figure. Draw parallelogram $OABC$. The ray intersects the line segment CB because $\alpha(q_{n-2}+q_{n-1}) > p_{n-2}+p_{n-1}$, and meets the extension of the line segment AB at Z . Denote X the farthest lattice point on the extension of AB before Z . In the figure, X happens to be the same as B . This is not necessarily true in general.

Theorem 3. X is (q_n, p_n) .

Theorem 1 can be proved similarly to Lemma 1. As expected from Corollary 1, (q_m, p_m) is a lower best approximation.

Putting the above steps together, Figure 4 illustrates the first four best approximations of some α with $0 < \alpha < 1/2$ and the parallelograms used to construct them.

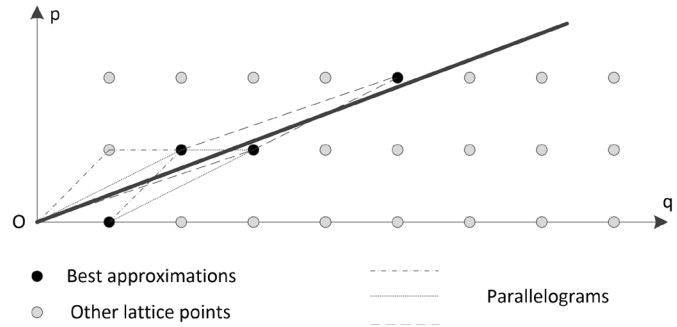


Figure 4: the first four best approximations of some α with $0 < \alpha < 1/2$.

Connection of Best Approximation and Continued Fractions:

Let us return to the construction of (q_m, p_m) . Recall that Z is the intersection of the extension of AB and the ray. The coordinates of Z are given by $(q_{n-2}+z_n q_{n-1}, p_{n-2}+z_n p_{n-1})$ where z_n is a positive real number satisfying

$$\frac{p_{n-2} + z_n p_{n-1}}{q_{n-2} + z_n q_{n-1}} = \alpha \tag{3}$$

Moreover, because X is the farthest lattice point on the AB and its extension before Z , we have the following recurrence relation,

$$q_n = q_{n-2} + m_n q_{n-1}, p_n = p_{n-2} + m_n p_{n-1} \tag{4}$$

where positive integer m_n is given by $m_n = [z_n]$. The exact expressions of m and thus (q_m, p_m) can be obtained via simple continued fractions, as explained next.

The idea of simple continued fractions works as follows. Write

$$\alpha = [\alpha] + \alpha_1.$$

Set $a_0 = [\alpha]$. $a_0 \geq 0$. Since α is irrational, $0 < \alpha_1 < 1$, and $1/\alpha_1 > 1$. Write

$$\frac{1}{\alpha_1} = \left[\frac{1}{\alpha_1} \right] + \alpha_2$$

Set $a_1 = \left[\frac{1}{\alpha_1} \right]$. $a_1 \geq 1$. Since α is irrational, $0 < \alpha_2 < 1$, and $1/\alpha_2 > 1$.

This procedure repeats and leads to an expression of the form

$$\alpha = a_0 + \alpha_1 = a_0 + \frac{1}{a_1 + \alpha_2} = a_0 + \frac{1}{a_1 + \frac{1}{a_2 + \alpha_3}} = \dots = a_0 + \frac{1}{a_1 + \frac{1}{a_2 + \frac{1}{a_3 + \dots + \frac{1}{a_n + \alpha_{n+1}}}}} \tag{5}$$

Note that $a_n \geq 1$ for $n \geq 1$. Since α is irrational, the sequence of $\{a_n\}$ goes on forever. To obtain a rational approximation of α , we stop at some a_n and set

$$\frac{h_n}{k_n} = a_0 + \frac{1}{a_1 + \frac{1}{a_2 + \frac{1}{a_3 + \dots + \frac{1}{a_n}}}} \quad (6)$$

$\left\{\frac{h_n}{k_n}\right\}, n = 1, 2, \dots$ are called convergents.

Lemma 4. Given $a_0, a_1, \dots, a_n, h_n, k_n$ can be calculated recurrently as follows.

$$k_n = k_{n-2} + a_n k_{n-1}, h_n = h_{n-2} + a_n h_{n-1} \quad (7)$$

with $k_0=1, h_0=a_0, k_1=a_1, h_1=1+a_0 a_1$.

Proof. We prove this recurrence relation by induction. It is easy to verify that the relation holds for $n=2$. Assuming that it holds for n , we next examine the case of $n+1$

$$\frac{h_{n+1}}{k_{n+1}} = a_0 + \frac{1}{a_1 + \frac{1}{a_2 + \frac{1}{a_3 + \dots + \frac{1}{a_n + \frac{1}{x}}}}} = a_0 + \frac{1}{a_1 + \frac{1}{a_2 + \frac{1}{a_3 + \dots + \frac{1}{a_n + \frac{1}{x}}}}}$$

with $x = \frac{a_n a_{n+1} + 1}{a_{n+1}}$. By the induction hypothesis, it follows that

$$\frac{h_{n+1}}{k_{n+1}} = \frac{h_{n-2} + x h_{n-1}}{k_{n-2} + x k_{n-1}} = \frac{h_{n-2} + \frac{a_n a_{n+1} + 1}{a_{n+1}} h_{n-1}}{k_{n-2} + \frac{a_n a_{n+1} + 1}{a_{n+1}} k_{n-1}} = \frac{a_{n+1} h_{n-2} + (a_n a_{n+1} + 1) h_{n-1}}{a_{n+1} k_{n-2} + (a_n a_{n+1} + 1) k_{n-1}} = \frac{h_{n-1} + a_{n+1} h_n}{k_{n-1} + a_{n+1} k_n}$$

Hence, we have completed the induction step.

The above recurrence relation of $\{h_n, k_n\}$ (7) derived from simple continued fractions is strikingly similar to that of $\{p_m, q_n\}$ (4) derived earlier from our geometric construction.

Theorem 5. For $n \geq 1$

$$m_n = a_n, p_n = h_n, q_n = k_n, z_n = a_n + \frac{1}{a_{n+1} + \frac{1}{a_{n+2} + \frac{1}{a_{n+3} + \dots}}} \quad (8)$$

Proof. To prove (8), we use induction again. It is easy to verify the cases of $n=1, 2$. Assuming that it holds for $3, \dots, n$, we next examine the case of $n+1$. We rewrite α of (5) in the recurrence form similar to,

$$\alpha = \frac{h_{n-1} + \frac{1}{a_{n+1}} h_n}{k_n + \frac{1}{a_{n+1}} k_n} = \frac{p_{n-1} + \frac{1}{a_{n+1}} p_n}{q_n + \frac{1}{a_{n+1}} q_n}$$

Comparison with our geometric construction (3) shows that

$$\frac{1}{a_{n+1}} = z_{n+1}$$

Therefore,

$$m_{n+1} = \lfloor z_{n+1} \rfloor = \left\lfloor \frac{1}{a_{n+1}} \right\rfloor = a_{n+1}.$$

Furthermore, by the recurrence relations (4) and (5), we know that $p_{n+1} = h_{n+1}, q_{n+1} = k_{n+1}$. Hence, we have completed the induction step.

In summary, what (8) in essence says is that for $n \geq 1$, every convergent is a best approximation and every best approximation is a convergent. This result is quite remarkable in connecting best approximations and simple continued fractions. Note that if $\alpha_1 > 1/2$, then $h_0/k_0 = \alpha_0$ is not a best ap-

proximation. Clearly the best approximation is $\alpha_0 + 1$. To avoid this complication, we ignore $n=0$ and focus on $n \geq 1$ in our statement.

■ Conclusions

In this paper we present a geometric interpretation of best rational approximation of an irrational number, discover a few interesting properties, and connect best approximations and simple continued fractions.

■ References

1. Wikipedia (2021a). Approximation of π . https://en.wikipedia.org/wiki/Approximations_of_%CF%80. Last edited on May 6, 2021.
2. Wikipedia (2021b). Continued Fraction. https://en.wikipedia.org/wiki/Continued_fraction. Last edited on May 5, 2021.
3. Irwin M.C. (1989). Geometry of Continued Fractions. The American Mathematical Monthly, Vol. 96, No. 8 (October 1989), pp. 696-703. <http://www.jstor.org/stable/2324717>.
4. Davenport H. (2008). The Higher Arithmetic – An Introduction to the Theory of Numbers. The 8th Edition. Cambridge University Press (June 2008). <https://doi.org/10.1017/CBO9780511818097>.

■ Authors

William Li is a rising freshman at Stanford University where he hopes to study symbolic systems. Will is a passionate math/CS researcher who works to promote science education and lead STEM outreach in underrepresented communities. Outside of science, Will is a nationally acclaimed debater who enjoys promoting tech policy.



American Commission for Accreditation
of Schools and Universities

STANDARDS

- * Governance
- * Education
- * Culture
- * Operations
- * Quality

Lifetime Qualities

MORAL

Caring, Modest,
Ethical, Respectful

THINKER

Knowledgeable, Inquirer,
Curious

PRODUCTIVE

Achiever,
Excellence Seeker

INNOVATIVE

Problem Solver, Explorer

VISIONARY

Global Citizen, Inclusive

ACASU BENEFITS

Enhances your institution's reputation and garners the esteem of Americans.

Assures students and their families that your institution meets American standards for high quality education.

Shows students and parents your institution's commitment to success and your ability to perform at high quality educational standards.

Shows your colleagues and the general public that your institution has a genuine interest in institutional improvement.

Sets your institution apart as a leader among others.

Provides you with a network of skilled professionals and resources to assist meeting your accreditation, enrollment, and college attainment goals.

Ensures that your standard operating procedures are compliant with U.S. international student regulations.



ACASU.ORG



The International Journal of High School Research is published
by Terra Science and Education